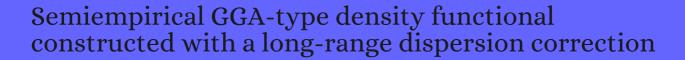
CITATION REPORT List of articles citing



DOI: 10.1002/jcc.20495 Journal of Computational Chemistry, 2006, 27, 1787-99.

Source: https://exaly.com/paper-pdf/40853306/citation-report.pdf

Version: 2024-04-28

This report has been generated based on the citations recorded by exaly.com for the above article. For the latest version of this publication list, visit the link given above.

The third column is the impact factor (IF) of the journal, and the fourth column is the number of citations of the article.

#	Paper	IF	Citations
2186	Surface-Mediated Hydrogen Bonding of Proteinogenic Amino Acids on Silicon.		
2185	Computational and Experimental Characterization of Five Crystal Forms of Thymine: Packing Polymorphism, Polytypism/Disorder and Stoichiometric 0.8-Hydrate.		
2184	Molecular Level Understanding of the Reversible Phase Transformation between Forms III and II of Dapsone.		
2183	Detailed Analysis of Packing Efficiency Allows Rationalization of Solvate Formation Propensity for Selected Structurally Similar Organic Molecules.		
2182	Influence of Axial Linkers on Polymerization in Paddle-Wheel Cu(II) Coordination Polymers for the Application of Optoelectronics Devices.		
2181	Crystal Structures, Stability, and Solubility Evaluation of Two Polymorphs of a 2:1 MelatoninPiperazine Cocrystal.		
2180	Determining and Controlling the Stoichiometry of Cu2ZnSnS4 Photovoltaics: The Physics and Its Implications.		
2179	Tailoring the Electronic Structure of Covalently Functionalized Germanane via the Interplay of Ligand Strain and Electronegativity.		
2178	Molecular Assembly-Induced Charge Transfer for Programmable Functionalities.		
2177	Gold ClusterCeO2 Nanostructured Hybrid Architectures as Catalysts for Selective Oxidation of Inert Hydrocarbons.		
2176	Effect of Copper Substrate Surface Orientation on the Reductive Functionalization of Graphene.		
2175	Experimental and Theoretical Study of the Extraction of UO22+ by Malonamides in Ionic Liquids.		
2174	Guest-Dependent Stabilization of the Low-Spin State in Spin-Crossover Metal-Organic Frameworks.		
2173	MetalLigand Cooperation in Single-Site Ruthenium Water Oxidation Catalysts: A Combined Experimental and Quantum Chemical Approach.		
2172	Emissive Azobenzenes Delivered on a Silver Coordination Polymer.		
2171	Transition Metal Carbonyl Complexes of an NHeterocyclic Carbene Stabilized Silyliumylidene Ion.		
2170	General Force-Field Parametrization Scheme for Molecular Dynamics Simulations of Conjugated		

2153

2152

Conformations.

How Accurate Are the Minnesota Density Functionals for Noncovalent Interactions, Isomerization Energies, Thermochemistry, and Barrier Heights Involving Molecules Composed of Main-Group 2169 Elements?. 2168 Ab Initio Evaluation of Henry Coefficients Using Importance Sampling. EnzyDock: ProteinLigand Docking of Multiple Reactive States along a Reaction Coordinate in 2167 Enzymes. 2166 Ab Initio Calculations for Spin-Gaps of Non-Heme Iron Complexes. Variational ForwardBackward Charge Transfer Analysis Based on Absolutely Localized Molecular 2165 Orbitals: Energetics and Molecular Properties. Exploring the Sponge Consortium Plakortis symbioticaXestospongia deweerdtae as a Potential 2164 Source of Antimicrobial Compounds and Probing the Pharmacophore for Antituberculosis Activity of Smenothiazole A by Diverted Total Synthesis. 1,2,3- versus 1,2-Indeno Ring Fusions Influence Structure Property and Chirality of Corannulene 2163 Bowls. Solvent-Free Enantioselective Michael Reactions Catalyzed by a Calixarene-Based Primary Amine 2162 Thiourea. 2161 Building Shape-Persistent Arylene Ethynylene Macrocycles as Scaffolds for 1,4-Diiodobutadiyne. Nonmonotonic Temperature Dependence of the Pressure-Dependent Reaction Rate Constant and 2160 Kinetic Isotope Effect of Hydrogen Radical Reaction with Benzene Calculated by Variational Transition-State Theory. Density Functional Theory for Microwave Spectroscopy of Noncovalent Complexes: A Benchmark 2159 Study. Time-Dependent Density-Functional Theory for Modeling Solid-State Fluorescence Emission of 2158 Organic Multicomponent Crystals. 2157 Ab Initio Studies of Exciton Interactions of Cy5 Dyes. 2156 . Hydration and Ion Pairing in Aqueous Mg2+ and Zn2+ Solutions: Force-Field Description Aided by 2155 Neutron Scattering Experiments and Ab Initio Molecular Dynamics Simulations. Chemisorption and Physisorption at the Metal/Organic Interface: Bond Energies of Naphthalene 2154 and Azulene on Coinage Metal Surfaces. Accurate Force Field Parameters and pH Resolved Surface Models for Hydroxyapatite to

Understand Structure, Mechanics, Hydration and Biological Interfaces.

Adsorption Behavior of Nonplanar Phthalocyanines: Competition of Different Adsorption

2151 Toward Accurate Adsorption Energetics on Clay Surfaces. Growth Mode Transition from Monolayer by Monolayer to Bilayer by Bilayer in Molecularly Flat 2150 Titanyl Phthalocyanine Film. Impact of Edge Oxidation State on Red-Ox Barriers during Hydrocarbon Oxydehydrogenation over 2149 Carbon Nanotube Catalysts: A Theoretical Study. 2148 Iron Intercalation in CovalentOrganic Frameworks: A Promising Approach for Semiconductors. Manganese(II) Molecular Sources for Plasma-Assisted CVD of Mn Oxides and Fluorides: From 2147 Precursors to Growth Process. Huge Absorption Edge Blueshifts of Layered 2146 -MoO{siComponents}amp;lt;sub{siComponents}gt;3{siComponents}amp;lt;/sub{siComponents}gt; Crystals upon Thickness Reduction Approaching 2D Nanosheets. 2145 . 2144 Two-Dimensional Organometallic Kondo Lattice with Long-Range Antiferromagnetic Order. 2143 Novel Solar Cell Materials: Insights from First-Principles. 2142 Flexoelectricity and the Formation of Carbon Nanoparticles in Flames. Exploration of AVP2O7/C (A = Li, Li0.5Na0.5, and Na) for High-Rate Sodium-Ion Battery 2141 Applications. 2140 Dual-Gated WTe2/MoSe2 van der Waals Tandem Solar Cells. Effect of Water on the Structural, Optical, and Hot-Carrier Cooling Properties of the Perovskite Material MASnI3. Toward Heterolytic Bond Dissociation of Dihydrogen: The Study of Hydrogen in Arsenolite under High Pressure. 2137 A Nanoscopic View of Photoinduced Charge Transfer in Organic Nanocrystalline Heterojunctions. 2136 Stabilization of Super Electrophilic Pd+2 Cations in Small-Pore SSZ-13 Zeolite. 2135 First-Principles Crystal Structure Prediction of Cu(I)-TCNQ Polymorphs. 2134 Chiral Monolayers with Achiral Tetrapod Molecules on Highly Oriented Pyrolytic Graphite.

2117

Transition.

Substantial Improvement of the Dielectric Strength of CelluloseLiquid Composites: Effects of Traps 2133 at the Nanoscale Interface. 2132 Band Alignment in Two-Dimensional Halide Perovskite Heterostructures: Type I or Type II?. 2131 . Tuning the Ambipolar Character of Copolymers with Substituents: A Density Functional Theory 2129 Facets and Defects in Perovskite Nanocrystals for Photocatalytic CO2 Reduction. Toward an Accurate Estimate of the Exfoliation Energy of Black Phosphorus: A Periodic Quantum 2128 Chemical Approach. 2127 Design of Efficient Catalysts with Double Transition Metal Atoms on C2N Layer. Gas-Phase Spectroscopic Signatures of CarboxylateLi+ Contact Ion Pairs: New Benchmarks For 2126 Characterizing Ion Pairing in Solution. Electrostatic Interaction-Induced Room-Temperature Phosphorescence in Pure Organic Molecules 2125 from QM/MM Calculations. Size of the Organic Cation Tunes the Band Gap of Colloidal Organolead Bromide Perovskite Nanocrystals. 2123 pKa at Quartz/Electrolyte Interfaces. 2122 Optical Dedoping Mechanism for P3HT:F4TCNQ Mixtures. Molecular Orbital Rule for Quantum Interference in Weakly Coupled Dimers: Low-Energy Giant 2121 Conductivity Switching Induced by Orbital Level Crossing. Decoupling the Effects of Mass Density and Hydrogen Oxygen, and Aluminum-Based Defects on Optoelectronic Properties of Realistic Amorphous Alumina. Inhibiting Low-Frequency Vibrations Explains Exceptionally High Electron Mobility in 2119 2,5-Difluoro-7,7,8,8-tetracyanoquinodimethane (F2TCNQ) Single Crystals. 2118 Molecular Dipole-Driven Electronic Structure Modifications of DNA/RNA Nucleobases on Graphene.

Insight into Electronic and Structural Reorganizations for Defect-Induced VO2 MetalInsulator

2116 Practical Density Functionals beyond the OverdelocalizationUnderbinding Zero-Sum Game.

5

Synthesis and Characterization of the Rare-Earth Hybrid Double Perovskites: (CH3NH3)2KGdCl6 2115 and (CH3NH3)2KYCl6. Electronic and Optical Properties of Pristine and Vertical and Lateral Heterostructures of Janus MoSSe and WSSe. 2113 Two-Dimensional Lattices of VN: Emergence of Ferromagnetism and Half-Metallicity on Nanoscale. Atomically Intercalating Tin Ions into the Interlayer of Molybdenum Oxide Nanobelt toward 2112 Long-Cycling Lithium Battery. 2111 First-Principles Investigation of Black Phosphorus Synthesis. Characterization of the PlatinumHydrogen Bond by Surface-Sensitive Time-Resolved Infrared 2110 Spectroscopy. Photo-oxidative Degradation and Protection Mechanism of Black Phosphorus: Insights from 2109 Ultrafast Dynamics. Synthesis of RNA Nucleotides in Plausible Prebiotic Conditions from ab Initio Computer 2108 Simulations. 2107 Concerted Metal Cation Desorption and Proton Transfer on Deprotonated Silica Surfaces. 2106 Revealing the Spectrum of Unknown Layered Materials with Superhuman Predictive Abilities. 2105 How a Solid Catalyst Determines the Chirality of the Single-Wall Carbon Nanotube Grown on It. 2104 Exotic Hydrogen Bonding in Compressed Ammonia Hydrides. 2103 Decreasing Exciton Binding Energy in Two-Dimensional Halide Perovskites by Lead Vacancies. Stable Surfaces That Bind Too Tightly: Can Range-Separated Hybrids or DFT+U Improve Paradoxical Descriptions of Surface Chemistry?. 2101 Spontaneous Decomposition of Fluorinated Phosphorene and Its Stable Structure. A Strong Test of Atomically Detailed Models of Molecular Adsorption in Zeolites Using 2100 Multilaboratory Experimental Data for CO2 Adsorption in Ammonium ZSM5. Self-Healing of Photocurrent Degradation in Perovskite Solar Cells: The Role of Defect-Trapped

6

Excitons.

2098 Effects of Plasmon Modes on Resonant Raman Images of a Single Molecule.

2099

- Computational Insights into LixOy Formation, Nucleation, and Adsorption on Carbon Nanotube 2097 Electrodes in Nonagueous LiO2 Batteries. Visible-Light-Induced Living/Controlled Radical Copolymerization of 1-Octene and Acrylic 2096 Monomers Mediated by Organocobalt Complexes. 2095 Structural Properties, OrderDisorder Phenomena and Phase Stability of Orotic Acid Crystal Forms. Size-Dependent Penetration of Gold Nanoclusters through a Defect-Free, Nonporous NaCl 2094 Membrane. 2093 Atomic Scale Study on Growth and Heteroepitaxy of ZnO Monolayer on Graphene. The Bright Future for Electrode Materials of Energy Devices: Highly Conductive Porous Na-Embedded Carbon. Raman Spectroscopy, Photocatalytic Degradation, and Stabilization of Atomically Thin Chromium 2091 Tri-iodide. Anomalous Shape Evolution of Ag2O2 Nanocrystals Modulated by Surface Adsorbates during 2090 Electron Beam Etching. 2089 Interface Modulation of Two-Dimensional Superlattices for Efficient Overall Water Splitting. 2088 Direct Observation of the Linear Dichroism Transition in Two-Dimensional Palladium Diselenide. Synthesis and Structural Characterization of Carbene-Stabilized Carborane-Fused Azaborolyl Radical Cation and Dicarbollyl-Fused Azaborole. 2086 Trends in Metallophilic Bonding in PdZn and PdCu Complexes. Fe(II) Hydride Complexes for the Homogeneous Dehydrocoupling of Hydrazine Borane: Catalytic Mechanism via DFT Calculations and Detailed Spectroscopic Characterization. 2084 Preparation of Ni(cod)2 Using Light as the Source of Energy. The Challenge of Reproducing with Calculations Raw Experimental Kinetic Data for an Organic 2083
- Reaction.
- Axial-Chiral Biisoquinoline N,NDioxides Bearing Polar Aromatic CH Bonds as Catalysts in 2082 Sakurai-Hosomi-Denmark Allylation.
- Strong Electron Coupling from the Sub-Nanometer Pd Clusters Confined in Porous Ceria Nanorods 2081 for Highly Efficient Electrochemical Hydrogen Evolution Reaction.
- Enhancing the Charge Extraction and Stability of Perovskite Solar Cells Using Strontium Titanate 2080 (SrTiO3) Electron Transport Layer.

Room-Temperature Stable Inorganic Halide Perovskite as Potential Solid Electrolyte for Chloride 2079 Ion Batteries. Highly Selective Separation of C2H2 from CO2 by a New Dichromate-Based Hybrid Ultramicroporous Material. Porous Two-Dimensional Monolayer MetalOrganic Framework Material and Its Use for the 2077 Size-Selective Separation of Nanoparticles. Magnetron Sputtering Deposition Cu@Onion-like NC as High-Performance Electrocatalysts for 2076 Oxygen Reduction Reaction. 2075 Lateral Heterostructures Formed by Thermally Converting nType SnSe2 to pType SnSe. Mn3O4 Quantum Dots Supported on Nitrogen-Doped Partially Exfoliated Multiwall Carbon Nanotubes as Oxygen Reduction Electrocatalysts for High-Performance ZnAir Batteries. Achieving High Efficiency in Solution-Processed Perovskite Solar Cells Using C60/C70 Mixed 2073 Fullerenes. Self-Powered and Highly Efficient Production of H2O2 through a ZnAir Battery with Oxygenated Carbon Electrocatalyst. MetalOrganic Frameworks with Potential Application for SO2 Separation and Flue Gas 2071 Desulfurization. Sulfur-Doped Mesoporous Carbon Nitride with an Ordered Porous Structure for Sodium-Ion 2070 Batteries. Self-Powered SnS1-xSex Alloy/Silicon Heterojunction Photodetectors with High Sensitivity in a 2069 Wide Spectral Range. Interfacial Engineering through Chloride-Functionalized Self-Assembled Monolayers for 2068 High-Performance Perovskite Solar Cells. Flowerlike Ti-Doped MoO3 Conductive Anode Fabricated by a Novel NiTi Dealloying Method: 2067 Greatly Enhanced Reversibility of the Conversion and Intercalation Reaction. Coordinated Water as New Binding Sites for the Separation of Light Hydrocarbons in MetalOrganic 2066 Frameworks with Open Metal Sites. Unraveling the Structural and Electronic Properties at the WSe2Graphene Interface for a Rational 2065 Design of van der Waals Heterostructures. Theoretical Study of GaN/BP van der Waals Nanocomposites with Strain-Enhanced Electronic and 2064 Optical Properties for Optoelectronic Applications. Mn Doping of CoP Nanosheets Array: An Efficient Electrocatalyst for Hydrogen Evolution Reaction 2063 with Enhanced Activity at All pH Values. 2062 MoS2 Quantum Dots as Efficient Catalyst Materials for the Oxygen Evolution Reaction.

2061 Well-Defined Diketiminatocobalt(II) Complexes for Alkene Cyclohydroamination of Primary Amines. Rational Design of FeN/C Hybrid for Enhanced Nitrogen Reduction Electrocatalysis under Ambient 2060 Conditions in Aqueous Solution. SDoped MoP Nanoporous Layer Toward High-Efficiency Hydrogen Evolution in pH-Universal 2059 Electrolyte. Structural Transformation Identification of Sputtered Amorphous MoSx as an Efficient Hydrogen-Evolving Catalyst during Electrochemical Activation. 2057 Carbon Dioxide-Catalyzed Stereoselective Cyanation Reaction. Distinct Catalytic Reactivity of Sn Substituted in Framework Locations and at Defect Grain Boundaries in Sn-Zeolites. COP Bonds as Atomic-Level Charge Transfer Channel To Boost Photocatalytic H2 Production of 2055 Co2P/Black Phosphorus Nanosheets Photocatalyst. 2054 Expediting Hydrogen Evolution through Topological Surface States on Bi2Te3. Composition-Graded CuPd Nanospheres with Ir-Doped Surfaces on NDoped Porous Graphene for 2053 Highly Efficient Ethanol Electro-Oxidation in Alkaline Media. Hydrothermal Decomposition of Amino Acids and Origins of Prebiotic Meteoritic Organic Compounds. Physicochemical Properties and Complexity of Amino Acids beyond Our Biosphere: Analysis of the 2051 Isoleucine Group from Meteorites. 2050 Surface Polarization Drives Photoinduced Charge Separation at the P3HT/Water Interface. 2049 Good Vibrations: Locking of Octahedral Tilting in Mixed-Cation Iodide Perovskites for Solar Cells. Microscopic Origin of Piezoelectricity in Lead-Free Halide Perovskite: Application in Nanogenerator 2048 Design. 2047 .

Corrugation in the Weakly Interacting Hexagonal-BN/Cu(111) System: Structure Determination by Combining Noncontact Atomic Force Microscopy and Xray Standing Waves.

2046 Proton and Li-Ion Permeation through Graphene with Eight-Atom-Ring Defects.

2045 Highly Oriented Atomically Thin Ambipolar MoSe2 Grown by Molecular Beam Epitaxy.

2043 Enhanced Photocatalytic Performance through Magnetic Field Boosting Carrier Transport. 2042 Boron Radicals Identified as the Source of the Unexpected Catalysis by Boron Nitride Nanosheets. 2041 Organic Radical-Linked Covalent Triazine Framework with Paramagnetic Behavior. Correction to Photochemical Creation of Covalent Organic 2D Monolayer Objects in Defined Shapes via a Lithographic 2D Polymerization. Phonon and Thermal Properties of Quasi-Two-Dimensional FePS3 and MnPS3 Antiferromagnetic 2039 Semiconductors. Solvent- and Catalyst-Free One-Pot Green Bound-Type Fused Bis-Heterocycles Synthesis via GroebkeBlackburnBienayme Reaction/SNAr/Ring-Chain Azido-Tautomerization Strategy. 2037 Adhesion of Epoxy Resin with Hexagonal Boron Nitride and Graphite. 2036 Enhanced Selective H2S Oxidation Performance on Mo2CModified qC3N4. Synthesis of NiCo Alloy Nanoparticle-Decorated B,N-Doped Carbon Nanosheet Networks via a 2035 Self-Template Strategy for Bifunctional Oxygen-Involving Reactions. Aluminum-Induced Interfacial Strengthening in Calcium Silicate Hydrates: Structure, Bonding, and 2034 Mechanical Properties. Formation of the End-on Bound Lanthanide Dinitrogen Complexes [(R2N)3LnNNLn(NR2)3]2 from 2033 Divalent [(R2N)3Ln]1 Salts (R = SiMe3). Zn-Promoted CH Reductive Elimination and H2 Activation via a Dual Unsaturated Heterobimetallic 2032 RuZn Intermediate. Driving Forces for Covalent Assembly of Porphyrins by Selective CH Bond Activation and Intermolecular Coupling on a Copper Surface. 2030 Microscopic Mechanism of Chiral Induction in a MetalOrganic Framework. 2029 Clocking Surface Reaction by In-Plane Product Rotation. Development of Enantiospecific Coupling of Secondary and Tertiary Boronic Esters with Aromatic 2028 Compounds. Substituent Directed Phototransformations of BN-Heterocycles: Elimination vs Isomerization via 2027 Selective BC Bond Cleavage. Bambusuril as a One-Electron Donor for Photoinduced Electron Transfer to Methyl Viologen in 2026 Mixed Crystals.

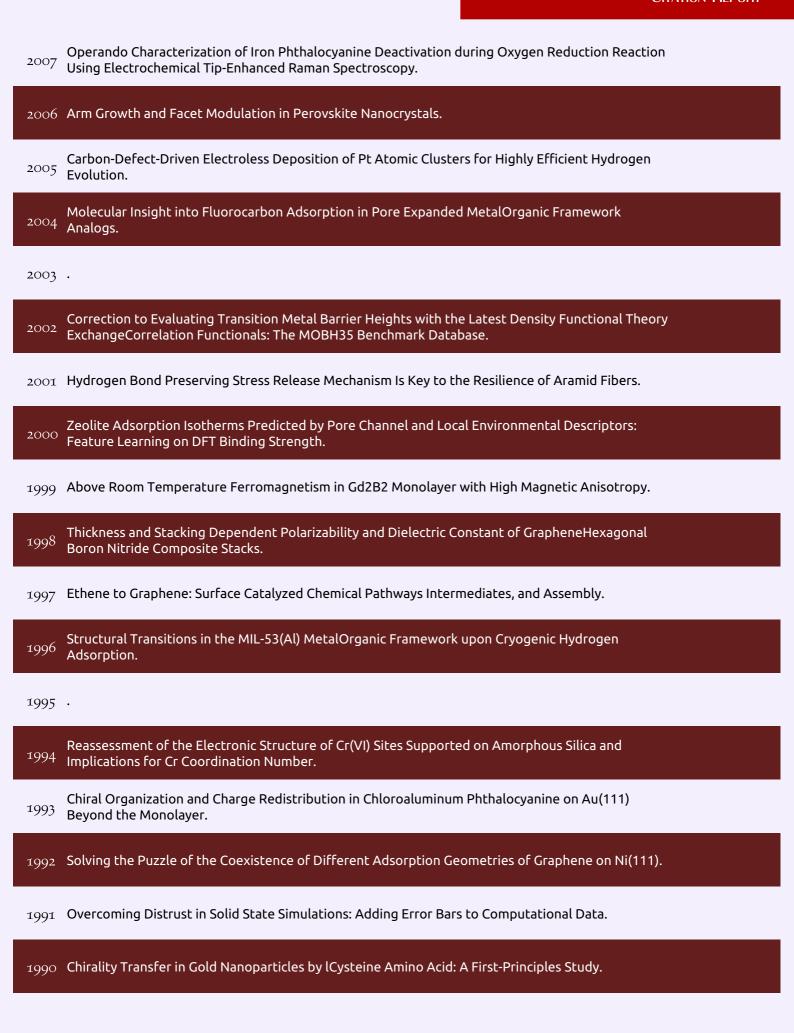
- 2025 Sodide and Organic Halides Effect Covalent Functionalization of Single-Layer and Bilayer Graphene. 2024 Direct and Delayed Dynamics in Electron-Induced Surface Reaction. Identifying the Recognition Site for Selective Trapping of 99TcO4 in a Hydrolytically Stable and 2023 Radiation Resistant Cationic MetalOrganic Framework. Catalytic Cyclopropanation by Myoglobin Reconstituted with Iron Porphycene: Acceleration of 2022 Catalysis due to Rapid Formation of the Carbene Species. 2021 Enacting Two-Electron Transfer from a Double-Triplet State of Intramolecular Singlet Fission. 2020 Single-Crystal Electrochemistry Reveals Why Metal Nanowires Grow. 2019 Effect of Structure on the SpinSpin Interactions of Tethered Dicyanomethyl Diradicals. 2018 . 2017 Controlling Proton-Coupled Electron Transfer in Bioinspired Artificial Photosynthetic Relays. Why and How Carbon Dioxide Conversion to Methanol Happens on Functionalized Semiconductor 2016 Photoelectrodes. Nucleophilicity and Electrophilicity Parameters for Predicting Absolute Rate Constants of Highly 2015 Asynchronous 1,3-Dipolar Cycloadditions of Aryldiazomethanes. 2014 Origin of the Immiscibility of Alkanes and Perfluoroalkanes. Room Temperature Iron-Catalyzed Transfer Hydrogenation and Regioselective Deuteration of 2013 CarbonCarbon Double Bonds. Proton Mobility, Intrinsic Acid Strength, and Acid Site Location in Zeolites Revealed by Varying Temperature Infrared Spectroscopy and Density Functional Theory Studies. Cyclometalated IridiumPhanePhos Complexes Are Active Catalysts in Enantioselective 2011 AlleneFluoral Reductive Coupling and Related Alcohol-Mediated Carbonyl Additions That Form Acyclic Quaternary Carbon Stereocenters.
- 2008 Imprinted Apportionment of Functional Groups in Multivariate MetalOrganic Frameworks.

2010 Bonding in 2D DonorAcceptor Heterostructures.

[Th(OC6H2tBu22,6-Me-4)4]1.

2009

Isolation of a Square-Planar Th(III) Complex: Synthesis and Structure of



1974

1973

Blocks.

Copper.

Nanoparticles.

Etching and Exfoliation Properties of Cr2AlC into Cr2CO2 and the Electrocatalytic Performances of 1989 2D Cr2CO2 MXene. Intrinsically Synergistic Active Centers Coupled with Surface Metal Doping To Facilitate Alkaline 1988 Hydrogen Evolution Reaction. MoleculeMetal Bond of Alternant versus Nonalternant Aromatic Systems on Coinage Metal Surfaces: Naphthalene versus Azulene on Ag(111) and Cu(111). 1986 Dynamics of RS-(Au-SR)x Staple Motifs on Metal Surfaces: From Nanoclusters to 2D Surfaces. Quantum Nature in the Interaction of Molecular Hydrogen with Porous Materials: Implications for 1985 Practical Hydrogen Storage. Room-Temperature Electrodeposition of Aluminum via Manipulating Coordination Structure in AlCl3 Solutions. Large-Scale Quantum-Mechanical Molecular Dynamics Simulations Using Density-Functional 1983 Tight-Binding Combined with the Fragment Molecular Orbital Method. Three Redox States of a Diradical AcceptorDonorAcceptor Triad: Gating the Magnetic Coupling and 1982 the Electron Delocalization. 1981 Spin Crossover in the {Fe(pz)[Pt(CN)4]} MetalOrganic Framework upon Pyrazine Adsorption. 1980 Prediction of Green Phosphorus with Tunable Direct Band Gap and High Mobility. Origin of the Substitution Mechanism for the Binding of Organic Ligands on the Surface of CsPbBr3 1979 Perovskite Nanocubes. 1978 Direct Prediction of Calcite Surface Wettability with First-Principles Quantum Simulation. Non-Transition-Metal Catalytic System for N2 Reduction to NH3: ADensity Functional Theory Study of Al-Doped Graphene. Molecular Electrostatic Potential: A New Tool to Predict the Lithiation Process of Organic Battery 1976 Materials. Charge Environment and Hydrogen Bond Dynamics in Binary Ionic Liquid Mixtures: A Computational Study.

Self-Assembly of Nanocubic Molecular Capsules via Solvent-Guided Formation of Rectangular

Experimental and Theoretical Study on the Nature of Adsorbed Oxygen Species on Shaped Ceria

Origin of the Selective Electroreduction of Carbon Dioxide to Formate by Chalcogen Modified

1971 Flat AgTe Honeycomb Monolayer on Ag(111). Dirac Electron Behavior for Spin-Up Electrons in Strongly Interacting Graphene on Ferromagnetic Mn5Ge3. Anisotropic Synthesis of Armchair Graphene Nanoribbon Arrays from Sub5 nm Seeds at Variable Pitches on Germanium. Real-Time Observing Ultrafast Carrier and Phonon Dynamics in Colloidal Tin Chalcogenide van der 1968 Waals Nanosheets. 1967 Dual-Facet Mechanism in Copper Nanocubes for Electrochemical CO2 Reduction into Ethylene. 1966 Electrically Tunable van der Waals Interaction in GrapheneMolecule Complex. Quantum Coherence Facilitates Efficient Charge Separation at a MoS2/MoSe2 van der Waals 1965 Junction. Wafer-Scale and Wrinkle-Free Epitaxial Growth of Single-Orientated Multilayer Hexagonal Boron 1964 Nitride on Sapphire. 1963 On the Mechanism of Hydrophilicity of Graphene. 1962 Large-Gap Quantum Spin Hall State in MXenes: dBand Topological Order in a Triangular Lattice. Ternary FexCo1xP Nanowire Array as a Robust Hydrogen Evolution Reaction Electrocatalyst with 1961 Pt-like Activity: Experimental and Theoretical Insight. Weak DonorAcceptor Interaction and Interface Polarization Define Photoexcitation Dynamics in 1960 the MoS2/TiO2 Composite: Time-Domain Ab Initio Simulation. Chemical Disorder in Topological Insulators: A Route to Magnetism Tolerant Topological Surface 1959 States. Environmental Screening Effects in 2D Materials: Renormalization of the Bandgap, Electronic Structure, and Optical Spectra of Few-Layer Black Phosphorus. Ferromagnetic and Antiferromagnetic Coupling of Spin Molecular Interfaces with High Thermal 1957 Stability. 1956 Size-Selective Carbon Clusters as Obstacles to Graphene Growth on a Metal. 1955 How the Complementarity at Vicinal Steps Enables Growth of 2D Monocrystals. 1954 Gap Opening in Twisted Double Bilayer Graphene by Crystal Fields.

Transition Metal Complexes of a Half-Parent Phosphasilene Adduct Representing 1953 SilvlenePhosphinideneMetal Complexes. 1952 Dinuclear NHC Gold(I) Allenyl and Propargyl Complexes: An Experimental and Theoretical Study. 1951 Azaindenocorannulenes: Synthesis, Properties, and Chirality. From Planar Macrocycle to Cylindrical Molecule: Synthesis and Properties of a Phenanthrene-Based 1950 Coronal Nanohoop as a Segment of [6,6]Carbon Nanotube. Synthesis of Synergistic Nitrogen-Doped NiMoO4/Ni3N Heterostructure for Implementation of an Efficient Alkaline Electrocatalytic Hydrogen Evolution Reaction. Development of Hybrid Pseudohalide Tin Perovskites for Highly Stable Carbon-Electrode Solar 1948 Cells. Promoting Effects of Au Submonolayer Shells on Structure-Designed CuPd/Ir Nanospheres: Greatly 1947 Enhanced Activity and Durability for Alkaline Ethanol Electro-Oxidation. 1946 Low Li+ Insertion Barrier Carbon for High Energy Efficient Lithium-Ion Capacitor. Synthesis of pH-Responsive Biodegradable Mesoporous SilicaCalcium Phosphate Hybrid 1945 Nanoparticles as a High Potential Drug Carrier. Porous Zr6L3 Metallocage with Synergetic Binding Centers for CO2. 1944 Toward Tunable Electroluminescent Devices by Correlating Function and Submolecular Structure in 1943 3D Crystals, 2D-Confined Monolayers, and Dimers. Welcoming Gallium- and Indium-Fumarate MOFs to the Family: Synthesis, Comprehensive 1942 Characterization, Observation of Porous Hydrophobicity, and CO2 Dynamics. Insight into the Nature of Iron Sulfide Surfaces During the Electrochemical Hydrogen Evolution and 1941 CO2 Reduction Reactions. Photocatalytic Hydrogen Generation from a Visible-Light-Responsive MetalOrganic Framework System: Stability versus Activity of Molybdenum Sulfide Cocatalysts. Oxide versus Nonoxide Cathode Materials for Aqueous Zn Batteries: An Insight into the Charge 1939 Storage Mechanism and Consequences Thereof.

Synergetic Effect of Substitutional Dopants and Sulfur Vacancy in Modulating the Ferromagnetism

MechanismProperty Correlation in Coordination Polymer Crystals toward Design of a Superior

1936 In Situ Tuning of Defects and Phase Transition in Titanium Dioxide by Lithiothermic Reduction.

of MoS2 Nanosheets.

Sorbent.

1937

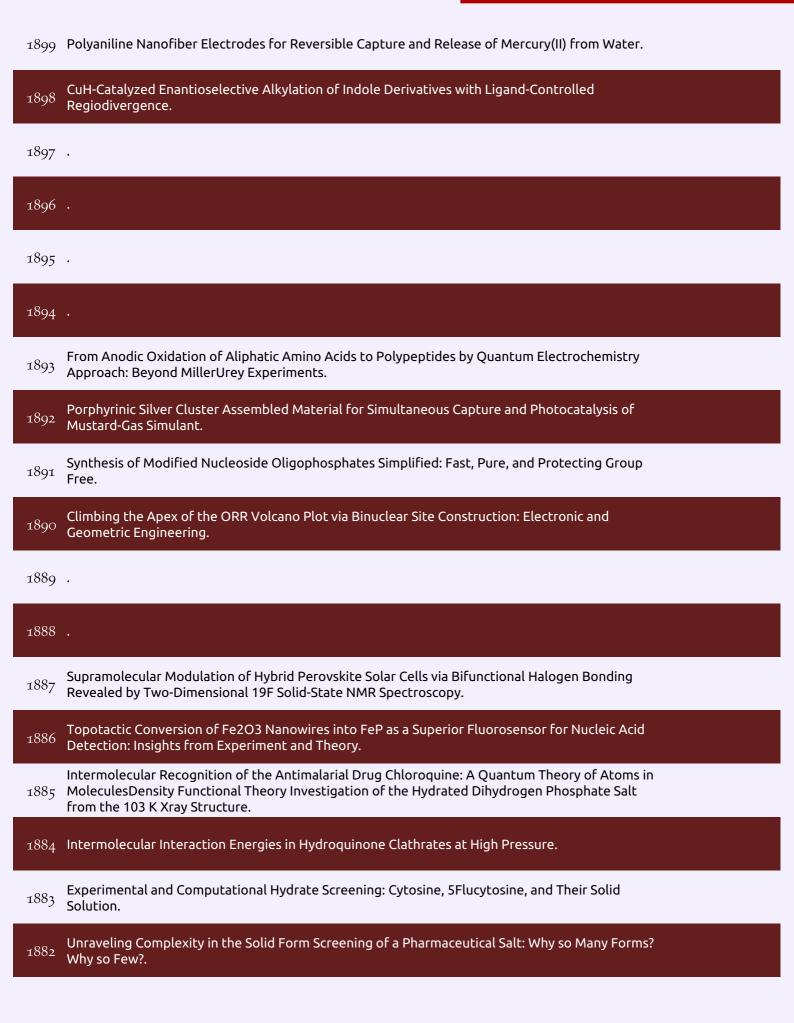
	Near Bandgap Excitation Inhibits the Interfacial Electron Transfer of Semiconductor/Cocatalyst.
1934	Densely Isolated FeN4 Sites for Peroxidase Mimicking.
1933	Hydrophosphination of Styrene and Polymerization of Vinylpyridine: A Computational Investigation of Calcium-Catalyzed Reactions and the Role of Fluxional Noncovalent Interactions.
1932	Revealing the Role of sp2@sp3 Structure of Nanodiamond in Direct Dehydrogenation: Insight from DFT study.
1931	Dynamic Kinetic Resolution of NProtected Amino Acid Esters via Phase-Transfer Catalytic Base Hydrolysis.
1930	Chromate Effect on Iodate Incorporation into Calcite.
1929	Hydrogen Evolution Reaction Activity of GrapheneMoS2 van der Waals Heterostructures.
1928	Controlling SolidLiquid Conversion Reactions for a Highly Reversible Aqueous Zinclodine Battery.
1927	Pyridinic-N-Dominated Doped Defective Graphene as a Superior Oxygen Electrocatalyst for Ultrahigh-Energy-Density ZnAir Batteries.
1926	Above 600 mV Open-Circuit Voltage BiI3 Solar Cells.
1926 1925	Above 600 mV Open-Circuit Voltage BiI3 Solar Cells. Heteroatom-Doped Transition Metal Electrocatalysts for Hydrogen Evolution Reaction.
1925	Heteroatom-Doped Transition Metal Electrocatalysts for Hydrogen Evolution Reaction. Scalable and Economic Synthesis of High-Performance Na3V2(PO4)2F3 by a
1925 1924	Heteroatom-Doped Transition Metal Electrocatalysts for Hydrogen Evolution Reaction. Scalable and Economic Synthesis of High-Performance Na3V2(PO4)2F3 by a SolvothermalBall-Milling Method. Bifunctional NCoSe2/3D-MXene as Highly Efficient and Durable Cathode for Rechargeable ZnAir
1925 1924 1923	Heteroatom-Doped Transition Metal Electrocatalysts for Hydrogen Evolution Reaction. Scalable and Economic Synthesis of High-Performance Na3V2(PO4)2F3 by a SolvothermalBall-Milling Method. Bifunctional NCoSe2/3D-MXene as Highly Efficient and Durable Cathode for Rechargeable ZnAir Battery.
1925 1924 1923 1922	Heteroatom-Doped Transition Metal Electrocatalysts for Hydrogen Evolution Reaction. Scalable and Economic Synthesis of High-Performance Na3V2(PO4)2F3 by a SolvothermalBall-Milling Method. Bifunctional NCoSe2/3D-MXene as Highly Efficient and Durable Cathode for Rechargeable ZnAir Battery. Cooperative Chemisorption-Induced Physisorption of CO2 Molecules by MetalOrganic Chains.
1925 1924 1923 1922	Heteroatom-Doped Transition Metal Electrocatalysts for Hydrogen Evolution Reaction. Scalable and Economic Synthesis of High-Performance Na3V2(PO4)2F3 by a SolvothermalBall-Milling Method. Bifunctional NCoSe2/3D-MXene as Highly Efficient and Durable Cathode for Rechargeable ZnAir Battery. Cooperative Chemisorption-Induced Physisorption of CO2 Molecules by MetalOrganic Chains. Characteristic Contrast in fmin Maps of Organic Molecules Using Atomic Force Microscopy.

1900

Framework.

Designing Optoelectronic Properties by On-Surface Synthesis: Formation and Electronic Structure 1917 of an IronTerpyridine Macromolecular Complex. Photochemical Creation of Covalent Organic 2D Monolayer Objects in Defined Shapes via a 1916 Lithographic 2D Polymerization. 1915 Point Defects and Localized Excitons in 2D WSe2. 1914 Temperature Driven Phase Transition at the Antimonene/Bi2Se3 van der Waals Heterostructure. Boron-carbon-nitride sheet as a novel surface for biological applications: insights from density 1913 functional theory. Fluorine-Terminated Diamond Surfaces as Dense Dipole Lattices: The Electrostatic Origin of Polar Hydrophobicity. Synthesis Structure, and Reactivity of the Sterically Crowded Th3+ Complex (C5Me5)3Th Including 1911 Formation of the Thorium Carbonyl, [(C5Me5)3Th(CO)][BPh4]. Parametrization of Non-covalent Interactions for Transition State Interrogation Applied to 1910 Asymmetric Catalysis. 1909 . Mechanistic Investigations of the Pd(0)-Catalyzed Enantioselective 1,1-Diarylation of Benzyl 1908 Acrylates. Phase Segregation in Cs, Rb- and KDoped Mixed-Cation (MA)x(FA)1xPbI3 Hybrid Perovskites from 1907 Solid-State NMR. 1906 End-On Bridging Dinitrogen Complex of Scandium. Enforced Tubular Assembly of Electronically Different Hexakis(mPhenylene Ethynylene) Macrocycles: Persistent Columnar Stacking Driven by Multiple Hydrogen-Bonding Interactions. Catalytic Silylation of N2 and Synthesis of NH3 and N2H4 by Net Hydrogen Atom Transfer 1904 Reactions Using a Chromium P4 Macrocycle. Formation of Stable Mixed GuanidiniumMethylammonium Phases with Exceptionally Long Carrier 1903 Lifetimes for High-Efficiency Lead Iodide-Based Perovskite Photovoltaics. 1902 Borylene Insertion into Cage BH Bond: A Route to Electron-Precise BB Single Bond. Phase Segregation in Potassium-Doped Lead Halide Perovskites from 39K Solid-State NMR at 21.1 1901 T.

Layer-Stacking-Driven Fluorescence in a Two-Dimensional Imine-Linked Covalent Organic



Two Self-Interpenetrating Copper(II)-Paddlewheel MetalOrganic Frameworks Constructed from 1881 Bifunctional TriazolateCarboxylate Linkers. Reversible, Two-Step Single-Crystal to Single-Crystal Phase Transitions between Desloratadine 1880 Forms I, II, and III. 1879 Identification of High-CO2Capacity Cationic Zeolites by Accurate Computational Screening. Eventual Chemical Transformation of Metals and Chalcogens into Metal Chalcogenide Nanoplates 1878 through a Surface Nucleation-Detachment-Reorganization Mechanism. 1877 Role of Graphene in Water-Assisted Oxidation of Copper in Relation to Dry Transfer of Graphene. 1876 Understanding the Effects of Cd and Ag Doping in Cu2ZnSnS4 Solar Cells. 1875 Shining Light on Carbon Nitrides: Leveraging Temperature To Understand Optical Gap Variations. Theoretical Prediction and Experimental Evaluation of Topological Landscape and Thermodynamic Stability of a Fluorinated Zeolitic Imidazolate Framework. Ozonation of Para-Substituted Phenolic Compounds Yields pBenzoquinones, Other Cyclic 1873 ,-Unsaturated Ketones, and Substituted Catechols. Electroactive Modified Carbon Nanotube Filter for Simultaneous Detoxification and Sequestration of Sb(III). Computational Estimate of the Photophysical Capabilities of Four Series of Organometallic Iron(II) 1871 Complexes. Unusual Tri, Hexa, and Nonanuclear Cu(II) Cage Methylsilsesquioxanes: Synthesis, Structures, and 1870 Catalytic Activity in Oxidations with Peroxides. 1869 Synthesis and Electronic Structure Diversity of Pyridine(diimine)iron Tetrazene Complexes. 1868 Perturbation Approach for Computing Infrared Spectra of the Local Mode of Probe Molecules. Formulation of Small Test Sets Using Large Test Sets for Efficient Assessment of Quantum 1867 Chemistry Methods. Density functional theory including dispersion corrections for intermolecular interactions in a large 1866 395 benchmark set of biologically relevant molecules. 2006, 8, 5287-93 1865 The use of atomic intrinsic polarizabilities in the evaluation of the dispersion energy. 2007, 127, 224105 30 1864 Calculations of the Stabilization Energies of the Building Blocks of Biomacromolecules. 2007,

1863	Resolution of identity density functional theory augmented with an empirical dispersion term (RI-DFT-D): a promising tool for studying isolated small peptides. 2007 , 111, 1146-54	66
1862	Semi-empirical molecular orbital methods including dispersion corrections for the accurate prediction of the full range of intermolecular interactions in biomolecules. 2007 , 9, 2362-70	117
1861	Double-hybrid density functional theory for excited electronic states of molecules. 2007 , 127, 154116	339
1860	Density functional theory with dispersion corrections for supramolecular structures, aggregates, and complexes of (bio)organic molecules. 2007 , 5, 741-58	636
1859	Non-covalent interactions in biomacromolecules. 2007 , 9, 5291-303	339
1858	Noncovalent Interactions between Graphene Sheets and in Multishell (Hyper)Fullerenes. 2007 , 111, 11199-11	l 2 ହି୕ଅ3
1857	On the properties of microsolvated molecules in the ground (S0) and excited (S1) states: the anisole-ammonia 1:1 complex. 2007 , 127, 144303	35
1856	The hydrolysis process of the anticancer complex [ImH][trans-RuCl4(Im)2]: a theoretical study. 2007 , 3507-15	19
1855	Density Functional and Semiempirical Molecular Orbital Methods Including Dispersion Corrections for the Accurate Description of Noncovalent Interactions Involving Sulfur-Containing Molecules. 2007 , 3, 1656-64	70
1854	Pseudohelical and helical primary structures of 1,2-spiroannelated four- and five-membered rings: syntheses and chiroptical properties. 2007 , 72, 9264-77	16
1853	A unified density-functional treatment of dynamical, nondynamical, and dispersion correlations. 2007 , 127, 124108	181
1852	Evaluation of the adsorption free energy of light guest molecules in nanoporous host structures. 2007 , 9, 2697-705	11
1851	Geometry Optimization of a Ru(IV) Allyl Dicationic Complex: A DFT Failure?. 2007, 3, 665-70	15
1850	Aluminosilicate surfaces as promoters for peptide bond formation: an assessment of Bernal's hypothesis by ab initio methods. 2007 , 129, 8333-44	64
1849	C-H bond activation by hyperconjugation with Al-C bonds and by chelating coordination of the hydride ion. 2007 , 129, 11259-64	29
1848	Ab Initio Modeling of Methanol Interaction with Single-Walled Carbon Nanotubes. 2007 , 111, 18917-18926	29
1847	Isotopomeric conformational changes in the anisole-water complex: new insights from HR-UV spectroscopy and theoretical studies. 2007 , 111, 12363-71	29
1846	On the Convergence of the Physicochemical Properties of [n]Helicenes. 2007 , 111, 14948-14955	65

(2008-2007)

1845	Density-functional, density-functional tight-binding, and wave function calculations on biomolecular systems. 2007 , 111, 5642-7	26
1844	How to compute isomerization energies of organic molecules with quantum chemical methods. 2007 , 72, 2118-26	210
1843	Density Functionals for Noncovalent Interaction Energies of Biological Importance. 2007 , 3, 289-300	528
1842	Double-hybrid density functionals with long-range dispersion corrections: higher accuracy and extended applicability. 2007 , 9, 3397-406	890
1841	Rapid intramolecular heterolytic dihydrogen activation by a four-membered heterocyclic phosphane-borane adduct. 2007 , 5072-4	516
1840	Theoretical Study of Binding Site Preference in [2]Rotaxanes. 2007 , 3, 2221-33	12
1839	London dispersion forces by range-separated hybrid density functional with second order perturbational corrections: the case of rare gas complexes. 2007 , 126, 044103	71
1838	A computational study of the adsorption of small Ag and Au nanoclusters on graphite. 2007 , 111, 12317-26	45
1837	The concept of protobranching and its many paradigm shifting implications for energy evaluations. 2007 , 13, 7731-44	173
1836	Homolytic substitution at phosphorus for the synthesis of alkyl and aryl phosphanes. 2007 , 46, 6533-6	56
1835	Homolytische Substitution am Phosphor zur Synthese von Alkyl- und Arylphosphanen. 2007 , 119, 6653-6656	17
1834	A comparative quantum chemical study of the ruthenium catalyzed olefin metathesis. <i>Journal of Computational Chemistry</i> , 2007 , 28, 2275-85	58
1833	Long-range corrected density functional study on weakly bound systems: balanced descriptions of various types of molecular interactions. 2007 , 126, 234114	133
1832	The M06 suite of density functionals for main group thermochemistry, thermochemical kinetics, noncovalent interactions, excited states, and transition elements: two new functionals and systematic testing of four M06-class functionals and 12 other functionals. 2008 , 120, 215-241	19079
1831	On the nature of the interaction between H2 and metal-organic frameworks. 2008 , 120, 543-550	35
1830	Why are dimethyl sulfoxide and dimethyl sulfone such good solvents?. 2008 , 14, 689-97	136
1829	Blue shifts vs red shifts in sigma-hole bonding. 2008 , 14, 699-704	221
1828	MP2, DFT-D, and PCM study of the HMBIICNE complex: Thermodynamics, electric properties, and solvent effects. 2008 , 108, 1533-1545	10

1827	Oxidative conversion of C1tt3 alkanes by vanadium oxide catalysts. DFT results and their accuracy. 2008 , 108, 2223-2229	58
1826	Simultaneous Ehole and hydrogen bonding by sulfur- and selenium-containing heterocycles. 2008 , 108, 2770-2781	157
1825	Resonating broken symmetry CI approach for ion-radical systems: Comparison with UHF, hybrid-DFT, and CASSCF-DFT. 2008 , 108, 2966-2977	8
1824	Solution structure of a functional biomimetic and mechanistic implications for nickel superoxide dismutases. 2008 , 9, 2135-46	36
1823	Potential-energy and free-energy surfaces of glycyl-phenylalanyl-alanine (GFA) tripeptide: experiment and theory. 2008 , 14, 4886-98	44
1822	Characterization of three members of the electron-transfer series [Fe(pda)2]n (n=2-, 1-, 0) by spectroscopy and density functional theoretical calculations [pda=redox non-innocent derivatives of N,N'-bis(pentafluorophenyl)-o-phenylenediamide(2-, 1, 0)]. 2008 , 14, 7608-22	40
1821	H2 adsorption in metal-organic frameworks: dispersion or electrostatic interactions?. 2008 , 14, 6597-600	63
1820	PP bond cleavage of tetraphenyltetraphosphane-1,4-diide facilitated by nickel(0). 2008 , 14, 8980-5	16
1819	Toluene dioxygenase-catalyzed synthesis of cis-dihydrodiol metabolites from 2-substituted naphthalene substrates: assignments of absolute configurations and conformations from circular dichroism and optical rotation measurements. 2008 , 14, 11500-11	21
1818	Calculation of conformational energies and optical rotation of the most simple chiral alkane. 2008 , 20, 1009-15	33
1817	Highly accurate CCSD(T) and DFT-SAPT stabilization energies of H-bonded and stacked structures of the uracil dimer. 2008 , 9, 1636-44	108
1816	IRMPD spectroscopy of a protonated, phosphorylated dipeptide. 2008 , 9, 2564-73	33
1815	Quantum chemical investigation of exciton coupling: super-molecular calculations of a merocyanine dimer aggregate. 2008 , 9, 2467-70	30
1814	Evaluation of the intramolecular basis set superposition error in the calculations of larger molecules: [n]helicenes and Phe-Gly-Phe tripeptide. <i>Journal of Computational Chemistry</i> , 2008 , 29, 861-7 θ .5	62
1813	Application of semiempirical long-range dispersion corrections to periodic systems in density functional theory. <i>Journal of Computational Chemistry</i> , 2008 , 29, 2088-97	247
1812	Different Reactivity Patterns in the Reactions of the Homologous Trimethylelement Compounds EMe3 (E = Al, Ga, In) with Methylhydrazine. 2008 , 2008, 543-551	24
1811	Theoretical Description of Substituent Effects in Electrophilic Aromatic Substitution Reactions. 2008 , 2008, 5928-5935	8
1810	Boron-Based Diastereomerism and Enantiomerism in Imine Complexes (Determination of the Absolute Configuration at Boron by CD Spectroscopy. 2008 , 2008, 5221-5225	19

(2010-2008)

1809	dihydropyridines. 2008 , 47, 779-82	95
1808	Do special noncovalent pi-pi stacking interactions really exist?. 2008 , 47, 3430-4	808
1807	Thiolkatalysierte stereoselektive Transferhydroaminierung von Olefinen mit N-aminierten Dihydropyridinen. 2008 , 120, 791-794	26
1806	Gibt es spezielle nicht-kovalente Æstapelwechselwirkungen wirklich?. 2008, 120, 3478-3483	122
1805	Testing the combination of Hartreeflock exchange and Wilsonllevy correlation for weakly bonded extended systems. 2008 , 451, 287-292	15
1804	Implementation and validation of DFT-D for molecular vibrations and dynamics: The benzene dimer as a case study. 2008 , 452, 333-339	46
1803	Theoretical investigation of equilibrium and transition state structures, binding energies and barrier heights of water-encapsulated open-cage [59]fullerenone complexes. 2008 , 465, 48-52	11
1802	A comparative study of single reference correlation methods of the coupled-pair type. 2008 , 343, 217-230	90
1801	Theoretical energetic and vibrational analysis of amide-templated pseudorotaxanes. 2008, 343, 186-199	9
1800	Weak intermolecular bonding in N,N?-dimethylethyleneurea dimers and N,N?-dimethylethyleneurealwater systems: The role of the dispersion effects in intermolecular interaction. 2008 , 354, 202-210	12
1799	Time-dependent density functional study of excimers and exciplexes of organic molecules. 2008 , 343, 362-371	67
1798	The role of dispersion correction to DFT for modelling weakly bound molecular complexes in the ground and excited electronic states. 2008 , 346, 247-256	72
1797	Density functionals with broad applicability in chemistry. 2008 , 41, 157-67	5345
1796	Intermolecular potential calculations for polynuclear aromatic hydrocarbon clusters. 2008, 112, 6249-56	92
1795	Geometries of Third-Row Transition-Metal Complexes from Density-Functional Theory. 2008 , 4, 1449-59	363
1794	Configurationally labile lithiated O-benzyl carbamates: application in asymmetric synthesis and quantum chemical investigations on the equilibrium of diastereomers. 2008 , 3, 78-87	28
1793	Structural Features of [(CpPPh2AuCl)2ZrCl2]: exploring the limits of aurophilic interactions. 2008 , 3, 753-8	9
1792	Thermodynamic stability versus kinetic lability of ZnS4 core. 2010 , 5, 1445-54	4

1791	Long-range corrected hybrid density functionals with damped atom-atom dispersion corrections. 2008 , 10, 6615-20	7709
1790	Performance of B3LYP Density Functional Methods for a Large Set of Organic Molecules. 2008 , 4, 297-306	601
1789	Implementation and Performance of DFT-D with Respect to Basis Set and Functional for Study of Dispersion Interactions in Nanoscale Aromatic Hydrocarbons. 2008 , 4, 2030-48	149
1788	OMx-D: semiempirical methods with orthogonalization and dispersion corrections. Implementation and biochemical application. 2008 , 10, 2159-66	87
1787	Highly accurate first-principles benchmark data sets for the parametrization and validation of density functional and other approximate methods. Derivation of a robust, generally applicable, double-hybrid functional for thermochemistry and thermochemical kinetics. 2008 , 112, 12868-86	578
1786	Estimate of Benzenellriphenylene and Triphenylenellriphenylene Interactions: A Topic Relevant to Columnar Discotic Liquid Crystals. 2008 , 112, 9501-9509	11
1785	Nature and magnitude of aromatic stacking of nucleic acid bases. 2008 , 10, 2595-610	300
1784	The interaction of carbohydrates and amino acids with aromatic systems studied by density functional and semi-empirical molecular orbital calculations with dispersion corrections. 2008 , 10, 2767-74	44
1783	B3LYP augmented with an empirical dispersion term (B3LYP-D*) as applied to molecular crystals. 2008 , 10, 405-410	642
1782	Computational characterization and modeling of buckyball tweezers: density functional study of concave-convex pipi interactions. 2008 , 10, 2813-8	179
1781	Structures and interaction energies of stacked graphene-nucleobase complexes. 2008, 10, 2722-9	231
1780	Assessment of Density Functionals for Intramolecular Dispersion-Rich Interactions. 2008, 4, 1610-9	65
1779	Empirical corrections to density functional theory highlight the importance of nonbonded intramolecular interactions in alkanes. 2008 , 112, 11495-500	46
1778	Assessment of the Performance of the M05-2X and M06-2X Exchange-Correlation Functionals for Noncovalent Interactions in Biomolecules. 2008 , 4, 1996-2000	555
1777	IR and Computational Characterization of CO Adsorption on a Model Surface, the Phenylene Periodic Mesoporous Organosilca with Crystalline Walls. 2008 , 112, 19560-19567	18
1776	A Prototype for Graphene Material Simulation: Structures and Interaction Potentials of Coronene Dimers. 2008 , 112, 4061-4067	135
1775	Axially chiral beta,beta'-bisporphyrins: synthesis and configurational stability tuned by the central metals. 2008 , 130, 17812-5	85
1774	Investigation of the benzene-dimer potential energy surface: DFT/CCSD(T) correction scheme. 2008 , 128, 114102	160

(2008-2008)

1773	MP2. 2008 , 10, 3327-34	51
1772	Popular Kohn-Sham density functionals strongly overestimate many-body interactions in van der Waals systems. 2008 , 78,	74
1771	Interactions in large, polyaromatic hydrocarbon dimers: application of density functional theory with dispersion corrections. 2008 , 112, 10968-76	131
1770	Exploring the Limit of Accuracy of the Global Hybrid Meta Density Functional for Main-Group Thermochemistry, Kinetics, and Noncovalent Interactions. 2008 , 4, 1849-68	784
1769	Accurate calculation of transport properties for organic molecular semiconductors with spin-component scaled MP2 and modern density functional theory methods. 2008 , 129, 024103	38
1768	Binding energy of adsorbates on a noble-metal surface: exchange and correlation effects. 2008 , 101, 266106	113
1767	New ruthenium(II) complexes with enantiomerically pure bis- and tris(pinene)-fused tridentate ligands. Synthesis, characterization and stereoisomeric analysis. 2008 , 47, 8016-24	15
1766	IR/UV spectra and quantum chemical calculations of Trp-Ser: stacking interactions between backbone and indole side-chain. 2008 , 10, 2844-51	33
1765	Validation of dispersion-corrected density functional theory approaches for ionic liquid systems. 2008 , 112, 8430-5	105
1764	The non-covalent functionalisation of carbon nanotubes studied by density functional and semi-empirical molecular orbital methods including dispersion corrections. 2008 , 10, 128-35	28
1763	Desorption electrospray ionization reactions between host crown ethers and the influenza neuraminidase inhibitor oseltamivir for the rapid screening of Tamiflu. 2008 , 133, 1513-22	36
1762	Physisorption and Chemisorption of Hydrocarbons in H-FAU Using QM-Pot(MP2//B3LYP) Calculations. 2008 , 112, 11796-11812	51
1761	Adsorption of aromatic hydrocarbons and ozone at environmental aqueous surfaces. 2008, 112, 4942-50	35
1760	On the importance of electron correlation effects for the intramolecular stacking geometry of a bis-thiophene derivative. 2008 , 112, 12469-74	22
1759	Multitechnique investigation of conformational features of small molecules: the case of methyl phenyl sulfoxide. 2008 , 112, 2095-101	7
1758	A quantum mechanical strategy to investigate the structure of liquids: the cases of acetonitrile, formamide, and their mixture. 2008 , 112, 6803-13	8
1757	Exploring the Stability of Golden Fullerenes. 2008, 112, 19311-19315	37
1756	Metahybrid density functional theory and correlated ab initio studies on microhydrated adenine-thymine base pairs. 2008 , 112, 9182-6	9

1755	Theoretical thermodynamics for large molecules: walking the thin line between accuracy and computational cost. 2008 , 41, 569-79	313
1754	Improved Description of Stereoelectronic Effects in Hydrocarbons Using Semilocal Density Functional Theory. 2008 , 4, 888-91	55
1753	Solvent smectic order parameters from solute nematic order parameters. 2008 , 129, 094509	9
1752	Quantum chemical studies of structures and binding in noncanonical RNA base pairs: the trans Watson-Crick:Watson-Crick family. 2008 , 25, 709-32	39
1751	Role of the van der Waals interactions on the bonding mechanism of pyridine on Cu(110) and Ag(110) surface: First-principles study. 2008 , 78,	51
1750	Adsorption and bonding mechanism of a N,N?-di(n-butyl)quinacridone monolayer studied by density functional theory including semiempirical dispersion corrections. 2008 , 78,	3
1749	Azobenzene at coinage metal surfaces: Role of dispersive van der Waals interactions. 2009, 80,	397
1748	Mechanism of alkane dehydrogenation catalyzed by acidic zeolites: Ab initio transition path sampling. 2009 , 131, 214508	50
1747	Complete basis set limit second-order Mler-Plesset calculations for the fcc lattices of neon, argon, krypton, and xenon. 2009 , 131, 244508	28
1746	Ab initio study of EMIM-BF4 crystal interaction with a Li (100) surface as a model for ionic liquid/Li interfaces in Li-ion batteries. 2009 , 131, 244705	31
1745	Efficient computation of the dispersion interaction with density-functional theory. 2009, 79,	53
1744	Assessment of double-hybrid energy functionals for pi-conjugated systems. 2009 , 131, 084108	70
1743	Fluorescence quenching in an organic donor-acceptor dyad: a first principles study. 2009 , 131, 034310	14
1742	Chemical versus van der Waals Interaction: the role of the heteroatom in the flat absorption of aromatic molecules C6H6, C5NH5, and C4N2H4 on the Cu(110) surface. 2009 , 102, 136809	130
1741	Density functional method including weak interactions: Dispersion coefficients based on the local response approximation. 2009 , 131, 224104	188
1740	Long-range-corrected hybrid density functionals including random phase approximation correlation: application to noncovalent interactions. 2009 , 131, 034110	78
1739	Oscillations in meta-generalized-gradient approximation potential energy surfaces for dispersion-bound complexes. 2009 , 131, 034111	146
1738	Dispersion-corrected Mller-Plesset second-order perturbation theory. 2009 , 131, 094106	172

1737	Surface ordering of molecular structures by dispersion forces. 2009 , 80,	8
1736	A new all-round density functional based on spin states and S(N)2 barriers. 2009 , 131, 094103	104
1735	Theoretical study of imidazoleNO complexes. 2009, 113, 14595-605	2
1734	The gas phase anisole dimer: a combined high-resolution spectroscopy and computational study of a stacked molecular system. 2009 , 113, 14343-51	51
1733	Study of the interaction between water and hydrogen sulfide with polycyclic aromatic hydrocarbons. 2009 , 130, 234307	26
1732	Approximate Density Functionals: Which Should I Choose?. 2009 ,	14
1731	Solvent-resistant structures of base-free lithium and potassium allyl complexes, $M[(SiMe3)nC3H5-n]$ (M = Li,n= 3; M = K,n= 2). 2009 , 8, 225-235	14
1730	The electronic structure of the primary electron donor of reaction centers of purple bacteria at atomic resolution as observed by photo-CIDNP 13C NMR. 2009 , 106, 22281-6	68
1729	Imaging hindered rotations of alkoxy species on TiO(2)(110). 2009, 131, 17926-32	37
1728	Photoinduced processes in hydrogen bonded system: photodissociation of imidazole clusters. 2009 , 113, 14583-90	20
1727	An efficient algorithm for the density-functional theory treatment of dispersion interactions. 2009 , 130, 124105	96
1726	The role of polymorphism in organic thin films: oligoacenes investigated from first principles. 2009 , 11, 125010	101
1725	Formation versus hydrolysis of the peptide bond from a quantum-mechanical viewpoint: The role of mineral surfaces and implications for the origin of life. 2009 , 10, 746-60	21
1724	Multimode simulation of dimer absorption spectra from first principles calculations: application to the 3,4,9,10-perylenetetracarboxylic diimide dimer. 2009 , 131, 154302	46
1723	Derivation of the dispersion energy as an explicit density- and exchange-hole functional. 2009 , 130, 084104	33
1722	Five-membered zirconacycloallenoids: synthesis and characterization of members of a unique class of internally metal-stabilized bent allenoid compounds. 2009 , 131, 1996-2007	77
1721	Aromatic adsorption on metals via first-principles density functional theory. 2009 , 465, 2949-2976	119
1720	Structure and Stability of Hydrogen Clathrates of Ammonia Borane. 2009 , 1216, 1	1

1719	An organometallic route to long helicenes. 2009 , 106, 13169-74	1	10
1718	A Ditopic Ion-Pair Receptor Based on Stacked Nucleobase Quartets. 2009 , 121, 3335-3337	2	-3
1717	Dihydrogen bonding: donor-acceptor bonding (AHHX) versus the H2 molecule (A-H2-X). 2009 , 15, 5814-2	2 3:	1
1716	Tetraaryl tetradecahydroporphyrazins: novel porphyrin derivatives featuring a cyclic benzene-ring tetramer. 2009 , 15, 10457-63	6	;
1715	Enantioselective nitroso-Diels-Alder reaction and its application for the synthesis of (-)-peracetylated conduramine A-1. 2009 , 15, 9078-84	8	9
1714	The stereospecific ligand exchange at a pseudo-benzylic T-4 iridium centre in planar-chiral cycloiridium (eta(6)-arene)tricarbonylchromium complexes. 2009 , 15, 10830-42	1.	4
1713	Structural analyses of N-acetylated 4-(dimethylamino)pyridine (DMAP) salts. 2009 , 15, 8548-57	5	·8
1712	Structural tracking of the potassium-mediated magnesiation of anisole. 2009 , 15, 10702-6	3.	3
1711	Analysis of energy stabilization inside the hydrophobic core of rubredoxin. 2009, 10, 543-8	4	-
1710	Ab initio study of the interactions between CO(2) and N-containing organic heterocycles. 2009 , 10, 374-83	1	64
1710 1709	Ab initio study of the interactions between CO(2) and N-containing organic heterocycles. 2009 , 10, 374-83 DFT/CCSD(T) investigation of the interaction of molecular hydrogen with carbon nanostructures. 2009 , 10, 1868-73	3	ĺ
•	DFT/CCSD(T) investigation of the interaction of molecular hydrogen with carbon nanostructures.		8
1709	DFT/CCSD(T) investigation of the interaction of molecular hydrogen with carbon nanostructures. 2009, 10, 1868-73 Treatment of Terminal Alkynes RC?CH with Dialkylaluminum Hydrides: Hydroalumination versus	33	8
1709 1708	DFT/CCSD(T) investigation of the interaction of molecular hydrogen with carbon nanostructures. 2009, 10, 1868-73 Treatment of Terminal Alkynes RC?CH with Dialkylaluminum Hydrides: Hydroalumination versus Deprotonation. 2009, 2009, 3307-3316 Noncovalent interactions in supramolecular complexes: a study on corannulene and the double concave buckycatcher. Journal of Computational Chemistry, 2009, 30, 51-6 Miler-Plesset perturbation energies and distances for HeC(20) extrapolated to the complete basis	3.	3
1709 1708 1707	DFT/CCSD(T) investigation of the interaction of molecular hydrogen with carbon nanostructures. 2009, 10, 1868-73 Treatment of Terminal Alkynes RT?CH with Dialkylaluminum Hydrides: Hydroalumination versus Deprotonation. 2009, 2009, 3307-3316 Noncovalent interactions in supramolecular complexes: a study on corannulene and the double concave buckycatcher. Journal of Computational Chemistry, 2009, 30, 51-6 Mller-Plesset perturbation energies and distances for HeC(20) extrapolated to the complete basis	3.	3
1709 1708 1707	DFT/CCSD(T) investigation of the interaction of molecular hydrogen with carbon nanostructures. 2009, 10, 1868-73 Treatment of Terminal Alkynes Rt.?CH with Dialkylaluminum Hydrides: Hydroalumination versus Deprotonation. 2009, 2009, 3307-3316 Noncovalent interactions in supramolecular complexes: a study on corannulene and the double concave buckycatcher. Journal of Computational Chemistry, 2009, 30, 51-6 MIler-Plesset perturbation energies and distances for HeC(20) extrapolated to the complete basis set limit. Journal of Computational Chemistry, 2009, 30, 379-88 Role and effective treatment of dispersive forces in materials: Polyethylene and graphite crystals	3. 3. 6	8 3 5 49
1709 1708 1707 1706	DFT/CCSD(T) investigation of the interaction of molecular hydrogen with carbon nanostructures. 2009, 10, 1868-73 Treatment of Terminal Alkynes RCPCH with Dialkylaluminum Hydrides: Hydroalumination versus Deprotonation. 2009, 2009, 3307-3316 Noncovalent interactions in supramolecular complexes: a study on corannulene and the double concave buckycatcher. Journal of Computational Chemistry, 2009, 30, 51-6 Mller-Plesset perturbation energies and distances for HeC(20) extrapolated to the complete basis set limit. Journal of Computational Chemistry, 2009, 30, 379-88 Role and effective treatment of dispersive forces in materials: Polyethylene and graphite crystals as test cases. Journal of Computational Chemistry, 2009, 30, 934-9 Can the hybrid meta GGA and DFT-D methods describe the stacking interactions in conjugated	3. 3. 6. 1. 5. 5. 1.	8 3 5 5 5

(2009-2010)

1701	How the choice of a computational model could rule the chemical interpretation: the Ni(II) catalyzed ethylene dimerization as a case study. <i>Journal of Computational Chemistry</i> , 2010 , 31, 1053-62 ^{3.5}	7
1700	Reversible, nicht metallunterstEzte Bindung von Kohlendioxid durch frustrierte Lewis-Paare. 2009 , 121, 6770-6773	208
1699	A ditopic ion-pair receptor based on stacked nucleobase quartets. 2009 , 48, 3285-7	64
1698	Reversible metal-free carbon dioxide binding by frustrated Lewis pairs. 2009, 48, 6643-6	586
1697	Modeling the noncovalent interactions at the metabolite binding site in purine riboswitches. 2009 , 15, 633-49	26
1696	Expansion of the sigma-hole concept. 2009 , 15, 723-9	596
1695	Performance of Becke's half-and-half functional for non-covalent interactions: energetics, geometries and electron densities. 2009 , 15, 1051-60	15
1694	Quinoline alkaloids as intercalative topoisomerase inhibitors. 2009 , 15, 1417-26	25
1693	Abstracts of the 2008 ISSOL Meeting. August 24-29, 2008. Florence, Italy. 2009 , 39, 179-392	3
1692	Density functional theory. 2009 , 102, 443-53	174
	Density functional theory. 2009 , 102, 443-53 Influence of Estacking on the N7 and O6 proton affinity of guanine. 2009 , 123, 105-111	174 11
1691	Influence of Estacking on the N7 and O6 proton affinity of guanine. 2009 , 123, 105-111 Interaction between uracil nucleobase and phenylalanine amino acid: the role of sodium cation in	11
1691 1690 1689	Influence of Estacking on the N7 and O6 proton affinity of guanine. 2009 , 123, 105-111 Interaction between uracil nucleobase and phenylalanine amino acid: the role of sodium cation in stacking. 2009 , 124, 115-122 Reactive desorption electrospray ionization mass spectrometry (DESI-MS) of natural products of a	33
1691 1690 1689	Influence of Estacking on the N7 and O6 proton affinity of guanine. 2009, 123, 105-111 Interaction between uracil nucleobase and phenylalanine amino acid: the role of sodium cation in stacking. 2009, 124, 115-122 Reactive desorption electrospray ionization mass spectrometry (DESI-MS) of natural products of a marine alga. 2009, 394, 245-54 Dialkyl-[5]trovacenylethinylaluminium- und Ballium Verbindungen {[5]Trovacenyl = ([7-C7H7)V(IS-C5H4-)} - Zur Frage magnetischer Austauschwechselwirkung Ber Trenngruppen mit	11 33 49
1691 1690 1689	Influence of Estacking on the N7 and O6 proton affinity of guanine. 2009, 123, 105-111 Interaction between uracil nucleobase and phenylalanine amino acid: the role of sodium cation in stacking. 2009, 124, 115-122 Reactive desorption electrospray ionization mass spectrometry (DESI-MS) of natural products of a marine alga. 2009, 394, 245-54 Dialkyl-[5]trovacenylethinylaluminium- und Ballium Verbindungen {[5]Trovacenyl = (IT-C7H7)V(IS-C5H4-)} - Zur Frage magnetischer Austauschwechselwirkung Ber Trenngruppen mit Elektronenmangel-Bindungssegmenten 2009, 635, 2027-2033	11 33 49 7
1691 1690 1689 1688 1687	Influence of Estacking on the N7 and O6 proton affinity of guanine. 2009, 123, 105-111 Interaction between uracil nucleobase and phenylalanine amino acid: the role of sodium cation in stacking. 2009, 124, 115-122 Reactive desorption electrospray ionization mass spectrometry (DESI-MS) of natural products of a marine alga. 2009, 394, 245-54 Dialkyl-[5]trovacenylethinylaluminium- und gallium Verbindungen {[5]Trovacenyl = (I7-C7H7)V(I5-C5H4-)} - Zur Frage magnetischer Austauschwechselwirkung Ber Trenngruppen mit Elektronenmangel-Bindungssegmenten[] 2009, 635, 2027-2033 Dispersion interactions in density-functional theory. 2009, 22, 1127-1135 MP2 and DFT study of IR spectra of TCNE-methylsubstituted benzene complexes: Is charge transfer	11 33 49 7 298

1683	Weak intra- and intermolecular interactions in a binaphthol imine: an experimental charge-density study on (+/-)-8'-benzhydrylideneamino-1,1'-binaphthyl-2-ol. 2009 , 65, 757-69	30
1682	Modeling of a Trgera tweezer and its complexation properties. 2009 , 934, 117-122	16
1681	IRDV double resonance spectra of pyrazine dimers: Competition between . 2009 , 467, 255-259	15
1680	A comparative study of modern and robust computational methods applied to . 2009 , 468, 138-142	9
1679	Long-range interactions between polar molecules and metallic surfaces: A comparison of classical and density functional theory based models. 2009 , 471, 239-243	31
1678	Six-coordination in Chlorophylls: The fundamental role of dispersion energy. 2009 , 472, 243-247	24
1677	Solvent effect on EPR, molecular and electronic properties of semiquinone radical derived from 3,4-dihydroxybenzoic acid as model for humic acid transient radicals: High-field EPR and DFT studies. 2009 , 473, 160-166	32
1676	Interaction energies in monosubstituted-benzene dimers in parallel- and antiparallel-displaced conformations. 2009 , 474, 101-106	36
1675	Toward spectroscopic studies of biologically relevant systems: Vibrational spectrum of adenine as a test case for performances of long-range/dispersion corrected density functionals. 2009 , 475, 105-110	46
1674	Molecular hydrogen encapsulation in spherophanes. 2009 , 480, 225-230	5
1673	Hydroxide anion at the airWater interface. 2009 , 481, 2-8	103
1672	An assessment of theoretical methods for nonbonded interactions: comparison to complete basis set limit coupled-cluster potential energy curves for the benzene dimer, the methane dimer, benzene-methane, and benzene-H2S. 2009 , 113, 10146-59	345
1671	Modelling singly ionized coronene clusters. 2009 , 52, 55-58	36
1670	"Mindless" DFT Benchmarking. 2009 , 5, 993-1003	191
1669	Evidence for a rapid degenerate hetero-Cope-type rearrangement in [Cp*W(S)2S-CH2-CH=CH2]. 2009 , 4, 1830-1833	1
1668	Conformational properties of six-membered heterocycles: accurate relative energy differences	53
	with DFT, the importance of dispersion interactions and silicon substitution effects. 2009 , 11, 8689-97	
1667	Accurate molecular van der Waals interactions from ground-state electron density and free-atom reference data. 2009 , 102, 073005	3885

(2009-2009)

1665	Silicon(100)-2 1. 2009 , 113, 5681-5689	24
1664	From monomer to bulk: appearance of the structural motif of solid iodine in small clusters. 2009 , 131, 1050-6	14
1663	Ligands for dinitrogen fixation at Schrock-type catalysts. 2009 , 48, 1638-48	54
1662	Insights into the (superoxo)Fe(III)Fe(III) intermediate and reaction mechanism of myo-inositol oxygenase: DFT and ONIOM(DFT:MM) study. 2009 , 131, 17206-14	56
1661	Van der Waals Interactions in Density-Functional Theory: Rare-Gas Diatomics. 2009 , 5, 719-27	131
1660	Performance of ab initio and density functional methods for conformational equilibria of $C(n)H(2n+2)$ alkane isomers (n = 4-8). 2009 , 113, 11974-83	134
1659	Metal-phosphine bond strengths of the transition metals: a challenge for DFT. 2009, 113, 11833-44	119
1658	Theoretical Investigation of Formamide Adsorption on Ag(111) Surfaces. 2009 , 113, 10541-10547	27
1657	Toward a combined DFT/QTAIM description of agostic bonds: the critical case of a Nb(III) complex. 2009 , 113, 12322-7	30
1656	Controlled formation of an axially bonded co-phthalocyanine dimer. 2009 , 131, 6096-8	30
1655	Quantum chemical modeling of zeolite-catalyzed methylation reactions: toward chemical accuracy for barriers. 2009 , 131, 816-25	265
1654	Conductance enhancement in nanographene-gold junctions by molecular pi-stacking. 2009 , 131, 14857-67	24
1653	Frequency and effect of the binding of Mg2+, Mn2+, and Co2+ ions on the guanine base in Watson-Crick and reverse Watson-Crick base pairs. 2009 , 113, 15670-8	44
1652	Origin of the Argon Nanocoating Shift in the OH Stretching Fundamental of n-Propanol: A Combined Experimental and Quantum Chemical Study. 2009 , 113, 10929-10938	22
1651	Effect of methoxy substituents on the structural and electronic properties of fluorinated cyclobutenes: a study of hexafluorocyclobutene and its vinyl methoxy derivatives by XRD and periodic DFT calculations. 2009 , 113, 3186-96	13
1650	Accurate calculations of intermolecular interaction energies using explicitly correlated coupled cluster wave functions and a dispersion-weighted MP2 method. 2009 , 113, 11580-5	141
1649	Theoretical Study of the Adsorption of RNA/DNA Bases on the External Surfaces of Na+-Montmorillonite. 2009 , 113, 13741-13749	66
1648	Pentacene Binds Strongly to Hydrogen-Terminated Silicon Surfaces Via Dispersion Interactions. 2009 , 113, 9969-9973	12

1647	Understanding the role of intra- and intermolecular interactions in the formation of single- and double-helical structures of aromatic oligoamides: a computational study. 2009 , 113, 1335-42	21
1646	Oxygen vacancy formation on clean and hydroxylated low-index V2O5 surfaces: A density functional investigation. 2009 , 79,	37
1645	Benchmark Data for Noncovalent Interactions in HCOOH Benzene Complexes and Their Use for Validation of Density Functionals. 2009 , 5, 2726-33	29
1644	Reactions of an intramolecular frustrated Lewis pair with unsaturated substrates: evidence for a concerted olefin addition reaction. 2009 , 131, 12280-9	205
1643	Accurate Quantum Chemical Description of Non-Covalent Interactions in Hydrogen Filled Endohedral Fullerene Complexes. 2009 , 113, 17006-17010	59
1642	Accurate interaction energies at density functional theory level by means of an efficient dispersion correction. 2009 , 130, 174101	40
1641	Application of dispersion-corrected density functional theory. 2009 , 113, 10321-6	33
1640	H/Br exchange in BBr3 by HSiR3 (R = H, CH3, C2H5): origin of DFT failures to describe a seemingly innocuous reaction barrier. 2009 , 113, 12035-43	12
1639	Phenylalanyl-Glycyl-Phenylalanine Tripeptide: A Model System for Aromatic-Aromatic Side Chain Interactions in Proteins. 2009 , 5, 2248-56	22
1638	DFT Study of the Hydrogen Spillover Mechanism on Pt-Doped Graphite. 2009 , 113, 14908-14915	114
1638 1637	DFT Study of the Hydrogen Spillover Mechanism on Pt-Doped Graphite. 2009 , 113, 14908-14915 Weak interactions between trivalent pnictogen centers: computational analysis of bonding in dimers X3EEX3 (E = pnictogen, X = halogen). 2009 , 48, 6740-7	114 64
	Weak interactions between trivalent pnictogen centers: computational analysis of bonding in	, i
1637	Weak interactions between trivalent pnictogen centers: computational analysis of bonding in dimers X3EEX3 (E = pnictogen, X = halogen). 2009 , 48, 6740-7 Unified Inter- and Intramolecular Dispersion Correction Formula for Generalized Gradient	64 70
1637 1636	Weak interactions between trivalent pnictogen centers: computational analysis of bonding in dimers X3EEX3 (E = pnictogen, X = halogen). 2009 , 48, 6740-7 Unified Inter- and Intramolecular Dispersion Correction Formula for Generalized Gradient Approximation Density Functional Theory. 2009 , 5, 2950-8	64 70
1637 1636 1635	Weak interactions between trivalent pnictogen centers: computational analysis of bonding in dimers X3EEX3 (E = pnictogen, X = halogen). 2009, 48, 6740-7 Unified Inter- and Intramolecular Dispersion Correction Formula for Generalized Gradient Approximation Density Functional Theory. 2009, 5, 2950-8 Self-Assembly of Diacid Molecules: A Theoretical Approach of Molecular Interactions. 2009, 113, 17566-17571 Stabilizing a molecular switch at solid surfaces: A density functional theory study of azobenzene on	64 7° 7
1637 1636 1635	Weak interactions between trivalent pnictogen centers: computational analysis of bonding in dimers X3EEX3 (E = pnictogen, X = halogen). 2009, 48, 6740-7 Unified Inter- and Intramolecular Dispersion Correction Formula for Generalized Gradient Approximation Density Functional Theory. 2009, 5, 2950-8 Self-Assembly of Diacid Molecules: A Theoretical Approach of Molecular Interactions. 2009, 113, 17566-17571 Stabilizing a molecular switch at solid surfaces: A density functional theory study of azobenzene on Cu(111), Ag(111), and Au(111). 2009, 80, Benzenium-ethene complex: a fundamental problem for standard second-order Mller-Plesset	64 70 7 47
1637 1636 1635 1634	Weak interactions between trivalent pnictogen centers: computational analysis of bonding in dimers X3EEX3 (E = pnictogen, X = halogen). 2009, 48, 6740-7 Unified Inter- and Intramolecular Dispersion Correction Formula for Generalized Gradient Approximation Density Functional Theory. 2009, 5, 2950-8 Self-Assembly of Diacid Molecules: A Theoretical Approach of Molecular Interactions. 2009, 113, 17566-17571 Stabilizing a molecular switch at solid surfaces: A density functional theory study of azobenzene on Cu(111), Ag(111), and Au(111). 2009, 80, Benzenium-ethene complex: a fundamental problem for standard second-order Mller-Plesset theory. 2009, 113, 3005-8 Combined DFT/CC and IR spectroscopic studies on carbon dioxide adsorption on the zeolite H-FER.	647074719

(2009-2009)

1629	Coulomb-only second-order perturbation theory in long-range-corrected hybrid density functionals. 2009 , 11, 9677-86	28
1628	Implementation and Optimization of DFT-D/COSab with Respect to Basis Set and Functional: Application to Polar Processes of Furfural Derivatives in Solution. 2009 , 5, 2772-86	8
1627	Long-range corrected double-hybrid density functionals. 2009 , 131, 174105	271
1626	Symmetry-Adapted Perturbation Theory Applied to Endohedral Fullerene Complexes: A Stability Study of H2@C60 and 2H2@C60. 2009 , 5, 1585-96	78
1625	The CrMn Interaction in syn-Facial [Tricarbonyl(benzyl)chromium]manganesetricarbonyl Complexes: A Non-Covalent MetalMetal Bond. 2009 , 28, 1001-1013	44
1624	Computations of Noncovalent Interactions. 2009, 1-38	38
1623	Averaging semiempirical NMR chemical shifts: dynamic effects on the subpicosecond time scale. 2009 , 113, 11723-33	5
1622	Periodic DFT modeling of bulk and surface properties of MgCl2. 2009 , 11, 6525-32	46
1621	Triplet excimer formation in platinum-based phosphors: a theoretical study of the roles of Pt-Pt bimetallic interactions and interligand pi-pi interactions. 2009 , 131, 11371-80	106
1620	The chemical structure of a molecule resolved by atomic force microscopy. 2009 , 325, 1110-4	1205
1620 1619	The chemical structure of a molecule resolved by atomic force microscopy. 2009, 325, 1110-4 Thermochemical Fragment Energy Method for Biomolecules: Application to a Collagen Model Peptide. 2009, 5, 1667-79	1205
1619	Thermochemical Fragment Energy Method for Biomolecules: Application to a Collagen Model	
1619	Thermochemical Fragment Energy Method for Biomolecules: Application to a Collagen Model Peptide. 2009 , 5, 1667-79	33
1619 1618	Thermochemical Fragment Energy Method for Biomolecules: Application to a Collagen Model Peptide. 2009 , 5, 1667-79 Dispersionless density functional theory. 2009 , 103, 263201	33 145
1619 1618 1617	Thermochemical Fragment Energy Method for Biomolecules: Application to a Collagen Model Peptide. 2009, 5, 1667-79 Dispersionless density functional theory. 2009, 103, 263201 Ab initio study of hydrogen adsorption in MOF-5. 2009, 131, 4143-50 The effect of Fe doping on adsorption of CO2/N2 within carbon nanotubes: a density functional	33 145 206
1619 1618 1617 1616	Thermochemical Fragment Energy Method for Biomolecules: Application to a Collagen Model Peptide. 2009, 5, 1667-79 Dispersionless density functional theory. 2009, 103, 263201 Ab initio study of hydrogen adsorption in MOF-5. 2009, 131, 4143-50 The effect of Fe doping on adsorption of CO2/N2 within carbon nanotubes: a density functional theory study with dispersion corrections. 2009, 20, 375701 Intermolecular interaction in density functional theory: Application to carbon nanotubes and fullerenes. 2009, 79, Magnetic properties and vapochromic reversible guest-induced transformation in a bispyrazolato	3314520619
1619 1618 1617 1616	Thermochemical Fragment Energy Method for Biomolecules: Application to a Collagen Model Peptide. 2009, 5, 1667-79 Dispersionless density functional theory. 2009, 103, 263201 Ab initio study of hydrogen adsorption in MOF-5. 2009, 131, 4143-50 The effect of Fe doping on adsorption of CO2/N2 within carbon nanotubes: a density functional theory study with dispersion corrections. 2009, 20, 375701 Intermolecular interaction in density functional theory: Application to carbon nanotubes and fullerenes. 2009, 79, Magnetic properties and vapochromic reversible guest-induced transformation in a bispyrazolato copper(II) polymer: an experimental and dispersion-corrected density functional theory study. 2009	331452061968

1611	Fluxionality of gold nanoparticles investigated by Born-Oppenheimer molecular dynamics. 2009 , 80,	57
1610	Noncovalent interactions in a transition-metal triphenylphosphine complex: a density functional case study. 2009 , 48, 4622-4	132
1609	Protonation of water clusters in the cavities of acidic zeolites: $(H2O)n.H$ -chabazite, $n = 1-4$. 2009 , 11, 1702-12	55
1608	Automatized parametrization of SCC-DFTB repulsive potentials: application to hydrocarbons. 2009 , 113, 11866-81	63
1607	Balance of Attraction and Repulsion in Nucleic-Acid Base Stacking: CCSD(T)/Complete-Basis-Set-Limit Calculations on Uracil Dimer and a Comparison with the Force-Field Description. 2009 , 5, 1524-44	44
1606	Understanding effects of molecular adsorption at a single-wall boron nitride nanotube interface from density functional theory calculations. 2009 , 20, 355705	45
1605	Assessment of Orbital-Optimized, Spin-Component Scaled Second-Order Many-Body Perturbation Theory for Thermochemistry and Kinetics. 2009 , 5, 3060-73	172
1604	The method of local increments for the calculation of adsorption energies of atoms and small molecules on solid surfaces. Part I. A single Cu atom on the polar surfaces of ZnO. 2009 , 11, 11196-206	25
1603	Impact of ligands on CO2 adsorption in metal-organic frameworks: first principles study of the interaction of CO2 with functionalized benzenes. I. Inductive effects on the aromatic ring. 2009 , 130, 194703	113
1602	Van der Waals interactions in density functional theory using Wannier functions. 2009 , 113, 5224-34	72
1601	Oxygen-doped nanodiamonds: synthesis and functionalizations. 2009 , 11, 3068-71	43
1600	Effects of the zeolite framework on the adsorptions and hydrogen-exchange reactions of unsaturated aliphatic, aromatic, and heterocyclic compounds in ZSM-5 zeolite: a combination of perturbation theory (MP2) and a newly developed density functional theory (M06-2X) in ONIOM	72
1599	Cooperativity in noncovalent interactions of biologically relevant molecules. 2009 , 11, 8440-7	45
1598	Investigation of Exchange Energy Density Functional Accuracy for Interacting Molecules. 2009 , 5, 2754-62	263
1597	An Overview of EHole Bonding, an Important and Widely-Occurring Noncovalent Interaction. 2009, 149-163	14
1596	Ab initio calculation of van der Waals bonded molecular crystals. 2009 , 102, 206411	126
1595	Affinity Scale for the Interaction of Amino Acids with Silica Surfaces. 2009 , 113, 5741-5750	95
1594	Design of an organic zeolite toward the selective adsorption of small molecules at the dispersion corrected density functional theory level. 2009 , 113, 16472-8	17

(2009-2009)

1593	Noncovalent metal-metal interactions: the crucial role of london dispersion in a bimetallic indenyl system. 2009 , 131, 14156-7	40
1592	Bridged bis-Trgerd base molecular tweezers as new cavitand family. 2009 , 74, 1091-1099	5
1591	Clathrate hydrates with hydrogen-bonding guests. 2009 , 11, 10245-65	133
1590	Density-based energy decomposition analysis for intermolecular interactions with variationally determined intermediate state energies. 2009 , 131, 164112	104
1589	Optimization and basis-set dependence of a restricted-open-shell form of B2-PLYP double-hybrid density functional theory. 2009 , 113, 9861-73	70
1588	Micro-chlorido, micro-hydroxo-bridged dicarbonyl ruthenacycles: synthesis, structure and catalytic properties in hydrogen atom transfer. 2009 , 2695-711	15
1587	Benchmark thermochemistry of the $C(n)H(2n+2)$ alkane isomers (n = 2-8) and performance of DFT and composite ab initio methods for dispersion-driven isomeric equilibria. 2009 , 113, 8434-47	110
1586	The conformational landscape of 5-methoxytryptamine studied by rotationally resolved fluorescence spectroscopy and resonant ionization spectroscopy. 2009 , 11, 2433-40	8
1585	Electronic spectrum of tryptophan-phenylalanine. A correlated ab initio and time-dependent density functional theory study. 2009 , 113, 16443-8	15
1584	Triangular tricopper(I) clusters supported by donor-substituted triazacyclohexanes. 2009 , 4556-68	13
1583	Non-bonded force field for the interaction between metals and organic molecules: a case study of olefins on aluminum. 2009 , 11, 10195-203	12
1582	Cis-trans conversion of the CH3S-Au-SCH3 complex on Au(111). 2009 , 11, 8601-5	20
1581	Metal-free dihydrogen activation chemistry: structural and dynamic features of intramolecular P/B pairs. 2009 , 1534-41	118
1580	Metal-ligand cooperation in the trans addition of dihydrogen to a pincer Ir(I) complex: a DFT study. 2009 , 9433-9	107
1579	Dispersion-corrected DFT calculations on C(60)-porphyrin complexes. 2009 , 11, 4365-74	23
1578	Nitrile insertion into a boryl-substituted five-membered zirconacycloallenoid: unexpected formation of a zwitterionic boratirane product. 2009 , 6572-3	21
1577	Computational organic chemistry. 2009 , 105, 398	6
1576	C60-derived nanobaskets: stability, vibrational signatures, and molecular trapping. 2009 , 20, 395701	7

1575	The interplay of van der Waals and weak chemical forces in the adsorption of salicylic acid on NaCl(001). 2009 , 11, 9337-40	9
1574	Charge-transport properties of prototype molecular materials for organic electronics based on graphene nanoribbons. 2009 , 11, 2741-6	43
1573	Trends and anomalies in H-AH(n) and CH(3)-AH(n) bond strengths (AH(n) = CH3, NH2, OH, F). 2009 , 11, 10317-22	10
1572	Hydrides and dimers of C(58) fullerenes: structures and stabilities. 2009 , 11, 1050-9	5
1571	The water-benzene interaction: insight from electronic structure theories. 2009 , 130, 154303	67
1570	Infrared spectroscopy of phenol-(H2O)(n>10): structural strains in hydrogen bond networks of neutral water clusters. 2009 , 113, 12134-41	48
1569	Role of dispersive interactions in layered materials: a periodic B3LYP and B3LYP-D* study of Mg(OH)2, Ca(OH)2 and kaolinite. 2009 , 19, 2564	70
1568	Are there stable ion-pairs in room-temperature ionic liquids? Molecular dynamics simulations of 1-n-butyl-3-methylimidazolium hexafluorophosphate. 2009 , 131, 15825-33	245
1567	Ammonia-water cation and ammonia dimer cation. 2009 , 113, 6859-64	19
1566	Suitability of double hybrid density functionals and their dispersion-corrected counterparts in producing the potential energy curves for CO2-Rg (Rg: He, Ne, Ar and Kr) systems. 2009 , 113, 1377-83	13
1566 1565		13
	A quantum mechanical study of TiCl3 alpha, beta and gamma crystal phases: geometry, electronic	
1565	producing the potential energy curves for CO2-Rg (Rg: He, Ne, Ar and Kr) systems. 2009 , 113, 1377-83 A quantum mechanical study of TiCl3 alpha, beta and gamma crystal phases: geometry, electronic structure and magnetism. 2009 , 11, 11264-75 The accuracy of geometries for iron porphyrin complexes from density functional theory. 2009 ,	10
1565 1564 1563	A quantum mechanical study of TiCl3 alpha, beta and gamma crystal phases: geometry, electronic structure and magnetism. 2009, 11, 11264-75 The accuracy of geometries for iron porphyrin complexes from density functional theory. 2009, 113, 11949-53 CH/pi interaction in benzene and substituted derivatives with halomethane: a combined density	10
1565 1564 1563	A quantum mechanical study of TiCl3 alpha, beta and gamma crystal phases: geometry, electronic structure and magnetism. 2009, 11, 11264-75 The accuracy of geometries for iron porphyrin complexes from density functional theory. 2009, 113, 11949-53 CH/pi interaction in benzene and substituted derivatives with halomethane: a combined density functional and dispersion-corrected density functional study. 2009, 113, 10113-8	10 43 27
1565 1564 1563	A quantum mechanical study of TiCl3 alpha, beta and gamma crystal phases: geometry, electronic structure and magnetism. 2009, 11, 11264-75 The accuracy of geometries for iron porphyrin complexes from density functional theory. 2009, 113, 11949-53 CH/pi interaction in benzene and substituted derivatives with halomethane: a combined density functional and dispersion-corrected density functional study. 2009, 113, 10113-8 Calculating the fluorescence of 5-hydroxytryptophan in proteins. 2009, 113, 14521-8 New intermolecular benchmark calculations on the water dimer: SAPT and supermolecular	10 43 27
1565 1564 1563 1562	A quantum mechanical study of TiCl3 alpha, beta and gamma crystal phases: geometry, electronic structure and magnetism. 2009, 11, 11264-75 The accuracy of geometries for iron porphyrin complexes from density functional theory. 2009, 113, 11949-53 CH/pi interaction in benzene and substituted derivatives with halomethane: a combined density functional and dispersion-corrected density functional study. 2009, 113, 10113-8 Calculating the fluorescence of 5-hydroxytryptophan in proteins. 2009, 113, 14521-8 New intermolecular benchmark calculations on the water dimer: SAPT and supermolecular post-Hartreeflock approaches. 2009, 109, 3259-3267 Reaction enthalpies using the neural-network-based X1 approach: the important choice of input	10 43 27 14 24

(2010-2009)

	Enantioselective HF loss promoted by resonant two-photon ionization of supersonically expanded (R)-1-phenyl-2,2,2-trifluoroethanol clusters. 2009 , 113, 15127-35	4
1556	Origin of Surface-Band Dispersion at the Pentacene/Cu Interface. 2010 , 3, 025701	9
1555	A simple approach for describing metal-supported cyclohexaphenylene dehydrogenation. 2010 , 75, 65-70	11
1554	Accurate Harmonic/Anharmonic Vibrational Frequencies for Open-Shell Systems: Performances of the B3LYP/N07D Model for Semirigid Free Radicals Benchmarked by CCSD(T) Computations. 2010 , 6, 828-38	109
1553	Ouantum chemical excited state calculations on pigmentBrotein complexes require thorough	43
1552	On the Structure and Geometry of Biomolecular Binding Motifs (Hydrogen-Bonding, Stacking, X-HIIII) WFT and DFT Calculations. 2010 , 6, 66-80	166
1551	DFT study on the catalytic reactivity of a functional model complex for intradiol-cleaving dioxygenases. 2010 , 114, 5878-85	21
1550	Adsorption of Aromatic and Anti-Aromatic Systems on Graphene through Lacking. 2010 , 1, 3407-3412	294
1549	Palladium-Catalyzed CH Activation/CN Bond Formation Reactions: DFT Study of Reaction Mechanisms and Reactive Intermediates. 2010 , 29, 821-834	65
1548	A consistent and accurate ab initio parametrization of density functional dispersion correction (DFT-D) for the 94 elements H-Pu. 2010 , 132, 154104	23773
1547	Activation of dihydrogen by non-metal systems. 2010 , 46, 8526-33	152
1546	Mutual relationship between stacking and hydrogen bonding in DNA. Theoretical study of guanine-cytosine, guanine-5-methylcytosine, and their dimers. 2010 , 114, 10217-27	68
1545	Exploring the limits of frustrated Lewis pair chemistry with alkynes: detection of a system that favors 1,1-carboboration over cooperative 1,2-P/B-addition. 2010 , 5, 2199-208	101
1544	The effect of pi-stacking, H-bonding, and electrostatic interactions on the ionization energies of nucleic acid bases: adenine-adenine, thymine-thymine and adenine-thymine dimers. 2010 , 12, 2292-307	83
	NUC catalyzed evidations of aldebydes to estars, shomers lective assulation of alsohols in assesses	
1543	NHC catalyzed oxidations of aldehydes to esters: chemoselective acylation of alcohols in presence of amines. 2010 , 132, 1190-1	374
1543 1542	of amines. 2010 , 132, 1190-1 Delineating origins of stereocontrol in asymmetric Pd-catalyzed alpha-hydroxylation of	374 8 ₄
	of amines. 2010 , 132, 1190-1 Delineating origins of stereocontrol in asymmetric Pd-catalyzed alpha-hydroxylation of 1,3-ketoesters. 2010 , 75, 3085-96	

1539	Hydrogen bonding in the urea dimers and adeninethymine DNA base pair: anharmonic effects in the intermolecular H-bond and intramolecular H-stretching vibrations. 2010 , 125, 253-268	23
1538	Dispersion-corrected energy barriers for silylene addition to white phosphorus, a density functional investigation into substituent effects. 2010 , 127, 223-229	6
1537	Theoretical study of challenging properties of intramolecularly Estacked oligo(dibenzofulvene) organic molecular semiconductors. 2010 , 127, 605-612	7
1536	Overcoming systematic DFT errors for hydrocarbon reaction energies. 2010 , 127, 429-442	45
1535	Performance of the M06-L density functional for a folded Tyrūly conformer. 2010 , 485, 40-44	13
1534	On the performance of van der Waals corrected-density functional theory in describing the atomic hydrogen physisorption on graphite. 2010 , 500, 283-286	23
1533	Structure of sodiated octa-glycine: IRMPD spectroscopy and molecular modeling. 2010 , 21, 728-38	44
1532	DFT molecular dynamics (DFTMD) simulations of carbohydrates: COSMO solvated Emaltose. 2010 , 953, 61-82	7
1531	Differential stabilization of adenine quartets by anions and cations. 2010 , 15, 387-97	16
1530	Validity of current force fields for simulations on boron nitride nanotubes. 2010 , 5, 150	38
1529	Influence of N-alkyl substituents and counterions on the structural and mesomorphic properties of guanidinium salts: experiment and quantum chemical calculations. 2010 , 11, 3752-65	29
1528	Experimental and Theoretical Conformational Analysis of 5-Benzylimidazolidin-4-one Derivatives II a Playground For Studying Dispersion Interactions and a Windshield-Wiper Effect in Organocatalysis. 2010, 93, 1-16	57
1527	Can DFT methods correctly and efficiently predict the coordination number of copper(I) complexes? A case study. <i>Journal of Computational Chemistry</i> , 2010 , 31, 75-83	16
1526	Atomistic insight into chondroitin-6-sulfate glycosaminoglycan chain through quantum mechanics calculations and molecular dynamics simulation. <i>Journal of Computational Chemistry</i> , 2010 , 31, 1670-80 ^{3.5}	9
1525	DFT study of the full catalytic cycle for the propene hydroformylation catalyzed by a heterobimetallic HPt(SnCl3)(PH3)2 model catalyst. <i>Journal of Computational Chemistry</i> , 2010 , 31, 1986-2000	11
1524	Comparison of aromatic NHIIIOHIIII and CHIIIInteractions of alanine using MP2, CCSD, and DFT methods. <i>Journal of Computational Chemistry</i> , 2010 , 31, 2874-82	95
1523	Assessment of density functionals with long-range and/or empirical dispersion corrections for conformational energy calculations of peptides. <i>Journal of Computational Chemistry</i> , 2010 , 31, 2915-23 ^{3.5}	44
1522	Water Dissociation and Dioxygen Binding in Phenylalanine Hydroxylase. 2010 , 2010, 351-356	5

1521	Neutral and Cationic Hydridoruthenium Tetrakiscarbene Complexes. 2010 , 2010, 918-925	24
1520	Anionic d8 Alkyl Hydrides Belective Formation and Reactivity of Anionic cis-PtII Methyl Hydride. 2010 , 2010, 1991-1999	6
1519	The Preparation and Structure of [Pt(S2N2){P(OR)nR?3fi}2] and [Pt(SeSN2)[[P(OMe)nPh3fi}2] (n = 0B). 2010 , 2010, 3185-3194	3
1518	A DFT Study of Site-Selectivity in Oxidative Addition Reactions with Pd0 Complexes: The Effect of an Azine Nitrogen and the Use of Different Types of Halogen Atoms in the Substrate. 2010 , 2010, 3152-3158	14
1517	Copper-Catalyzed Enantioselective [2+2] Cycloadditions of 2-Nitrosopyridine with Ketenes. 2010 , 352, 945-948	38
1516	Intermediates involved in the oxidation of nitrogen monoxide: photochemistry of the cis-N(2)O(2)O(2) complex and of sym-N(2)O(4) in solid Ne matrices. 2010 , 16, 1506-20	40
1515	On the mechanism of ruthenium-catalyzed formation of hydrogen from alcohols: a DFT study. 2010 , 16, 13487-99	31
1514	A computational study of rhodium pincer complexes with classical and nonclassical hydride centres as catalysts for the hydroamination of ethylene with ammonia. 2010 , 16, 9203-14	22
1513	Kinetic isotope effects in asymmetric reactions. 2010 , 16, 10616-28	64
1512	Towards a molecular understanding of cation-anion interactionsprobing the electronic structure of imidazolium ionic liquids by NMR spectroscopy, X-ray photoelectron spectroscopy and theoretical calculations. 2010 , 16, 9018-33	241
1511	Mechanical properties of dense zeolitic imidazolate frameworks (ZIFs): a high-pressure X-ray diffraction, nanoindentation and computational study of the zinc framework Zn(Im)2, and its lithium-boron analogue, LiB(Im)4. 2010 , 16, 10684-90	105
1510	Lewis base catalyzed enantioselective allylation of alpha,beta-unsaturated aldehydes. 2010 , 16, 9442-5	48
1509	Lewis acid assisted stabilization of side-on bonded N2 in [Ru(NCN)]-pincer complexescomputational catalyst design directed at NH3 synthesis from N2 and H2. 2010 , 16, 14266-71	16
1508	Frustrierte Lewis-Paare: metallfreie Wasserstoffaktivierung und mehr. 2010 , 122, 50-81	611
1507	Neue Einblicke in den Mechanismus der Diwasserstoff-Aktivierung durch frustrierte Lewis-Paare. 2010 , 122, 1444-1447	110
1506	Cyclische Allene und Cumulene durch kooperative Addition frustrierter Lewis-Paare an konjugierte Enine und Diine. 2010 , 122, 2464-2467	53
1505	Ab-initio-Thermochemie fester Stoffe. 2010 , 122, 5370-5395	16
1504	Das tert-Butylkation in H-Zeolithen: Deprotonierung zu Isobuten und Umwandlung in Oberflühenalkoxide. 2010 , 122, 4783-4786	9

1503	Flexibility in a Metal Drganic Framework Material Controlled by Weak Dispersion Forces: The Bistability of MIL-53(Al). 2010 , 122, 7663-7665	30
1502	Frustrated Lewis pairs: metal-free hydrogen activation and more. 2010 , 49, 46-76	1585
1501	The mechanism of dihydrogen activation by frustrated Lewis pairs revisited. 2010 , 49, 1402-5	350
1500	Formation of cyclic allenes and cumulenes by cooperative addition of frustrated Lewis pairs to conjugated enynes and diynes. 2010 , 49, 2414-7	118
1499	Ab initio thermochemistry of solid-state materials. 2010 , 49, 5242-66	126
1498	The tert-butyl cation in H-zeolites: deprotonation to isobutene and conversion into surface alkoxides. 2010 , 49, 4678-80	81
1497	Flexibility in a metal-organic framework material controlled by weak dispersion forces: the bistability of MIL-53(Al). 2010 , 49, 7501-3	141
1496	Thermally-driven processes on rutile TiO2(110)-(11): A direct view at the atomic scale. 2010 , 85, 161-205	269
1495	Electron-density and electrostatic-potential features of orthorhombic chlorine trifluoride. 2010 , 20, 161-164	24
1494	Unsymmetrically substituted triazacyclohexanes and their chromium complexes. 2010 , 29, 1399-1404	2
1493	Theoretical prediction of a peptide binding to major histocompatibility complex II. 2010, 29, 240-5	5
1492	Evaluation of dispersion-corrected density functional theory (B3LYP-DCP) for compounds of biochemical interest. 2010 , 29, 178-87	18
1491	Infrared spectroscopic characterization of the oxidative dehydrogenation of propane by V4O10+. 2010 , 297, 102-106	29
1490	Assessment of density functionals for predicting the infrared spectrum of sodiated octa-glycine. 2010 , 297, 152-161	21
1489	Atomistic theoretical models for nanoporous hybrid materials. 2010 , 129, 304-318	46
1488	Interaction of CO, CO2 and CH4 with mesoporous organosilica: Periodic DFT calculations with dispersion corrections. 2010 , 129, 62-67	21
1487	Binding energy of d10 transition metals to alkenes by wave function theory and density functional theory?. 2010 , 324, 80-88	47
1486	On the nature of the active site in ruthenium olefin coordination[hsertion polymerization catalysts?. 2010 , 324, 64-74	7

1485	Could N-(diethylcarbamothioyl)benzamide be a good ionophore for sensor membranes?. 2010 , 981, 86-92	20
1484	A performance study of density functional theory with empirical dispersion corrections and spin-component scaled second-order Mller P lesset perturbation theory on adsorbateDeolite interactions. 2010 , 945, 85-88	11
1483	Theoretical studies on the pKa values of perfluoroalkyl carboxylic acids. 2010 , 949, 60-69	69
1482	van der Waals interactions in sterically crowded disilenes. 2010 , 957, 66-71	5
1481	Theoretical study of tautomerization and isomerization of methylamino- and phenylamino-substituted cyclic azaphospholines, oxaphospholines and thiaphospholines in gas and aqueous phases. 2010 , 962, 101-107	5
1480	Adsorption mechanisms of fluorocarbon polymers at ultra low-k surfaces. 2010 , 604, 1808-1812	11
1479	NWChem: A comprehensive and scalable open-source solution for large scale molecular simulations. 2010 , 181, 1477-1489	3430
1478	Promiscuous DNA alkyladenine glycosylase dramatically favors a bound lesion over undamaged adenine. 2010 , 152, 118-27	8
1477	The effect of van der Waals interactions on the properties of intrinsic defects in graphite. 2010 , 48, 4145-416	1 32
1476	Terahertz absorption spectra of 1,3,5,7-tetranitro-1,3,5,7-tetrazocane (HMX) polymorphs. 2010 , 489, 48-53	42
1475	Alkane dimers interaction: A semi-local MGGA functional study. 2010 , 492, 183-186	17
1474	Assessment of density functional methods for the study of olefin metathesis catalysed by ruthenium alkylidene complexes. 2010 , 493, 273-278	58
1473	Interactions of hydrophobic and hydrophilic self-assembled monolayers with water as probed by sum-frequency-generation spectroscopy. 2010 , 494, 193-197	18
1472	Application of an empirical dispersion potential to van der Waals binding in nitromethane, pentaerythritol, and pentaerythritol tetranitrate. 2010 , 498, 97-100	11
1471	A theoretical study of Batacking tetracene derivatives as promising organic molecular semiconductors. 2010 , 499, 146-151	26
1470	Insight in Structures of Superbulky Metallocenes with the CpBIG Ligand: Theoretical Considerations of Decaphenyl Metallocenes. 2010 , 636, 2257-2261	15
1469	Porous graphene as an atmospheric nanofilter. 2010 , 6, 2266-71	284
1468	Assessing the performances of some recently proposed density functionals for the description of bond dissociations involving organic radicals. 2010 , 110, 2320-2329	11

1467	Directional tendencies of halogen and hydrogen bonds. 2010 , 110, 2823-2832	214
1466	Theoretical studies on the all-anti zigzag geometries of perfluoro-n-alkyl chains. 2010,	3
1465	Performance of the M062X density functional against the ISOL set of benchmark isomerization energies for large organic molecules. 2010 ,	6
1464	Comparative theoretical investigation on the isomerization energies of long-chain perfluoroalkanes: A case study with perfluorooctane sulfonic acid congeners. 2010 ,	
1463	Comparative density functional theory study on the relative gas phase enthalpies and free energies of formation for the mono- through hepta-halogenated (X=F, Cl, Br) anthraquinones. 2010 ,	
1462	Anomalous molecular orbital variation upon adsorption on a wide band gap insulator. 2010 , 132, 214706	12
1461	The Aromatic Amino Acid Hydroxylase Mechanism: A Perspective From Computational Chemistry. 2010 , 437-500	8
1460	#bctabromo-meso-tris(pentafluorophenyl)corrole: reductive demetalation-based synthesis of a heretofore inaccessible, perhalogenated free-base corrole. 2010 , 14, 509-512	22
1459	Ab initio investigation of benzene clusters: molecular tailoring approach. 2010 , 133, 164308	68
1458	Tests of the RPBE, revPBE, tau-HCTHhyb, omegaB97X-D, and MOHLYP density functional approximations and 29 others against representative databases for diverse bond energies and barrier heights in catalysis. 2010 , 132, 164117	178
1457	Free energy surface of two- and three-dimensional transitions of Au 12 nanoclusters obtained by ab initio metadynamics. 2010 , 81,	24
1456	Effect of metallic surfaces on the electronic structure, magnetism, and transport properties of Co-phthalocyanine molecules. 2010 , 82,	38
1455	Atodiresei et al. Reply:. 2010 , 104,	1
1454	Periodic local Mller-Plesset second order perturbation theory method applied to molecular crystals: study of solid NH3 and CO2 using extended basis sets. 2010 , 132, 134706	74
1453	Density fitting and Cholesky decomposition approximations in symmetry-adapted perturbation theory: Implementation and application to probe the nature of Einteractions in linear acenes. 2010 , 132, 184111	225
1452	Improving the density functional theory description of water with self-consistent polarization. 2010 , 132, 164102	30
1451	Density functional study of 1,3,5-trinitro-1,3,5-triazine molecular crystal with van der Waals interactions. 2010 , 132, 094106	39
1450	Diffusion of 1,4-butanedithiol on Au(100)[[11]]: A DFT-based master-equation approach. 2010 , 82,	4

(2010-2010)

1449	First-principles study of 1,4-butanedithiol molecules and radicals adsorbed on unreconstructed Au(111) and Au(100). 2010 , 81,	9
1448	Structure and properties of surface and subsurface defects in graphite accounting for van der Waals and spin-polarization effects. 2010 , 82,	16
1447	Structure and energetics of azobenzene on Ag(111): benchmarking semiempirical dispersion correction approaches. 2010 , 104, 036102	214
1446	Dynamics of electron localization in warm versus cold water clusters. 2010 , 105, 043002	61
1445	Atomistic insight into the adsorption site selectivity of stepped Au(111) surfaces. 2010 , 82,	16
1444	The assessment of density functionals for DNAprotein stacked and T-shaped complexes. 2010 , 88, 815-830	36
1443	Local response dispersion method. II. Generalized multicenter interactions. 2010 , 133, 194101	82
1442	Correcting for dispersion interaction and beyond in density functional theory through force matching. 2010 , 133, 174115	23
1441	IR spectroscopy on isolated $Co(n)(alcohol)m$ cluster anions (n=1-4, m=1-3): structures and spin states. 2010 , 133, 194304	9
1440	Communication: Thermodynamics of water modeled using ab initio simulations. 2010 , 133, 141101	30
1439	Entropy effects in hydrocarbon conversion reactions: free-energy integrations and transition-path sampling. 2010 , 22, 384201	21
1438	Density Functional Theory Study of Catechol Adhesion on Silica Surfaces. 2010 , 114, 20793-20800	97
1437	Importance of London dispersion effects for the packing of molecular crystals: a case study for intramolecular stacking in a bis-thiophene derivative. 2010 , 12, 8500-4	100
1436	Van der waals interactions in molecular assemblies from first-principles calculations. 2010 , 114, 1944-52	48
1435	Transition state models for probing stereoinduction in Evans chiral auxiliary-based asymmetric aldol reactions. 2010 , 132, 12319-30	48
1434	Ab initio transition state theory for polar reactions in solution. 2010 , 145, 487-505	87
1433	Ab initio vibrational dynamics of molecular hydrogen on graphene: An effective interaction potential. 2010 , 132, 194708	12
1432	Probing substituent effects in aryl-aryl interactions using stereoselective Diels-Alder cycloadditions. 2010 , 132, 3304-11	159

1431	Theoretical Investigation of Solvent Effects and Complex Systems: Toward the calculations of bioinorganic systems from ab initio molecular dynamics simulations and static quantum chemistry. 2010 , 62, 111-142	8
1430	Hydroalumination and Hydrogallation of 1,2-Bis(trimethylsilylethynyl)benzene: Formation of Molecular Capsules and Ca Bond Activation. 2010 , 29, 1406-1412	36
1429	Controlling the Magnetic Properties of a Single Phthalocyanine Molecule through its Strong Coupling with the GaAs Surface. 2010 , 1, 2757-2762	14
1428	Describing Both Dispersion Interactions and Electronic Structure Using Density Functional Theory: The Case of Metal-Phthalocyanine Dimers. 2010 , 6, 81-90	100
1427	What determines the inhibition effectiveness of ATA, BTAH, and BTAOH corrosion inhibitors on copper?. 2010 , 132, 16657-68	224
1426	Comparative van der Waals density-functional study of graphene on metal surfaces. 2010 , 82,	247
1425	Significant van der Waals Effects in Transition Metal Complexes. 2010 , 6, 2040-4	176
1424	Coverage-Dependent Architectures of Iron Phthalocyanine on Ag(110): a Comprehensive STM/DFT Study. 2010 , 114, 2144-2153	41
1423	Hydrogen forms in water by proton transfer to a distorted electron. 2010 , 114, 915-20	32
1422	Adsorption of small aromatic molecules on the (111) surfaces of noble metals: A density functional theory study with semiempirical corrections for dispersion effects. 2010 , 132, 224701	201
1421	Two- and three-body interatomic dispersion energy contributions to binding in molecules and solids. 2010 , 132, 234109	180
1420	Weak Chemical Interaction and van der Waals Forces: A Combined Density Functional and Intermolecular Perturbation Theory [Application to Graphite and Graphitic Systems. 2010 , 45-79	5
1419	The Relevance of Dispersion Interactions for the Stability of Oxide Phases. 2010 , 114, 22718-22726	55
1418	Viologen-based redox-switchable anion-binding receptors. 2010 , 34, 1373	59
1417	Stability of Hydrocarbons of the Polyhedrane Family Containing Bridged CH Groups: A Case of Failure of the Colle-Salvetti Correlation Density Functionals. 2010 , 6, 3442-55	16
1416	Using Nonempirical Semilocal Density Functionals and Empirical Dispersion Corrections to Model Dative Bonding in Substituted Boranes. 2010 , 6, 1825-33	20
1415	Benchmark calculations of water-acene interaction energies: Extrapolation to the water-graphene limit and assessment of dispersion-corrected DFT methods. 2010 , 12, 6375-81	98
1414	Designing molecular switches based on DNA-base mispairing. 2010 , 114, 15311-8	53

(2010-2010)

1413	Assessing the quality of the random phase approximation for lattice constants and atomization energies of solids. 2010 , 81,	335
1412	The contribution of computational studies to organometallic catalysis: descriptors, mechanisms and models. 2010 , 296-310	93
1411	A General Database for Main Group Thermochemistry, Kinetics, and Noncovalent Interactions - Assessment of Common and Reparameterized (meta-)GGA Density Functionals. 2010 , 6, 107-26	340
1410	Using Density Functional Theory Methods for Modeling Induction and Dispersion Interactions in Ligand B rotein Complexes. 2010 , 6, 96-112	4
1409	Water Adsorption on Coordinatively Unsaturated Sites in CuBTC MOF. 2010 , 1, 3354-3359	142
1408	van der Waals Interactions in Density-Functional Theory: Intermolecular Complexes. 2010 , 6, 1081-1088	137
1407	Accurate modelling of Pd(0) + PhX oxidative addition kinetics. 2010 , 39, 10833-6	163
1406	Failure of Conventional Density Functionals for the Prediction of Molecular Crystal Polymorphism: A Quantum Monte Carlo Study. 2010 , 1, 1789-1794	58
1405	Hydrophobic Behavior of Dehydroxylated Silica Surfaces: A B3LYP Periodic Study. 2010 , 114, 19984-19992	22
1404	A New Empirical Correction to the AM1 Method for Macromolecular Complexes. 2010 , 6, 2153-66	21
1403	Effects of London dispersion on the isomerization reactions of large organic molecules: a density functional benchmark study. 2010 , 12, 6940-8	110
1402	Computational study of silica-supported transition metal fragments for Kubas-type hydrogen storage. 2010 , 132, 17296-305	27
1401	Extension of the Hartree Bock Plus Dispersion Method by First-Order Correlation Effects. 2010, 1, 550-555	75
1400	Interactions Studied with Electronic Structure Methods: The Ethyne Methyl Isocyanide Complex and Thioanisole. 2010 , 6, 2687-700	7
1399	Noncovalent Interaction between Aniline and Carbon Nanotubes: Effect of Nanotube Diameter and the Hydrogen-Bonded Solvent Methanol on the Adsorption Energy and the Photophysics. 2010 , 114, 5898-5905	13
1398	Mechanism of the hydride transfer between Anabaena Tyr303Ser FNR(rd)/FNR(ox) and NADP+/H. A combined pre-steady-state kinetic/ensemble-averaged transition-state theory with multidimensional tunneling study. 2010 , 114, 3368-79	25
1397	Ligand effects in bimetallic high oxidation state palladium systems. 2010 , 49, 11249-53	36
1396	n-Alkane isodesmic reaction energy errors in density functional theory are due to electron correlation effects. 2010 , 12, 4670-3	51

1395	Brightening and locking a weak and floppy N-H chromophore: the case of pyrrolidine. 2010 , 114, 10492-9	11
1394	Analysis of the interactions taking place in the recognition site of a bimetallic Mg(II)-Zn(II) enzyme, isopentenyl diphosphate isomerase. a parallel quantum-chemical and polarizable molecular mechanics study. 2010 , 114, 4884-95	18
1393	Developing a Reliable Synthetic Route to cis-1,3-Bridge-Disubstituted [3]Ferrocenophane Systems. 2010 , 29, 3852-3861	6
1392	Controlling half-metallicity of graphene nanoribbons by using a ferroelectric polymer. 2010 , 4, 1345-50	82
1391	Theoretical study on the repair mechanism of the (6-4) photolesion by the (6-4) photolyase. 2010 , 132, 16285-95	61
1390	Structural and Electronic Properties of the Methyl-Terminated Si(111) Surface. 2010 , 114, 11898-11902	14
1389	Assessment of DFT and DFT-D for Potential Energy Surfaces of Rare Gas Trimers-Implementation and Analysis of Functionals and Extrapolation Procedures. 2010 , 6, 1951-65	7
1388	Oxygen superbases as polar binding pockets in nonpolar solvents. 2010 , 132, 12660-7	24
1387	The ⊞and ∰orms of oxalic acid di-hydrate at high pressure: a theoretical simulation and a neutron diffraction study. 2010 , 12, 2596	22
1386	Synthesis and Reactivity of an Iridium(I) Acetonyl PNP Complex. Experimental and Computational Study of Metal Ligand Cooperation in H and C Bond Activation via Reversible Ligand Dearomatization. 2010 , 29, 3817-3827	87
1385	Ambipolar Charge Transport in ⊞Oligofurans: A Theoretical Study 2010, 114, 20436-20442	55
1384	Calculations of alkane energies using long-range corrected DFT combined with intramolecular van der Waals correlation. 2010 , 12, 1440-3	56
1383	Intramolecular proton transfer in calixphyrin derivatives. 2010 , 114, 3649-54	6
1382	A computational investigation of the nitrogen-boron interaction in o-(N,N-dialkylaminomethyl)arylboronate systems. 2010 , 114, 12531-9	54
1381	Toward an Accurate Modeling of the Water Deolite Interaction: Calibrating the DFT Approach. 2010 , 1, 763-768	11
1380	A carbene-carbene complex equilibrium. 2010 , 132, 10677-9	23
1379	Noncovalent interactions in the gas-phase conformers of anionic iduronate (methyl 2-o-sulfo-L-iduronate): variation of subconformer versus ring conformer energetics for a prototypical anionic monosaccharide studied using computational methods. 2010 , 114, 11153-60	2
1378	Coverage Dependence of the Structure of Acrolein Adsorbed on Ag(111). 2010 , 1, 2546-2549	16

1377	An Error and Efficiency Analysis of Approximations to MllerPlesset Perturbation Theory. 2010 , 6, 3681-3687	12
1376	Theoretical study of chlorophyll a hydrates formation in aqueous organic solvents. 2010 , 114, 681-7	20
1375	Theoretical and experimental comparison of SnPc, PbPc, and CoPc adsorption on Ag(111). 2010 , 81,	87
1374	Configurationally labile enantioenriched lithiated 3-arylprop-2-enyl carbamates: joint experimental and quantum chemical investigations on the equilibrium of epimers. 2010 , 75, 5716-20	7
1373	Electrons in Cold Water Clusters: An ab Initio Molecular Dynamics Study of Localization and Metastable States 2010 , 114, 20489-20495	34
1372	Auxiliary Density Matrix Methods for Hartree-Fock Exchange Calculations. 2010 , 6, 2348-64	321
1371	The structure of geminal imidazolium bis(trifluoromethylsulfonyl)amide ionic liquids: a theoretical study of the gas phase ionic complexes. 2010 , 114, 12506-12	22
1370	Ligand effects on the [Cu(PhO)(PhOH)]+ redox active complex. 2010, 49, 8421-9	17
1369	Understanding the Resonance Raman Scattering of Donor-Acceptor Complexes using Long-Range Corrected DFT. 2010 , 6, 2845-55	20
1368	Fluxionality of [(Ph3P)3M(X)] (M = Rh, Ir). The red and orange forms of [(Ph3P)3Ir(Cl)]. Which phosphine dissociates faster from Wilkinson's catalyst?. 2010 , 132, 12013-26	47
1367	Hole Mobility for Thin-Film Organic Molecular Solids in the Presence of Defects or Surface Adsorbates: Theory and Implications for Gas Detection. 2010 , 114, 12173-12189	9
1366	NMR-spectroscopic and solid-state investigations of cometal-free asymmetric conjugate addition: a dinuclear paracyclophaneimine zinc methyl complex. 2010 , 132, 12899-905	28
1365	Geometry Optimization of Large and Flexible van der Waals Dimers: A Fragmentation-Reconstruction Approach. 2010 , 6, 2536-46	6
1364	Competing thermal electrocyclic ring-closure reactions of (2Z)-hexa-2,4,5-trienals and their Schiff bases. Structural, kinetic, and computational studies. 2010 , 75, 4453-62	15
1363	Insight from First-Principles Calculations into the Interactions between Hydroxybenzoic Acids and Alkali Chloride Surfaces. 2010 , 114, 460-467	14
1362	Simulations of nanocylinders self-assembled from cyclic 毗ripeptides. 2010 , 114, 11948-52	4
1361	Stacking and spreading interaction in N-heteroaromatic systems. 2010 , 114, 9606-16	55
1360	Microhydration of the selenite dianion: a theoretical study of structures, hydration energies, and electronic stabilities of $SeO(3)(2-)(H(2)O)(n)$ (n = 0-6, 9) clusters. 2010 , 114, 8948-60	8

1359	Applications of Screened Hybrid Density Functionals with Empirical Dispersion Corrections to Rare Gas Dimers and Solids. 2010 , 6, 864-72	16
1358	Treatment of Layered Structures Using a Semilocal meta-GGA Density Functional. 2010 , 1, 515-519	51
1357	Spin- and energy-dependent tunneling through a single molecule with intramolecular spatial resolution. 2010 , 105, 047204	240
1356	The mechanisms underlying the enhanced resolution of atomic force microscopy with functionalized tips. 2010 , 12, 125020	118
1355	Simulating proton transport through a simplified model for trans-membrane proteins. 2010 , 114, 7047-55	12
1354	Origin of the Enhanced Interaction of Molecular Hydrogen with Extraframework Cu+ and FeO+ Cations in Zeolite Hosts. A Periodic DFT Study. 2010 , 114, 13926-13934	19
1353	Effect of charge distribution on RDX adsorption in IRMOF-10. 2010 , 26, 5942-50	25
1352	In situ transformation of TON silica zeolite into the less dense ITW: structure-direction overcoming framework instability in the synthesis of SiO2 zeolites. 2010 , 132, 3461-71	45
1351	Latent porosity in potassium dodecafluoro-closo-dodecaborate(2-). Structures and rapid room temperature interconversions of crystalline K2B12F12, K2(H2O)2B12F12, and K2(H2O)4B12F12 in the presence of water vapor. 2010 , 132, 13902-13	35
1350	Exchange-Enhanced H-Abstraction Reactivity of High-Valent Nonheme Iron(IV)-Oxo from Coupled Cluster and Density Functional Theories. 2010 , 1, 1533-1540	96
1349	What is the Real Nature of Ferrous Soybean Lipoxygenase-1? A New Two-Conformation Model Based on Combined ONIOM(DFT:MM) and Multireference Configuration Interaction Characterization. 2010 , 1, 901-906	21
1348	An Assessment of Density Functional Methods for Potential Energy Curves of Nonbonded Interactions: The XYG3 and B97-D Approximations. 2010 , 6, 727-34	86
1347	A System-Dependent Density-Based Dispersion Correction. 2010 , 6, 1990-2001	118
1346	Hydrogen generation from alcohols catalyzed by ruthenium-triphenylphosphine complexes: multiple reaction pathways. 2010 , 132, 8056-70	202
1345	One-Pot Generation of a Tris-cationic Homobimetallic Planar-Chiral Ruthenacycle. 2010 , 29, 1675-1679	10
1344	Experimental and theoretical investigation of the aromatic-aromatic interaction in isolated capped dipeptides. 2010 , 114, 2973-82	49
1343	Toward Molecular Nanowires Self-Assembled on an Insulating Substrate: Heptahelicene-2-carboxylic acid on Calcite (101 4). 2010 , 114, 1547-1552	72
1342	H-Bonding of Furan and Its Hydrogenated Derivatives with the Isolated Hydroxyl of Amorphous Silica: An IR Spectroscopic and Thermodynamic Study. 2010 , 114, 18233-18239	18

(2010-2010)

	Oxidation of Methanol to Formaldehyde on Silica-Supported Molybdena: Density Functional Theory Study on Models of Mononuclear Sites. 2010 , 114, 2967-2979	36
1340	Inclusion of Dispersion Effects Significantly Improves Accuracy of Calculated Reaction Barriers for Cytochrome P450 Catalyzed Reactions. 2010 , 1, 3232-3237	137
1339	Mono- versus dinuclear Pt(II) 6-(5-trifluoromethyl-pyrazol-3-yl)-2,2'-bipyridine complexes: synthesis, characterization, and remarkable difference in luminescent properties. 2010 , 49, 1372-83	48
1338	Thermochemical benchmarking of hydrocarbon bond separation reaction energies: Jacob's ladder is not reversed!. 2010 , 108, 2655-2666	45
1337	Computational and Experimental Studies on the Adsorption of CO, N2, and CO2 on Mg-MOF-74. 2010 , 114, 11185-11191	267
1336	DSD-BLYP: A General Purpose Double Hybrid Density Functional Including Spin Component Scaling and Dispersion Correction 2010 , 114, 20801-20808	261
1335	Molecular modeling of phenothiazine derivatives: self-assembling properties. 2010 , 114, 12479-89	15
1334	How Well Can Kohn-Sham DFT Describe the HO2 + O3 Reaction?. 2010 , 6, 2751-61	20
1333	Estimating the hydrogen bond energy. 2010 , 114, 9529-36	234
1332	Thermodynamic properties of cementite (Fe3C). 2010 , 34, 129-133	64
1331	Molecular, electronic, and crystal structures of self-assembled hydrothermally synthesized Zn(II)-mercaptonicotinate: a combined spectroscopic and theoretical approach. 2010 , 49, 4099-108	13
		13
	Zn(II)-mercaptonicotinate: a combined spectroscopic and theoretical approach. 2010 , 49, 4099-108	13 8 71
1330	Zn(II)-mercaptonicotinate: a combined spectroscopic and theoretical approach. 2010 , 49, 4099-108 Ab initio calculations for industrial materials engineering: successes and challenges. 2010 , 22, 384215 Empirically corrected DFT and semi-empirical methods for non-bonding interactions. 2010 , 12, 307-22	8
1330	Zn(II)-mercaptonicotinate: a combined spectroscopic and theoretical approach. 2010 , 49, 4099-108 Ab initio calculations for industrial materials engineering: successes and challenges. 2010 , 22, 384215 Empirically corrected DFT and semi-empirical methods for non-bonding interactions. 2010 , 12, 307-22	8
1329 1328	Zn(II)-mercaptonicotinate: a combined spectroscopic and theoretical approach. 2010 , 49, 4099-108 Ab initio calculations for industrial materials engineering: successes and challenges. 2010 , 22, 384215 Empirically corrected DFT and semi-empirical methods for non-bonding interactions. 2010 , 12, 307-22 Synthesis, structure and properties of decakis(phenylthio)corannulene. 2010 , 8, 53-5	8 71 39
1329 1328 1327	Zn(II)-mercaptonicotinate: a combined spectroscopic and theoretical approach. 2010 , 49, 4099-108 Ab initio calculations for industrial materials engineering: successes and challenges. 2010 , 22, 384215 Empirically corrected DFT and semi-empirical methods for non-bonding interactions. 2010 , 12, 307-22 Synthesis, structure and properties of decakis(phenylthio)corannulene. 2010 , 8, 53-5 Stability and dynamics of small molecules trapped on graphene. 2010 , 82, Hydroxyapatite as a key biomaterial: quantum-mechanical simulation of its surfaces in interaction	8 71 39 61

1323	Environmental effects in computational spectroscopy: accuracy and interpretation. 2010 , 11, 1812-32	47
1322	Bonding of Methyl Phosphonate to TiO2(110) 2010 , 114, 16983-16988	21
1321	JuNoLo DIIch nonlocal code for parallel post-processing evaluation of vdW-DF correlation energy. 2010 , 181, 371-379	38
1320	Improved interaction energy benchmarks for dimers of biological relevance. 2010 , 12, 5974-9	98
1319	Halogen bonding: an electrostatically-driven highly directional noncovalent interaction. 2010 , 12, 7748-57	1239
1318	Density functional theory study of ATA, BTAH, and BTAOH as copper corrosion inhibitors: adsorption onto Cu(111) from gas phase. 2010 , 26, 14582-93	99
1317	Periodic density functional theory calculations for 3-dimensional polyacetylene with empirical dispersion terms. 2010 , 12, 3289-93	23
1316	Molecular packing and charge transport parameters in crystalline organic semiconductors from first-principles calculations. 2010 , 12, 9381-8	56
1315	Performance of the Empirical Dispersion Corrections to Density Functional Theory: Thermodynamics of Hydrocarbon Isomerizations and Olefin Monomer Insertion Reactions. 2010 , 6, 477-90	41
1314	Adsorption of Na and Hg on the Ice(Ih) Surface: A Density-Functional Study. 2010 , 114, 2941-2946	6
1313	Accurate dispersion interactions from standard density-functional theory methods with small basis sets. 2010 , 12, 6092-8	46
1312	DFT/CC investigation of physical adsorption on a graphite (0001) surface. 2010 , 12, 6438-44	89
1311	Stereoselectivity in Oxyallyl-Furan 4+3 Cycloadditions: Control of Intermediate Conformations and Dispersive Stabilisation with Evans' Oxazolidinones. 2010 , 1, 387-392	60
1310	Frontiers in electronic structure theory. 2010 , 132, 110902	126
1309	Enhanced Catalytic Activity of Carbon Alloy Catalysts Codoped with Boron and Nitrogen for Oxygen Reduction Reaction. 2010 , 114, 8933-8937	66
1308	Direct observation and quantification of COIbinding within an amine-functionalized nanoporous solid. 2010 , 330, 650-3	794
1307	Density functional theoretical study of pentacene/noble metal interfaces with van der Waals corrections: vacuum level shifts and electronic structures. 2010 , 132, 134703	114
1306	Theoretical Predictions of Energetic Molecular Crystals at Ambient and Hydrostatic Compression Conditions Using Dispersion Corrections to Conventional Density Functionals (DFT-D). 2010 , 114, 6734-6748	122

1305	Study of the interaction between short alkanethiols from ab initio calculations. 2010 , 12, 7555-65	16
1304	Ionization of cytosine monomer and dimer studied by VUV photoionization and electronic structure calculations. 2010 , 12, 2860-72	58
1303	Mechanism of the Swern oxidation: significant deviations from transition state theory. 2010 , 75, 8088-99	20
1302	Detection of weak intramolecular interactions in Ru(3)(CO)(12) by topological analysis of charge density distributions. 2010 , 114, 9368-73	11
1301	Study of polycyclic aromatic hydrocarbons adsorbed on graphene using density functional theory with empirical dispersion correction. 2010 , 12, 6483-91	72
1300	Van der Waals Interactions Between Organic Adsorbates and at Organic/Inorganic Interfaces. 2010 , 35, 435-442	244
1299	Improved description of the structure of molecular and layered crystals: ab initio DFT calculations with van der Waals corrections. 2010 , 114, 11814-24	737
1298	Accurate Prediction of Hydrogen Adsorption in MetalDrganic Frameworks with Unsaturated Metal Sites via a Combined Density-Functional Theory and Molecular Mechanics Approach. 2010 , 114, 19116-19126	42
1297	Implementation and assessment of a simple nonlocal van der Waals density functional. 2010 , 132, 164113	69
1296	Role of van der Waals bonding in the layered oxide V2O5: First-principles density-functional calculations. 2010 , 82,	73
1295	Quantum chemical modeling of benzene ethylation over H-ZSM-5 approaching chemical accuracy: a hybrid MP2:DFT study. 2010 , 132, 11525-38	127
1294	Ab Initio Path Integral Simulations of Floppy Molecular Systems. 2010 , 675-686	
1293	Importance of the nature of Bubstituents in pyrrolidine organocatalysts in asymmetric Michael additions. 2010 , 75, 7310-21	30
1292	Chirality influence on the aggregation of methyl mandelate. 2010 , 34, 1266	34
1291	Comparative Study of Selected Wave Function and Density Functional Methods for Noncovalent Interaction Energy Calculations Using the Extended S22 Data Set. 2010 , 6, 2365-76	194
1290	Ethanol monomers and dimers revisited: a Raman study of conformational preferences and argon nanocoating effects. 2010 , 114, 8223-33	48
1289	A density functional theory study of CO2 and N2 adsorption on aluminium nitride single walled nanotubes. 2010 , 20, 10426	54
1288	Enzymatic ring-opening mechanism of verdoheme by the heme oxygenase: a combined X-ray crystallography and QM/MM study. 2010 , 132, 12960-70	33

1287	Practical Aspects of Computational Chemistry. 2010 ,	11
1286	Theoretical Study of the Hydrolysis of Pentameric Aluminum Complexes. 2010 , 6, 993-1007	17
1285	Role of dispersive interactions in the CO adsorption on MgO(001): periodic B3LYP calculations augmented with an empirical dispersion term. 2010 , 12, 6382-6	58
1284	Theoretical Chemistry of Zeolite Reactivity. 2010 , 301-334	3
1283	A DFT periodic study on the interaction between O2 and cation exchanged chabazite MCHA ($M = H+$, $Na+$ or $Cu+$): effects in the triplet-singlet energy gap. 2010 , 12, 442-52	16
1282	Electronic peculiarities of the excited states of [RuN5C]+ vs. [RuN6]2+ polypyridine complexes: insight from theory. 2010 , 39, 10959-66	25
1281	Application of high level wavefunction methods in quantum mechanics/molecular mechanics hybrid schemes. 2010 , 12, 5041-52	18
1280	Structure of the gas-phase glycine tripeptide. 2010 , 12, 3463-73	21
1279	Inclusion complexes of buckycatcher with C(60) and C(70). 2010 , 12, 7091-7	95
1278	Azobenzene versus 3,3',5,5'-tetra-tert-butyl-azobenzene (TBA) at Au(111): characterizing the role of spacer groups. 2010 , 12, 6404-12	44
1277	A highly ordered, aromatic bidentate self-assembled monolayer on Au(111): a combined experimental and theoretical study. 2010 , 12, 6445-54	19
1276	The dehydrogenation of ammonia-borane catalysed by dicarbonylruthenacyclic(II) complexes. 2010 , 39, 8893-905	40
1275	Enantioselective interaction of carbamoylated quinine and (S)-3,5-dinitrobenzoyl alanine: theoretical and experimental circular dichroism study. 2010 , 12, 11487-97	7
1274	The 1,4-phenylenediisocyanide dimer: gas-phase properties and insights into organic self-assembled monolayers. 2010 , 12, 82-96	4
1273	Simultaneous adsorption of benzene and dioxygen in CuHY zeolites as a precursor process to the aerobic oxidation of benzene to phenol. 2010 , 12, 6345-51	11
1272	Physisorption of aromatic organic contaminants at the surface of hydrophobic/hydrophilic silica geosorbents: a B3LYP-D modeling study. 2010 , 12, 6357-66	59
1271	Symmetry and polar-leffects on the dynamics of enshrouded aryl-alkyne molecular rotors. 2010 , 1, 102	34
1270	Ab initio study of van der Waals and hydrogen-bonded molecular crystals with a periodic local-MP2 method. 2010 , 12, 2429	48

1269	Structural changes in the water tetramer. A combined Monte Carlo and DFT study. 2010 , 12, 13657-66	13
1268	Reference MP2/CBS and CCSD(T) quantum-chemical calculations on stacked adenine dimers. Comparison with DFT-D, MP2.5, SCS(MI)-MP2, M06-2X, CBS(SCS-D) and force field descriptions. 2010 , 12, 3522-34	78
1267	A comparative analysis of the role of water in the binding pockets of ionotropic glutamate receptors. 2010 , 12, 14057-66	12
1266	DFT-MD and vibrational anharmonicities of a phosphorylated amino acid. Success and failure. 2010 , 12, 3501-10	13
1265	Noncovalent interactions of a benzo[a]pyrene diol epoxide with DNA base pairs: insight into the formation of adducts of (+)-BaP DE-2 with DNA. 2010 , 114, 2038-44	33
1264	Enantioselective helical folding inside a self-assembled, cylindrical capsule. 2010 , 46, 1625-7	18
1263	The role of van der Waals interactions in surface-supported supramolecular networks. 2010 , 12, 992-9	42
1262	Interpretation of the ultrafast photoinduced processes in pentacene thin films. 2010, 132, 3431-9	54
1261	Low-lying structures and stabilities of large water clusters: investigation based on the combination of the AMOEBA potential and generalized energy-based fragmentation approach. 2010 , 114, 9253-61	39
1260	Calculation of One- and Two-Photon Absorption Spectra of Thiolated Gold Nanoclusters using Time-Dependent Density Functional Theory. 2010 , 6, 2809-21	38
1259	Imaging and characterization of activated CO2 species on Ni(110). 2010 , 82,	28
1258	Structure and dynamics of liquid water on rutile TiO2(110). 2010 , 82,	162
1257	Adsorption of n-butane on Cu(100), Cu(111), Au(111), and Pt(111): Van der Waals density-functional study. 2010 , 82,	48
1256	Molecular packing and chemical association in liquid water simulated using ab initio hybrid Monte Carlo and different exchange-correlation functionals. 2010 , 132, 204509	14
1255	Theoretical study of the adsorption of C1-C4 primary alcohols in H-ZSM-5. 2010 , 12, 9481-93	62
1254	Polycyclic aromatic hydrocarbon formation mechanism in the "particle phase". A theoretical study. 2010 , 12, 9429-40	23
1253	Accurate quantum chemical energies for the interaction of hydrocarbons with oxide surfaces: CH(4)/MgO(001). 2010 , 12, 14330-40	113
1252	Experimental and computational study of the ring opening of tricyclic oxanorbornenes to polyhydro isoindole phosphonates. 2010 , 8, 3644-54	14

1251	(51)V NMR parameters of VOCl(3): static and dynamic density functional study from the gas phase to the bulk. 2011 , 13, 619-27	16
1250	Stability of noble-gas hydrocarbons in an organic liquid-like environment: HXeCCH in acetylene. 2011 , 13, 19601-6	26
1249	Liquid structures of water, methanol, and hydrogen fluoride at ambient conditions from first principles molecular dynamics simulations with a dispersion corrected density functional. 2011 , 13, 19943-50	59
1248	Adjusting framework ionicity to favour crystallisation of zeolites with strained structural units. Periodic quantum chemical studies. 2011 , 1, 868	7
1247	Alanine at 13.6 GPa and its pressure-induced amorphisation at 15 GPa. 2011 , 13, 5841	39
1246	Gas-phase study of new organozinc reagents by IRMPD-spectroscopy, computational modelling and tandem-MS. 2011 , 13, 13255-67	14
1245	Doubly hybrid density functional for accurate description of thermochemistry, thermochemical kinetics and nonbonded interactions. 2011 , 30, 115-160	106
1244	An infrared study of solid glycine in environments of astrophysical relevance. 2011 , 13, 12268-76	36
1243	Dispersion interactions of carbohydrates with condensate aromatic moieties: theoretical study on the CH-IInteraction additive properties. 2011 , 13, 14215-22	25
1242	Benzoannelation stabilizes the d(xy)1 state of low-spin iron(III) porphyrinates. 2011 , 50, 3567-81	12
1241	Adsorption and Diffusion of Fructose in Zeolite HZSM-5: Selection of Models and Methods for Computational Studies. 2011 , 115, 21785-21790	26
1240	Perpendicular growth of carbon chains on graphene from first-principles. 2011 , 83,	43
1239	Energetics and dynamics of proton transfer reactions along short water wires. 2011, 13, 13207-15	43
1238	Structural characterization of the {3[BPMTU]+ []3[X]IInH2O} salts (BPMTU = 1,3-bis(3-pyridylmethyl)-2-thiourea and X = Cl, Br, I). A polychlorine network based on O IIIClIand OH IIIClInteractions. 2011 , 64, 202-221	
1237	Exploring the structure and chemical activity of 2-D gold islands on graphene moir (Ru(0001). 2011 , 152, 267-76; discussion 293-306	32
1236	Approaches to the solvation of the molecular probe N-methyl-6-quinolone in its excited state. 2011 , 13, 16395-403	15
1235	Dimers of cyclic carbonates: chirality recognition in battery solvents and energy storage. 2011 , 13, 14176-82	16
1234	Thermal Cℍ Bond Activation of Benzene, Toluene, and Methane with Cationic [M(X)(bipy)]+ (M = Ni, Pd, Pt; X = CH3, Cl; bipy = 2,2?-bipyridine): A Mechanistic Study. 2011 , 30, 1588-1598	44

1233	Dissolution thermochemistry of alkali metal dianion salts (M2X1, $M = Li+$, Na+, and K+ with X = CO3(2-), SO4(2-), C8H8(2-), and B12H12(2-)). 2011 , 50, 11412-22	10
1232	Axial chirality of donor-donor, donor-acceptor, and tethered 1,1'-binaphthyls: a theoretical revisit with dynamics trajectories. 2011 , 115, 5488-95	36
1231	Computational studies of room temperature ionic liquid-water mixtures. 2011 , 47, 6228-41	96
1230	Structure of the indole-benzene dimer revisited. 2011 , 115, 9485-92	28
1229	From a localized H3O radical to a delocalized H3O+Me-solvent-separated pair by sequential hydration. 2011 , 13, 14003-9	16
1228	Interlayer interaction and relative vibrations of bilayer graphene. 2011 , 13, 5687-95	125
1227	C6H6/Au(111): interface dipoles, band alignment, charging energy, and van der Waals interaction. 2011 , 134, 044701	56
1226	Free energy of reaction by density functional theory: oxidative addition of ammonia by an iridium complex with PCP pincer ligands. 2011 , 1, 1526	39
1225	Mechanistic differences between methanol and dimethyl ether carbonylation in side pockets and large channels of mordenite. 2011 , 13, 2603-12	123
1224	Enhanced binding strengths of acyclic porphyrin hosts with endohedral metallofullerenes. 2011 , 2, 1530	36
1223	Enthalpy difference between conformations of normal alkanes: effects of basis set and chain length on intramolecular basis set superposition error. 2011 , 109, 943-953	23
1222	Aromatic pathways in mono- and bisphosphorous singly MBius twisted [28] and [30]hexaphyrins. 2011 , 13, 20659-65	37
1221	Prediction of high-valent iron K-edge absorption spectra by time-dependent density functional theory. 2011 , 40, 11070-9	84
1220	A molecular dynamics study of 1,1-diamino-2,2-dinitroethylene (FOX-7) crystal using a symmetry adapted perturbation theory-based intermolecular force field. 2011 , 13, 16629-36	41
1219	Laws of thermal diffusion of individual molecules on the gold surface. 2011 , 13, 13690-7	5
1218	High pressure modification of organic NLO materials: large conformational re-arrangement of 4-aminobenzophenone. 2011 , 13, 6845	12
1217	An alternative approach for the calculation of correlation energy in periodic systems: a hybrid MP2(B3LYP) study of the He-MgO(100) interaction. 2011 , 47, 4385-7	7
1216	Periodic ab initio estimates of the dispersive interaction between molecular nitrogen and a monolayer of hexagonal BN. 2011 , 13, 4434-43	20

1215	Subtle effects control the polymerisation mechanism in Ediimine iron catalysts. 2011 , 40, 8419-28	18
1214	[6]Saddlequat: a [6]helquat captured on its racemization pathway. 2011 , 2, 2314-2320	35
1213	Reactivity studies on [Cp?Fel]2: From iron hydrides to P4-activation. 2011 , 2, 2120	55
1212	Transition from one-dimensional water to ferroelectric ice within a supramolecular architecture. 2011 , 108, 3481-6	89
1211	A consistent picture of the proton release mechanism of oNBA in water by ultrafast spectroscopy and ab initio molecular dynamics. 2011 , 115, 1075-83	26
1210	Isolated monohydrates of a model peptide chain: effect of a first water molecule on the secondary structure of a capped phenylalanine. 2011 , 133, 3931-42	60
1209	Adsorption of Carbon Dioxide on Mesoporous Zirconia: Microcalorimetric Measurements, Adsorption Isotherm Modeling, and Density Functional Theory Calculations. 2011 , 115, 10097-10103	38
1208	Energetics of direct and water-mediated proton-coupled electron transfer. 2011 , 133, 19040-3	27
1207	Will P450cam Hydroxylate or Desaturate Alkanes? QM and QM/MM Studies. 2011 , 2, 2229-2235	18
1206	Self-organization of 1-methylnaphthalene on the surface of artificial snow grains: a combined experimental-computational approach. 2011 , 115, 11412-22	38
1205	Competitive photocyclization/rearrangement of 4-aryl-1,1-dicyanobutenes controlled by intramolecular charge-transfer interaction. Effect of medium polarity, temperature, pressure, excitation wavelength, and confinement. 2011 , 10, 1405-14	12
1204	Interaction Between Gold Atoms and Thio-Aryl Ligands on the Au(111) Surface. 2011 , 115, 24871-24879	11
1203	Olefin-borane "van der Waals complexes": intermediates in frustrated Lewis pair addition reactions. 2011 , 133, 12448-50	110
1202	Adsorption of C60 on Au(111) revisited: A van der Waals density functional study. 2011 , 83,	50
1201	QTAIM application in drug development: prediction of relative stability of drug polymorphs from experimental crystal structures. 2011 , 115, 12809-17	26
1200	The effects of protein environment and dispersion on the formation of ferric-superoxide species in myo-inositol oxygenase (MIOX): a combined ONIOM(DFT:MM) and energy decomposition analysis. 2011 , 115, 11278-85	25
1199	Energetics and structure of organic molecules embedded in single-wall carbon nanotubes from first principles: The example of benzene. 2011 , 84,	13
1198	A theoretical discussion on the relationships among molecular packings, intermolecular interactions, and electron transport properties for naphthalene tetracarboxylic diimide derivatives. 2011 , 21, 15558	53

1197	Density Functional Theory Study of O2 and NO Adsorption on Heteroatom-Doped Graphenes Including the van der Waals Interaction. 2011 , 115, 10971-10978	32
1196	Molybdenum oxides versus molybdenum sulfides: geometric and electronic structures of Mo $\mathbb{K}(y)$? (X = O, S and y = 6, 9) clusters. 2011 , 115, 2291-6	23
1195	Theoretical study of polaron formation in poly(G)-poly(C) cations. 2011 , 115, 3136-45	9
1194	On the cause of controlling affinity to small molecules of imprinted polymeric membranes prepared by noncovalent approach: a computational and experimental investigation. 2011 , 115, 9345-51	18
1193	Bonding nature and vibrational signatures of oxirane:(water)(n=1-3). Assessment of the performance of the dispersion-corrected DFT methods compared to the ab initio results and Fourier transform infrared experimental data. 2011 , 115, 6688-701	12
1192	Density functional theory investigations of the structural and electronic properties of Ag2V4O11. 2011 , 83,	21
1191	Sensitivity Analysis of Cluster Models for Calculating Adsorption Energies for Organic Molecules on Mineral Surfaces. 2011 , 115, 10044-10055	12
1190	Theoretical and Experimental Study of Bonding and Optical Properties of Self-Assembly Metallophthalocyanines Complexes on a Gold Surface. A Survey of the SubstrateBurface Interaction 2011 , 115, 23512-23518	18
1189	Computational Investigations of Ligand Fluxionality in Fe3(C8H8)3. 2011 , 30, 5196-5201	
1188	Electron and Electrostatic Properties of Three Crystal Forms of Piracetam. 2011 , 11, 2528-2539	9
1187	Density Functional Theoretical Study of Perfluoropentacene/Noble Metal Interfaces with van der Waals Corrections: Adsorption States and Vacuum Level Shifts. 2011 , 115, 5767-5772	22
1186	Silanol-Related and Unspecific Adsorption of Molecular Ammonia on Highly Dehydrated Silica. 2011	
	, 115, 23344-23353	17
1185	Main-chain boron-containing oligophenylenes via ring-opening polymerization of 9-H-9-borafluorene. 2011 , 133, 4596-609	109
1185 1184	Main-chain boron-containing oligophenylenes via ring-opening polymerization of	
	Main-chain boron-containing oligophenylenes via ring-opening polymerization of 9-H-9-borafluorene. 2011 , 133, 4596-609 Theoretical study of corundum as an ideal gate dielectric material for graphene transistors. 2011 ,	109
1184	Main-chain boron-containing oligophenylenes via ring-opening polymerization of 9-H-9-borafluorene. 2011 , 133, 4596-609 Theoretical study of corundum as an ideal gate dielectric material for graphene transistors. 2011 , 84, Versatile Electronic and Magnetic Properties of Corrugated V2O5 Two-Dimensional Crystal and Its	109 46
1184	Main-chain boron-containing oligophenylenes via ring-opening polymerization of 9-H-9-borafluorene. 2011, 133, 4596-609 Theoretical study of corundum as an ideal gate dielectric material for graphene transistors. 2011, 84, Versatile Electronic and Magnetic Properties of Corrugated V2O5 Two-Dimensional Crystal and Its Derived One-Dimensional Nanoribbons: A Computational Exploration. 2011, 115, 11983-11990 Terahertz spectroscopy and solid-state density functional theory simulations of the improvised explosive oxidizers potassium nitrate and ammonium nitrate. 2011, 115, 12410-8	109 46 32

1179	Aurophilic Interactions from Wave Function, Symmetry-Adapted Perturbation Theory, and Rangehybrid Approaches. 2011 , 7, 2399-407	34
1178	Nuclear shieldings with the SSB-D functional. 2011 , 115, 1250-6	16
1177	Fully computational lead-development of fluoro-olefin polymerization catalysts. 2011 , 115, 13885-95	5
1176	Formal Estimation of Errors in Computed Absolute Interaction Energies of Protein-ligand Complexes. 2011 , 7, 790-797	116
1175	Single Electron Tunneling through a Tailored Arylthio-coronene. 2011 , 115, 9204-9209	9
1174	Locating Instantons in Many Degrees of Freedom. 2011 , 7, 690-8	94
1173	Ab Initio Modeling of Donor-Acceptor Interactions and Charge-Transfer Excitations in Molecular Complexes: The Case of Terthiophene-Tetracyanoquinodimethane. 2011 , 7, 2068-77	38
1172	Aldimines generated from aza-Wittig reaction between bis(iminophosphoranes) derived from 1,1'-diazidoferrocene and aromatic or heteroaromatic aldehydes: electrochemical and optical behaviour towards metal cations. 2011 , 40, 12548-59	19
1171	Singular Value Decomposition for Analyzing Temperature- and Pressure-Dependent Radial Distribution Functions: Decomposition into Grund RDFs (GRDFs). 2011 , 7, 3035-9	2
1170	Trimethoxybenzene complexes of pentafluorophenylchlorocarbene. 2011 , 115, 8113-8	9
1169	Noncovalent interactions between modified cytosine and guanine DNA base pair mimics investigated by terahertz spectroscopy and solid-state density functional theory. 2011 , 115, 14391-6	22
1168	An ab initio insight into the Cu(111)-mediated Ullmann reaction. 2011 , 13, 154-60	68
1167	Structures of the Ordered Water Monolayer on MgO(001). 2011, 115, 6764-6774	78
1166	Electronic Structure and Optical Properties of Ca(NH2BH3)2 Studied from GW Calculations. 2011 , 115, 18795-18801	13
1165	Transient innermolecular carbene-hemicarcerand complex of fluorophenylcarbene. 2011 , 115, 13799-803	3
1164	Anomalous Wetting Layer at the Au(111) Surface. 2011 , 2, 2582-2586	43
1163	Aminophenylnitronylnitroxides: Highly Networked Hydrogen-Bond Assembly in Organic Radical Materials. 2011 , 23, 4844-4856	7
1162	Stability of Hydrocarbons of the Polyhedrane Family: Convergence of ab Initio Calculations and Corresponding Assessment of DFT Main Approximations. 2011 , 7, 2761-5	3

1161	Structural and vibrational properties of arsenic sulfides: alacranite (As8S9). 2011 , 115, 4558-62	14
1160	Rhenium in homogeneous catalysis: [ReBrH(NO)(labile ligand)(large-bite-angle diphosphine)] complexes as highly active catalysts in olefin hydrogenations. 2011 , 133, 8168-78	56
1159	Theoretical study on the regioselectivity of the B80 buckyball in electrophilic and nucleophilic reactions using DFT-based reactivity indices. 2011 , 115, 9069-80	29
1158	Selective homogeneous hydrogenation of biogenic carboxylic acids with [Ru(TriPhos)H]+: a mechanistic study. 2011 , 133, 14349-58	213
1157	Method of local increments for the calculation of adsorption energies of atoms and small molecules on solid surfaces. 2. CO/MgO(001). 2011 , 115, 7153-60	27
1156	Addressing Methionine in Molecular Design through Directed Sulfur-Halogen Bonds. 2011 , 7, 2307-15	39
1155	Stereoselectivities and regioselectivities of (4 + 3) cycloadditions between allenamide-derived chiral oxazolidinone-stabilized oxyallyls and furans: experiment and theory. 2011 , 133, 14443-51	50
1154	Modeling CH Abstraction Reactivity of Nonheme Fe(IV)O Oxidants with Alkanes: What Role Do Counter Ions Play?. 2011 , 2, 2610-2617	59
1153	Self-Assembling of Poly(3-hexylthiophene). 2011 , 115, 576-581	60
1152	Bond Length Alternation of Conjugated Oligomers: Wave Function and DFT Benchmarks. 2011 , 7, 369-76	119
1152 1151	Bond Length Alternation of Conjugated Oligomers: Wave Function and DFT Benchmarks. 2011 , 7, 369-76 Binding Structures of Pyrrole on Si(5 5 12) Surfaces. 2011 , 115, 17111-17117	119
1151	Binding Structures of Pyrrole on Si(5 5 12)	2
1151	Binding Structures of Pyrrole on Si(5 5 12)	2
1151 1150 1149	Binding Structures of Pyrrole on Si(5 5 12) Surfaces. 2011, 115, 17111-17117 Synthesis and Structure of Bifunctional Zirconocene/Borane Complexes and Their Activation for Ethylene Polymerization. 2011, 30, 6372-6382 Application of London-Type Dispersion Corrections in Solid-State Density Functional Theory for Predicting the Temperature-Dependence of Crystal Structures and Terahertz Spectra. 2011, 11, 2006-2010 Charge density analysis of 2-methyl-4-nitro-1-phenyl-1H-imidazole-5-carbonitrile: an experimental	2 22 19
1151 1150 1149 1148	Binding Structures of Pyrrole on Si(5 5 12) Surfaces. 2011, 115, 17111-17117 Synthesis and Structure of Bifunctional Zirconocene/Borane Complexes and Their Activation for Ethylene Polymerization. 2011, 30, 6372-6382 Application of London-Type Dispersion Corrections in Solid-State Density Functional Theory for Predicting the Temperature-Dependence of Crystal Structures and Terahertz Spectra. 2011, 11, 2006-2010 Charge density analysis of 2-methyl-4-nitro-1-phenyl-1H-imidazole-5-carbonitrile: an experimental and theoretical study of C?NIIIC?N interactions. 2011, 115, 12941-52	2 22 19 21
1151 1150 1149 1148	Binding Structures of Pyrrole on Si(5 5 12) Surfaces. 2011, 115, 17111-17117 Synthesis and Structure of Bifunctional Zirconocene/Borane Complexes and Their Activation for Ethylene Polymerization. 2011, 30, 6372-6382 Application of London-Type Dispersion Corrections in Solid-State Density Functional Theory for Predicting the Temperature-Dependence of Crystal Structures and Terahertz Spectra. 2011, 11, 2006-2010 Charge density analysis of 2-methyl-4-nitro-1-phenyl-1H-imidazole-5-carbonitrile: an experimental and theoretical study of C?NIIIC?N interactions. 2011, 115, 12941-52 Investigation of Boron Nitride Nanomesh Interacting with Water. 2011, 115, 13685-13692 Acetylacetone, an interesting anchoring group for ZnO-based organic-inorganic hybrid materials: a	2 22 19 21 39

1143	VOPO4[H2O: a stacking faults structure studied by X-ray powder diffraction and DFT-D calculations. 2011 , 50, 4378-83	11
1142	Coverage-Driven Electronic Decoupling of Fe-Phthalocyanine from a Ag(111) Substrate. 2011 , 115, 12173-12	17 9 1
1141	Heat-to-connect: surface commensurability directs organometallic one-dimensional self-assembly. 2011 , 5, 9093-103	62
1140	Assessment of dispersion corrected atom centered pseudopotentials: application to energetic molecular crystals. 2011 , 115, 803-10	30
1139	Corroles cannot ruffle. 2011 , 50, 3247-51	29
1138	Surface-confined conformers and coassembly-induced conformer resolution. 2011 , 27, 9994-9	3
1137	Nature of the Transition MetalCarbene Bond in Grubbs Olefin Metathesis Catalysts. 2011 , 30, 3522-3529	37
1136	Comparison of intermolecular interaction energies from SAPT and DFT including empirical dispersion contributions. 2011 , 115, 11321-30	44
1135	Free energy simulations of a GTPase: GTP and GDP binding to archaeal initiation factor 2. 2011 , 115, 6749-63	26
1134	Large Induced Interface Dipole Moments without Charge Transfer: Buckybowls on Metal Surfaces. 2011 , 2, 2805-2809	39
1133	Effect of counterions on the protonation state in a poly(G)-poly(C) radical cation. 2011 , 115, 14885-90	4
1132	Understanding the interaction of the porphyrin macrocycle to reactive metal substrates: structure, bonding, and adatom capture. 2011 , 5, 1831-8	55
1131	Electron correlation decides the stability of cubic versus hexagonal boron nitride. 2011, 83,	24
1130	Tracking of the polyproline folding by density functional computations and Raman optical activity spectra. 2011 , 115, 15079-89	30
1129	Analysis of the Reaction between O2and Nitrogen-Containing Char Using the Density Functional Theory. 2011 , 25, 670-675	19
1128	Initial Growth Mechanisms of Gold-Phosphine Clusters. 2011 , 115, 6305-6316	22
1127	Computational insight into the Rh-mediated activation of white phosphorus. 2011 , 50, 22-9	5
1126	Charge Transfer in Molecular Complexes with 2,3,5,6-Tetrafluoro-7,7,8,8-tetracyanoquinodimethane (F4-TCNQ): A Density Functional Theory Study. 2011 , 23, 5149-5159	87

1125	Do Short CHM (M = Cu(I), Ag(I)) Distances Represent Agostic Interactions in Pincer-Type Complexes? Unusual NHC Transmetalation from Cu(I) to Ag(I). 2011 , 30, 3302-3310	51
1124	Electron distribution in partially reduced mixed metal oxide systems: infrared spectroscopy of CemVnOo(+) gas-phase clusters. 2011 , 115, 11187-92	42
1123	Dispersion-corrected energy decomposition analysis for intermolecular interactions based on the BLW and dDXDM methods. 2011 , 115, 5467-77	38
1122	Revisiting the Aufbau Reaction with Acetylene: Further Insights from Experiment and Theory. 2011 , 30, 1569-1576	9
1121	Competition between amide stacking and intramolecular H bonds in peptide derivatives: controlling nearest-neighbor preferences. 2011 , 115, 11960-70	39
1120	Adsorption of Gases in Microporous Organic Molecular Crystal, a Multiscale Computational Investigation. 2011 , 115, 4935-4942	13
1119	Theoretical Study of the Adsorption of the Butanol Isomers in H-ZSM-5. 2011 , 115, 8658-8669	39
1118	First Principles-Based Calculations of Free Energy of Binding: Application to Ligand Binding in a Self-Assembling Superstructure. 2011 , 7, 1102-8	17
1117	Q-band EPR spectroscopy of photogenerated quartet state organic nitreno radicals. 2011 , 115, 4922-8	6
1116	Adsorption of Single Platinum Atom on the Graphene Oxide: The Role of the Carbon Lattice. 2011 , 115, 12023-12032	8
1115	Vibrational and thermodynamic properties of ℍMX: a first-principles investigation. 2011 , 134, 204509	21
1114	Density functional theory study of pyrophyllite and M-montmorillonites (M = Li, Na, K, Mg, and Ca): role of dispersion interactions. 2011 , 115, 9695-703	55
1113	New Insights into the Structure of the Vapor/Water Interface from Large-Scale First-Principles Simulations. 2011 , 2, 105-13	114
1112	Peculiar Behavior of Azolium Azolate Energetic Ionic Liquids. 2011 , 2, 2571-2576	6
1111	Role of Multicentered Bonding in Controlling Magnetic Interactions in Estacked Bis-dithiazolyl Radical. 2011 , 11, 3137-3140	45
1110	Polymer Crystallinity and Transport Properties at the Poly(3-hexylthiophene)/Zinc Oxide Interface. 2011 , 115, 9651-9655	30
1109	Complexation, computational, magnetic, and structural studies of the Maillard reaction product isomaltol including investigation of an uncommon [Interaction with copper(II). 2011 , 50, 1498-505	16
1108	Cation-cation "attraction": when London dispersion attraction wins over Coulomb repulsion. 2011 , 50, 2619-28	112

1107	A step beyond the Feltham-Enemark notation: spectroscopic and correlated ab initio computational support for an antiferromagnetically coupled M(II)-(NO)- description of Tp*M(NO) (M = Co, Ni). 2011 , 133, 18785-801	83
1106	Density Functional Theory Study of Alkane-Alkoxide Hydride Transfer in Zeolites. 2011 , 1, 105-115	33
1105	Weak Molecular Interactions Studied with Parallel Implementations of the Local Pair Natural Orbital Coupled Pair and Coupled Cluster Methods. 2011 , 7, 76-87	127
1104	Overcoming lability of extremely long alkane carbon-carbon bonds through dispersion forces. 2011 , 477, 308-11	298
1103	Aryl C-H amination by diruthenium nitrides in the solid state and in solution at room temperature: experimental and computational study of the reaction mechanism. 2011 , 133, 13138-50	56
1102	First-principles calculations of the structural and dynamic properties, and the equation of state of crystalline iodine oxides I2O4, I2O5, and I2O6. 2011 , 134, 204501	6
1101	Intermolecular interaction energies in molecular crystals: comparison and agreement of localized Mler-Plesset 2, dispersion-corrected density functional, and classical empirical two-body calculations. 2011 , 115, 11179-86	149
1100	Ab initio molecular dynamics simulations of a binary system of ionic liquids. 2011 , 13, 13617-20	65
1099	Creating carboxylic acid co-crystals: The application of Hammett substitution constants. 2011 , 13, 6583	25
1098	Electronic structure and chemical bond in naphthalene and anthracene. 2011 , 13, 5679-86	45
1097	Differences in structure, energy, and spectrum between neutral, protonated, and deprotonated phenol dimers: comparison of various density functionals with ab initio theory. 2011 , 13, 991-1001	33
1096	Modeling interactions between lignocellulose and ionic liquids using DFT-D. 2011 , 13, 11393-401	93
1095	Ab initio study of lithium-doped graphane for hydrogen storage. 2011 , 96, 27013	44
1094	Relativity and the lead-acid battery. 2011 , 106, 018301	80
1093	Van der Waals effects in ab initio water at ambient and supercritical conditions. 2011 , 135, 154503	127
1092	Aerobic Oxidation of Hydrocarbons Catalyzed by Mn-Doped Nanoporous Aluminophosphates (II): Hydroperoxide Decomposition. 2011 , 1, 945-955	15
1091	Aerobic Oxidation of Hydrocarbons Catalyzed by Mn-Doped Nanoporous Aluminophosphates (IV): Regeneration Mechanism. 2011 , 1, 1475-1486	21
1090	Ab initio theoretical study of non-covalent adsorption of aromatic molecules on boron nitride nanotubes. 2011 , 13, 11766-72	39

1089	Halogen bond involving hypervalent halogen: CSD search and theoretical study. 2011 , 115, 9294-9	49
1088	Fluorine-Centered Halogen Bonding: A Factor in Recognition Phenomena and Reactivity. 2011 , 11, 4238-4246	211
1087	New heteroleptic bis-phenanthroline copper(I) complexes with dipyridophenazine or imidazole fused phenanthroline ligands: spectral, electrochemical, and quantum chemical studies. 2011 , 50, 11309-22	52
1086	Adsorption of Cu, Ag, and Au atoms on graphene including van der Waals interactions. 2011 , 23, 395001	99
1085	Directional Dependence of Hydrogen Bonds: a Density-based Energy Decomposition Analysis and Its Implications on Force Field Development. 2011 , 7, 4038-4049	33
1084	Relating Trends in First-Principles Electronic Structure and Open-Circuit Voltage in Organic Photovoltaics. 2011 , 2, 2531-2537	43
1083	Viability of clathrate hydrates as CO2 capturing agents: a theoretical study. 2011 , 115, 7633-7	45
1082	Approximate Density Functionals: Which Should I Choose?. 2011 ,	3
1081	Parameterization of a B3LYP specific correction for non-covalent interactions and basis set superposition error on a gigantic dataset of CCSD(T) quality non-covalent interaction energies. 2011 , 7, 658-668	59
1080	Evaluation of a combination of local hybrid functionals with DFT-D3 corrections for the calculation of thermochemical and kinetic data. 2011 , 115, 8990-6	25
1079	Electronic structures of silver oxides. 2011 , 84,	51
1078	A computational investigation on singlet and triplet exciton couplings in acene molecular crystals. 2011 , 13, 18615-25	34
1077	Structural and Vibrational Properties of Liquid Water from van der Waals Density Functionals. 2011 , 7, 3054-61	134
1076	Systematic study of the performance of density functional theory methods for prediction of energies and geometries of organoselenium compounds. 2011 , 115, 4827-31	22
1075	An ab initio study of van der Waals potential energy parameters for silver clusters. 2011 , 115, 2332-9	6
1074	Accuracy of Density Functionals in the Prediction of Electronic Proton Affinities of Amino Acid Side Chains. 2011 , 7, 3898-908	35
1073	Ab Initio Studies of Cellulose I: Crystal Structure, Intermolecular Forces, and Interactions with Water. 2011 , 115, 11533-11539	65
1072	The reactivity of endohedral fullerenes. What can be learnt from computational studies?. 2011 , 13, 3585-603	117

1071	A theoretical study of a ZnO graphene analogue: adsorption on Ag(111) and hydrogen transport. 2011 , 23, 334215	5
1070	Importance of accurate spectral simulations for the analysis of terahertz spectra: citric acid anhydrate and monohydrate. 2011 , 115, 11039-44	20
1069	Ab initio study of structure and interconversion of native cellulose phases. 2011 , 115, 10097-105	38
1068	Theoretical insights into heme-catalyzed oxidation of cyclohexane to adipic acid. 2011 , 50, 1194-202	30
1067	A potent ruthenium(II) antitumor complex bearing a lipophilic levonorgestrel group. 2011 , 50, 9164-71	65
1066	Benchmarking Semiempirical Methods for Thermochemistry, Kinetics, and Noncovalent Interactions: OMx Methods Are Almost As Accurate and Robust As DFT-GGA Methods for Organic Molecules. 2011 , 7, 2929-36	83
1065	Protein-ligand interaction energies with dispersion corrected density functional theory and high-level wave function based methods. 2011 , 115, 11210-20	73
1064	On the mechanism of the copper-mediated C-S bond formation in the intramolecular disproportionation of imine disulfides. 2011 , 50, 9968-79	16
1063	Density functional theory studies of interactions of ruthenium-arene complexes with base pair steps. 2011 , 115, 11293-302	21
1062	Quantitative detection of human tumor necrosis factor by a resonance raman enzyme-linked immunosorbent assay. 2011 , 83, 297-302	78
1061	First principle kinetic studies of zeolite-catalyzed methylation reactions. 2011 , 133, 888-99	133
1060	Theoretical investigation into the mechanism of reductive elimination from bimetallic palladium complexes. 2011 , 50, 6449-57	45
1059	Nitrogenase structure and function relationships by density functional theory. 2011 , 766, 267-91	5
1058	Energy decomposition analysis based on a block-localized wavefunction and multistate density functional theory. 2011 , 13, 6760-75	171
1057	Electronic Structure of Organic Materials Investigated by Quantum Chemical Calculations. 2011 , 1-22	
1056	Density Functional Theory for Transition Metal Chemistry: The Case of a Water-Splitting Ruthenium Cluster. 2011 , 137-163	2
1055	Nature and strength of C-HIIIO interactions involving formyl hydrogen atoms: computational and experimental studies of small aldehydes. 2011 , 13, 14076-91	69
1054	Accurate Dispersion-Corrected Density Functionals for General Chemistry Applications. 2011 , 1-16	1

1053	Heats of Adsorption of CO and CO2 in MetalØrganic Frameworks: Quantum Mechanical Study of CPO-27-M (M = Mg, Ni, Zn). 2011 , 115, 21777-21784	112
1052	Aerobic Oxidation of Hydrocarbons Catalyzed by Mn-Doped Nanoporous Aluminophosphates (III): Propagation Mechanism. 2011 , 1, 1487-1497	15
1051	Quasiparticle band gap engineering of graphene and graphone on hexagonal boron nitride substrate. 2011 , 11, 5274-8	186
1050	Interfacial Electronic Structure of the Dipolar Vanadyl Naphthalocyanine on Au(111): P ush-Back vs Dipolar Effects. 2011 , 115, 21128-21138	38
1049	Does DFT-D estimate accurate energies for the binding of ligands to metal complexes?. 2011 , 40, 11176-83	72
1048	Redox noninnocence of nitrosoarene ligands in transition metal complexes. 2011 , 50, 5763-76	49
1047	Effect of layer stacking on the electronic structure of graphene nanoribbons. 2011 , 5, 6096-101	29
1046	Exploiting CH-IInteractions in supramolecular hydrogels of aromatic carbohydrate amphiphiles. 2011 , 2, 1349	70
1045	DFT Study on the Mechanism of the Activation and Cleavage of CO2 by (NHC)CuEPh3 (E = Si, Ge, Sn). 2011 , 30, 1340-1349	60
1044	Quantum mechanics/molecular mechanics methods can be more accurate than full quantum mechanics in systems involving dispersion correlations. 2011 , 13, 10520-6	18
1043	Electrostatic model for treating long-range lateral interactions between polar molecules adsorbed on metal surfaces. 2011 , 84,	45
1042	Density functional theory modeling of the adsorption of small analyte and indicator dye 9-(diphenylamino)acridine molecules on the surface of amorphous silica nanoparticles. 2011 , 13, 1440-7	17
1041	Energetic Molecules Encapsulated Inside Carbon Nanotubes and between Graphene Layers: DFT Calculations. 2011 , 115, 10985-10989	54
1040	Relativity and the mercury battery. 2011 , 13, 16510-2	13
1039	Point defects on graphene on metals. 2011 , 107, 116803	181
1038	Linear alkane polymerization on a gold surface. 2011 , 334, 213-6	278
1037	Phosphine and solvent effects on oxidative addition of CH3Br to Pd(PR3) and Pd(PR3)2 complexes. 2011 , 40, 11089-94	44
1036	Polymorphism of a Model Arylboronic Azaester: Combined Experimental and Computational Studies. 2011 , 11, 1835-1845	25

1035	Organometallic reactivity: the role of metal-ligand bond energies from a computational perspective. 2011 , 40, 11184-91	48
1034	Computational Study of Copper-Free Sonogashira Cross-Coupling Reaction. 2011 , 30, 5656-5664	29
1033	Water thin film-silica interaction on ⊞quartz (0001) surfaces. 2011 , 84,	27
1032	Does the TauD enzyme always hydroxylate alkanes, while an analogous synthetic non-heme reagent always desaturates them?. 2011 , 133, 176-9	51
1031	Like-charge guanidinium pairing from molecular dynamics and ab initio calculations. 2011 , 115, 11193-201	48
1030	Current approaches to predicting molecular organic crystal structures. 2011 , 17, 3-52	169
1029	Theoretical evaluation of structural models of the S2 state in the oxygen evolving complex of Photosystem II: protonation states and magnetic interactions. 2011 , 133, 19743-57	249
1028	Theoretical study of mechanism and selectivity of copper-catalyzed C-H bond amidation of indoles. 2011 , 76, 9246-52	42
1027	Interaction of 1,2,5-chalcogenadiazole derivatives with thiophenolate: hypercoordination with formation of interchalcogen bond versus reduction to radical anion. 2011 , 115, 4851-60	46
1026	A STM perspective on covalent intermolecular coupling reactions on surfaces. 2011 , 44, 464011	116
1025	Accurate Conformational Energy Differences of Carbohydrates: A Complete Basis Set Extrapolation. 2011 , 7, 988-97	21
1024	Application of London-type dispersion corrections to the solid-state density functional theory simulation of the terahertz spectra of crystalline pharmaceuticals. 2011 , 13, 4250-9	70
1023	Role of water in atomic resolution AFM in solutions. 2011 , 13, 12584-94	51
1022	Doping of graphene by a Au(111) substrate: Calculation strategy within the local density approximation and a semiempirical van der Waals approach. 2011 , 83,	82
1021	A DFT study of substituent effects in corannulene dimers. 2011 , 13, 21139-45	41
1020	CO2 adsorption on TiO2(110) rutile: insight from dispersion-corrected density functional theory calculations and scanning tunneling microscopy experiments. 2011 , 134, 104707	83
1019	Analytic energy gradient for second-order Mller-Plesset perturbation theory based on the fragment molecular orbital method. 2011 , 135, 044110	44
1018	Novel C-HTTC contacts involving 3,5-dimethylpyrazole ligands in a tetracoordinate Co(II) complex. 2011 , 40, 11605-12	22

1017	Combined Experimental and Computational Hydrostatic Compression Study of Crystalline Ammonium Perchlorate. 2011 , 115, 18782-18788	23
1016	Performance of Density Functional Theory and Mller-Plesset Second-Order Perturbation Theory for Structural Parameters in Complexes of Ru. 2011 , 7, 2325-32	116
1015	Formation of self-assembled chains of tetrathiafulvalene on a Cu(100) surface. 2011 , 115, 13080-7	5
1014	Dispersion corrections essential for the study of chemical reactivity in fullerenes. 2011 , 115, 3491-6	108
1013	Conformational analysis of a nitroxide side chain in an Ehelix with density functional theory. 2011 , 115, 397-405	31
1012	Vapor-liquid coexistence curves for methanol and methane using dispersion-corrected density functional theory. 2011 , 115, 11688-92	35
1011	Structural and electronic properties of the graphene/Al/Ni(111) intercalation system. 2011 , 13, 113028	95
1010	Which DFT functional performs well in the calculation of methylcobalamin? Comparison of the B3LYP and BP86 functionals and evaluation of the impact of empirical dispersion correction. 2011 , 115, 9308-13	66
1009	DFT study of the interaction free energy of Leomplexes of fullerenes with buckybowls and viologen dimers. 2011 , 35, 1453	32
1008	Tunable band gaps in bilayer transition-metal dichalcogenides. 2011 , 84,	442
	Tunable band gaps in bilayer transition-metal dichalcogenides. 2011 , 84, Quantum mechanical modeling of catalytic processes. 2011 , 2, 453-77	58
	Quantum mechanical modeling of catalytic processes. 2011 , 2, 453-77	
1007	Quantum mechanical modeling of catalytic processes. 2011 , 2, 453-77 On the dissociation of molecular hydrogen by Au supported on transition metal carbides: choice of the most active support. 2011 , 13, 6865-71 Tin Monoxide: Structural Prediction from First Principles Calculations with van der Waals	58
1007	Quantum mechanical modeling of catalytic processes. 2011 , 2, 453-77 On the dissociation of molecular hydrogen by Au supported on transition metal carbides: choice of the most active support. 2011 , 13, 6865-71 Tin Monoxide: Structural Prediction from First Principles Calculations with van der Waals Corrections. 2011 , 115, 19916-19924 A theoretical study on structural, spectroscopic and energetic properties of acetamide clusters.	58 25
1007	Quantum mechanical modeling of catalytic processes. 2011, 2, 453-77 On the dissociation of molecular hydrogen by Au supported on transition metal carbides: choice of the most active support. 2011, 13, 6865-71 Tin Monoxide: Structural Prediction from First Principles Calculations with van der Waals Corrections. 2011, 115, 19916-19924 A theoretical study on structural, spectroscopic and energetic properties of acetamide clusters [CH3CONH2] (n=1-15). 2011, 13, 15211-20	58 25 79
1007 1006 1005	Quantum mechanical modeling of catalytic processes. 2011, 2, 453-77 On the dissociation of molecular hydrogen by Au supported on transition metal carbides: choice of the most active support. 2011, 13, 6865-71 Tin Monoxide: Structural Prediction from First Principles Calculations with van der Waals Corrections. 2011, 115, 19916-19924 A theoretical study on structural, spectroscopic and energetic properties of acetamide clusters [CH3CONH2] (n=1-15). 2011, 13, 15211-20 Fe(CO)4 and related compounds as isolobal fragments. 2011, 50, 4428-36	58 25 79 34
1007 1006 1005 1004	Quantum mechanical modeling of catalytic processes. 2011, 2, 453-77 On the dissociation of molecular hydrogen by Au supported on transition metal carbides: choice of the most active support. 2011, 13, 6865-71 Tin Monoxide: Structural Prediction from First Principles Calculations with van der Waals Corrections. 2011, 115, 19916-19924 A theoretical study on structural, spectroscopic and energetic properties of acetamide clusters [CH3CONH2] (n=1-15). 2011, 13, 15211-20 Fe(CO)4 and related compounds as isolobal fragments. 2011, 50, 4428-36 GGA versus van der Waals density functional results for mixed gold/mercury molecules and pure Au and Hg cluster properties. 2011, 13, 20863-70	58 25 79 34 5

999	Multiscale magnetic study of Ni(111) and graphene on Ni(111). 2011 , 84,	46
998	Ab initio studies of aromatic excimers using multiconfiguration quasi-degenerate perturbation theory. 2011 , 115, 7687-99	60
997	Evaluation of theoretical approaches for describing the interaction of water with linear acenes. 2011 , 115, 5955-64	23
996	Steric and electronic effects in the host-guest hydrogen bonding in clathrate hydrates. 2011 , 115, 6149-54	16
995	Binding of 6-mer single-stranded homo-nucleotides to poly(3,4-ethylenedioxythiophene): specific hydrogen bonds with guanine. 2011 , 7, 9922	13
994	On the physisorption of water on graphene: a CCSD(T) study. 2011 , 13, 12041-7	152
993	Reaction mechanism of the reverse water-gas shift reaction using first-row middle transition metal catalysts L'M (M = Fe, Mn, Co): a computational study. 2011 , 50, 8782-9	24
992	Preparation of RSn(I)-Sn(I)R with two unsymmetrically coordinated Sn(I) atoms and subsequent gentle activation of P4. 2011 , 133, 17889-94	87
991	Testing a Variety of Electronic-Structure-Based Methods for the Relative Energies of 5-Formyluracil Crystals. 2011 , 7, 2685-8	20
990	Engineering Homologous Molecular Organization in 2D and 3D. Cocrystallization of Pyridyl-Substituted Diaminotriazines with Alkanecarboxylic Acids. 2011 , 115, 12908-12919	13
990		13
	Pyridyl-Substituted Diaminotriazines with Alkanecarboxylic Acids. 2011 , 115, 12908-12919	
989	Pyridyl-Substituted Diaminotriazines with Alkanecarboxylic Acids. 2011 , 115, 12908-12919 Azobenzene-functionalized carbon nanotubes as high-energy density solar thermal fuels. 2011 , 11, 3156-62 A Failure of DFT Is Not Necessarily a DFT Failure-Performance Dependencies on Model System	188
989 988	Pyridyl-Substituted Diaminotriazines with Alkanecarboxylic Acids. 2011, 115, 12908-12919 Azobenzene-functionalized carbon nanotubes as high-energy density solar thermal fuels. 2011, 11, 3156-62 A Failure of DFT Is Not Necessarily a DFT Failure-Performance Dependencies on Model System Choices. 2011, 7, 3019-25 Accurate Interaction Energies for Problematic Dispersion-Bound Complexes: Homogeneous Dimers	188
989 988 987	Azobenzene-functionalized carbon nanotubes as high-energy density solar thermal fuels. 2011, 11, 3156-62 A Failure of DFT Is Not Necessarily a DFT Failure-Performance Dependencies on Model System Choices. 2011, 7, 3019-25 Accurate Interaction Energies for Problematic Dispersion-Bound Complexes: Homogeneous Dimers of NCCN, P2, and PCCP. 2011, 7, 2842-51 Calibration of DFT Functionals for the Prediction of Fe MBsbauer Spectral Parameters in	188 15 41
989 988 987 986	Azobenzene-functionalized carbon nanotubes as high-energy density solar thermal fuels. 2011, 11, 3156-62 A Failure of DFT Is Not Necessarily a DFT Failure-Performance Dependencies on Model System Choices. 2011, 7, 3019-25 Accurate Interaction Energies for Problematic Dispersion-Bound Complexes: Homogeneous Dimers of NCCN, P2, and PCCP. 2011, 7, 2842-51 Calibration of DFT Functionals for the Prediction of Fe MBsbauer Spectral Parameters in Iron-Nitrosyl and Iron-Sulfur Complexes: Accurate Geometries Prove Essential. 2011, 7, 3232-3247	188 15 41 59
989 988 987 986 985	Pyridyl-Substituted Diaminotriazines with Alkanecarboxylic Acids. 2011, 115, 12908-12919 Azobenzene-functionalized carbon nanotubes as high-energy density solar thermal fuels. 2011, 11, 3156-62 A Failure of DFT Is Not Necessarily a DFT Failure-Performance Dependencies on Model System Choices. 2011, 7, 3019-25 Accurate Interaction Energies for Problematic Dispersion-Bound Complexes: Homogeneous Dimers of NCCN, P2, and PCCP. 2011, 7, 2842-51 Calibration of DFT Functionals for the Prediction of Fe MBsbauer Spectral Parameters in Iron-Nitrosyl and Iron-Sulfur Complexes: Accurate Geometries Prove Essential. 2011, 7, 3232-3247 Energy-Specific Linear Response TDHF/TDDFT for Calculating High-Energy Excited States. 2011, 7, 3540-7 How Different Are Aromatic Interactions from Aliphatic Interactions and Non-IStacking	188 15 41 59 83

981	Electronic structure of 2,2'-bipyridine organotransition-metal complexes. Establishing the ligand oxidation level by density functional theoretical calculations. 2011 , 50, 9773-93	146
980	Comparison of microhydration methods: protonated glycine as a working example. 2011 , 115, 3604-13	16
979	Accurate Prediction of Methane Adsorption in a Metal D rganic Framework with Unsaturated Metal Sites by Direct Implementation of an ab Initio Derived Potential Energy Surface in GCMC Simulation. 2011 , 115, 23074-23080	82
978	Noncovalent interactions in paired DNA nucleobases investigated by terahertz spectroscopy and solid-state density functional theory. 2011 , 115, 9467-78	43
977	Energy barriers for trimethylaluminum reaction with varying surface hydroxyl density. 2011 , 258, 225-229	20
976	Theoretical study of tetracyclo[3.3.3.13,10.17,10]tridecane (bowlane) and its methylene spacer edge and lip expanded (CH2)h(n=14) homologs. 2011 , 969, 53-55	1
975	QTAIMC study of the Xℍ/H?O bond order indices (X=O, N, C) in molecular systems. 2011 , 973, 33-39	20
974	A comparison of density functional theory (DFT) methods for estimating the singlet@riplet (SOII1) excitation energies of benzene and polyacenes. 2011 , 976, 105-112	31
973	Gas-phase conformational and intramolecular Interaction studies on some pyrazolo[3,4-d]pyrimidine derivatives. 2011 , 977, 134-139	25
972	Density Functional Theory. 2011 , 255-368	3
971	Hierarchical interactions and their influence upon the adsorption of organic molecules on a graphene film. 2011 , 133, 9208-11	55
970	Interactions of the N3 dye with the iodide redox shuttle: quantum chemical mechanistic studies of the dye regeneration in the dye-sensitized solar cell. 2011 , 13, 15148-57	28
969	Structural flexibility and role of vicinal 2-thienyl rings in 2,3-dicyano-5,6-di(2-thienyl)-1,4-pyrazine, [(CN)2Th2Pyz], its palladium(II) complex [(CN)2Th2Pyz(PdCl2)2], and the related pentametallic pyrazinoporphyrazines [(PdCl2)4Th8TPyzPzM] (M = Mg(II)(H2O), Zn(II)). 2011 , 50, 12116-25	7
968	Can ferric-superoxide act as a potential oxidant in P450(cam)? QM/MM investigation of hydroxylation, epoxidation, and sulfoxidation. 2011 , 133, 5444-52	48
967	Fingerprints of Dirac points in first-principles calculations of scanning tunneling spectra of graphene on a metal substrate. 2011 , 84,	17
966	Nucleic Acid G-quartets: Insights into Diverse Patterns and Optical Properties. 2011 , 115, 12530-12546	62
966	Nucleic Acid G-quartets: Insights into Diverse Patterns and Optical Properties. 2011 , 115, 12530-12546 Validation of electronic structure methods for isomerization reactions of large organic molecules. 2011 , 13, 13683-9	62 67

963	Efficient and Accurate Double-Hybrid-Meta-GGA Density Functionals-Evaluation with the Extended GMTKN30 Database for General Main Group Thermochemistry, Kinetics, and Noncovalent Interactions. 2011 , 7, 291-309	841
962	Dimerization of Radical-Anions: Nitride Clusterfullerenes versus Empty Fullerenes. 2011 , 2, 1592-1600	20
961	Real-world predictions from ab initio molecular dynamics simulations. 2012 , 307, 109-53	74
960	Dispersion interactions in density-functional theory: an adiabatic-connection analysis. 2011 , 135, 194109	18
959	Synthesis and characterization of chiral mono N-heterocyclic carbene-substituted rhodium complexes and their catalytic properties in hydrosilylation reactions. 2011 , 696, 3945-3954	17
958	Adventitious formation of a new oxopentadienyl Mn(I) tricarbonyl complex: Structural study and bonding investigation of (IB-CH2C(Fc)CHC(Fc)O)Mn(CO)3. 2011 , 696, 3268-3273	2
957	Benzene under high pressure: a story of molecular crystals transforming to saturated networks, with a possible intermediate metallic phase. 2011 , 133, 9023-35	125
956	How reliable are DFT transition structures? Comparison of GGA, hybrid-meta-GGA and meta-GGA functionals. 2011 , 9, 689-700	186
955	Spectroscopic detection of DNA quadruplexes by vibrational circular dichroism. 2011 , 133, 15055-64	38
954	Benchmark results for empirical post-GGA functionals: difficult exchange problems and independent tests. 2011 , 13, 19325-37	71
953	Ring-expanded bicyclic <code>#actams</code> : a structure-chiroptical properties relationship investigation by experiment and calculations. 2011 , 76, 3306-19	21
952	Computational Approaches Towards Modeling Finite Molecular Assemblies: Role of Cation-₪ and Hydrogen Bonding Interactions. 2011 , 517-555	2
951	Substituent effects in cation-linteractions: a unified view from inductive, resonance, and through-space effects. 2011 , 115, 5660-4	26
950	Interacting Lewis-X carbohydrates in condensed phase: a first-principles molecular dynamics study. 2011 , 115, 12599-606	2
949	Enzyme-free colorimetric assay of serum uric acid. 2011 , 47, 11498-500	34
948	Polymorphism of Crystalline 4-Amino-2-Nitroacetanilide. 2011 , 11, 2074-2083	10
947	Nature of adhesion of condensed organic films on platinum by first-principles simulations. 2011 , 13, 11827-37	7
946	Comprehensive Benchmarking of a Density-Dependent Dispersion Correction. 2011 , 7, 3567-77	322

945	Density, structure, and dynamics of water: the effect of van der Waals interactions. 2011 , 134, 024516	220
944	DFT study of [2.2]-, [3.3]-, and [4.4]paracyclophanes: strain energy, conformations, and rotational barriers. 2011 , 115, 2396-401	51
943	An examination of density functional theories on isomerization energy calculations of organic molecules. 2011 , 130, 851-857	24
942	Dissociation of strong acid revisited: X-ray photoelectron spectroscopy and molecular dynamics simulations of HNO3 in water. 2011 , 115, 9445-51	42
941	A Comparative Study of Lattice Dynamics of Three- and Two-Dimensional MoS2. 2011 , 115, 16354-16361	250
940	Local nature of substituent effects in stacking interactions. 2011 , 133, 10262-74	356
939	On the Binding Strength Sequence for Nucleic Acid Bases and C(60) with Density Functional and Dispersion-corrected Density Functional Theories: Whether C(60) could protect nucleic acid bases from radiation-induced damage?. 2011 , 115, 3220-3228	24
938	What Makes for a Bad Catalytic Cycle? A Theoretical Study on the SuzukiMiyaura Reaction within the Energetic Span Model. 2011 , 1, 246-253	106
937	Detailed ab initio first-principles study of the magnetic anisotropy in a family of trigonal pyramidal iron(II) pyrrolide complexes. 2011 , 50, 7460-77	120
936	Selectivity in DNA replication. Interplay of steric shape, hydrogen bonds, Estacking and solvent effects. 2011 , 47, 7326-8	47
935	Accurate static and dynamic properties of liquid electrolytes for Li-ion batteries from ab initio molecular dynamics. 2011 , 115, 3085-90	104
934	Anthracene-resorcin[4]arene-based capsules: synthesis and photoswitchable features. 2011 , 9, 7491-9	24
933	Hydrogen-bond strengths by magnetically induced currents. 2011 , 13, 434-7	34
932	Further evidences of the quality of double-hybrid energy functionals for Łonjugated systems. 2011 , 134, 234102	6
931	Performance of the van der Waals Density Functional VV10 and (hybrid)GGA Variants for Thermochemistry and Noncovalent Interactions. 2011 , 7, 3866-71	175
930	Organometallic complexes of graphene: toward atomic spintronics using a graphene web. 2011 , 5, 9939-49	67
929	Comparison of the performance of dispersion-corrected density functional theory for weak hydrogen bonds. 2011 , 13, 13942-50	119
928	Origins of aryl substituent effects on the stereoselectivities of additions of silyl enol ethers to a chiral oxazolinium ion. 2011 , 13, 6572-5	8

927	Does Nitric Acid Dissociate at the Aqueous Solution Surface?. 2011 , 115, 21183-21190	64
926	Semiempirical, Hartree-Fock, density functional, and second order Moller-Plesset perturbation theory methods do not accurately predict ionization energies and electron affinities of short-through long-chain [n]acenes. 2011 ,	1
925	Intermolecular vs molecule-substrate interactions: A combined STM and theoretical study of supramolecular phases on graphene/Ru(0001). 2011 , 2, 365-73	34
924	First-principles Theoretical Study of Organic-metal Interfaces. 2011 , 32, 9-14	
923	An introduction to quantum chemical methods applied to drug design. 2011 , 3, 1061-78	
922	Modeling Photobiology Using Quantum Mechanics and Quantum Mechanics/Molecular Mechanics Calculations. 2011 , 397-433	1
921	Derivatives and dimers of C50-D5h and C50-D3: a comparison of two closely related but quite differently behaving fullerenes. 2011 , 135, 044310	6
920	Surface-assisted cyclodehydrogenation provides a synthetic route towards easily processable and chemically tailored nanographenes. 2011 , 3, 61-7	345
919	Giant magnetoresistance through a single molecule. 2011 , 6, 185-9	262
918	The relative stability of zeolite precursor tetraalkylammoniumBilicate oligomer complexes. 2011 , 146, 82-87	21
917	A higher energy conformer of (S)-proline is the active catalyst in intermolecular aldol reaction: Evidence from DFT calculations. 2011 , 345, 37-43	20
916	Silver(I)-mediated Hoogsteen-type base pairs. 2011 , 105, 1398-404	56
915	The ground states of iron(III) porphines: role of entropy-enthalpy compensation, Fermi correlation, dispersion, and zero-point energies. 2011 , 105, 1286-92	24
914	Theoretical studies on the dimerization of substituted paraphenylenediamine radical cations. 2011 , 83, 368-78	3
913	In situ infrared spectroscopy study of sucrose up to 14GPa. 2011 ,	
912	Structure of singly hydrated, protonated phospho-tyrosine. 2011 , 308, 338-347	20
911	Anisotropic crystal deformation measurements determined using powder X-ray diffraction and a new in situ compression stage. 2011 , 418, 199-206	11
910	Dehydrogenation of propane over ZnMOR. Static and dynamic reaction energy diagram. 2011 , 277, 104-116	40

909	Monomolecular cracking of propane over acidic chabazite: An ab initio molecular dynamics and transition path sampling study. 2011 , 279, 220-228	85
908	Microkinetic modeling of the fast selective catalytic reduction of nitrogen oxide with ammonia on H-ZSM5 based on first principles. 2011 , 283, 178-191	19
907	The influence of density functional approximations on the description of LiH + NH3 -> LiNH2 + H2 reaction. 2011 , 511, 427-433	8
906	The geometric and electronic structure of Xe-adsorbed Fe(001) surface by first-principles calculations. 2011 , 512, 99-103	1
905	ConvexBoncave stacking of curved conjugated networks: Benchmark calculations on the corannulene dimer. 2011 , 512, 155-160	63
904	Packing effects in organic donor\(\text{Bcceptor molecular heterojunctions.}\) 2011, 514, 146-150	6
903	A new polymorph (IV) of benzamide: Structural characterization and mechanism of the I <-> IV phase transition. 2011 , 514, 274-277	9
902	Raman and infrared spectra of cellobiose in the solid state: What can be learned from single-molecule calculations?. 2011 , 514, 284-290	12
901	Cooperativity in the stacking of benzene-1,3,5-tricarboxamide: The role of dispersion. 2011 , 515, 226-230	37
900	2D vs. 3D titanium dioxide: Role of dispersion interactions. 2011 , 516, 72-75	18
899	A combined quantum chemical and crystallographic study on the oxidized binuclear center of cytochrome c oxidase. 2011 , 1807, 769-78	30
898	Stabilization of the peroxy intermediate in the oxygen splitting reaction of cytochrome cbb(3). 2011 , 1807, 813-8	14
897	Proline-based chiral stationary phases: a molecular dynamics study of the interfacial structure. 2011 , 1218, 6331-47	22
896	Computational Study on the Catalytic Role of Pincer Ruthenium(II)-PNN Complex in Directly Synthesizing Amide from Alcohol and Amine: The Origin of Selectivity of Amide over Ester and Imine. 2011 , 30, 5233-5247	138
895	High Capacity Hydrogen Storage in Ca Decorated Graphyne: A First-Principles Study. 2011 , 115, 23221-23225	179
894	A thorough benchmark of density functional methods for general main group thermochemistry, kinetics, and noncovalent interactions. 2011 , 13, 6670-88	1347
893	Assessment of the Performance of DFT and DFT-D Methods for Describing Distance Dependence of Hydrogen-Bonded Interactions. 2011 , 7, 88-96	342
892	Semiempirical self-consistent polarization description of bulk water, the liquid-vapor interface, and cubic ice. 2011 , 115, 6046-53	21

891	Optical rotation calculated with time-dependent density functional theory: the OR45 benchmark. 2011 , 115, 10930-49	97
890	Confinement effect on p-nitroaniline electronic spectrum and electric properties. 2011 , 115, 5210-20	18
889	Reversible Hydrogen Storage by Controlled Buckling of Graphene Layers. 2011 , 115, 25523-25528	133
888	TRAVIS - a free analyzer and visualizer for Monte Carlo and molecular dynamics trajectories. 2011 , 51, 2007-23	692
887	Density-functional approaches to noncovalent interactions: a comparison of dispersion corrections (DFT-D), exchange-hole dipole moment (XDM) theory, and specialized functionals. 2011 , 134, 084107	526
886	Excited-State Electronic Structure with Configuration Interaction Singles and Tamm-Dancoff Time-Dependent Density Functional Theory on Graphical Processing Units. 2011 , 7, 1814-1823	154
885	A main group metal sandwich: five lithium cations jammed between two corannulene tetraanion decks. 2011 , 333, 1008-11	187
884	Do H-bond features of silica surfaces affect the H2O and NH3 adsorption? Insights from periodic B3LYP calculations. 2011 , 115, 11221-8	18
883	X-ray emission spectroscopy evidences a central carbon in the nitrogenase iron-molybdenum cofactor. 2011 , 334, 974-7	659
882	Electronic structure and absorption spectra of supramolecular complexes of a fullerene crown ether with a Eextended TTF derivative. 2011 , 13, 11965-75	14
881	On the accuracy of DFT-SAPT, MP2, SCS-MP2, MP2C, and DFT+Disp methods for the interaction energies of endohedral complexes of the C(60) fullerene with a rare gas atom. 2011 , 13, 732-43	77
880	Radical-transfer hydroamination of olefins with N-aminated dihydropyridines. 2011 , 6, 1197-209	45
879	The Origin of Regioselectivity in 2-Butanol Dehydration on Solid Acid Catalysts. 2011, 3, 1557-1561	26
878	Approximations to complete basis set-extrapolated, highly correlated non-covalent interaction energies. 2011 , 135, 134318	69
877	Polar distortions in hydrogen-bonded organic ferroelectrics. 2011 , 84,	43
876	Key building block of photoresponsive biomimetic systems. 2011 , 115, 1232-42	6
875	四And 四nteractions are equally important: multilayered graphanes. 2011 , 133, 20036-9	65
874	Dispersion-corrected density functional theory comparison of hydrogen adsorption on boron-nitride and carbon nanotubes. 2011 , 84,	23

873	Selective alignment of carbon nanotubes on sapphire surfaces: bond formation between nanotubes and substrates. 2011 , 107, 065501	5
872	Prediction of the Unknown Crystal Structure of Creatine Using Fully Quantum Mechanical Methods. 2011 , 11, 5733-5740	33
871	Exciton Dissociation at Thiophene/Fullerene Interfaces: The Electronic Structures and Quantum Dynamics. 2011 , 115, 10205-10210	94
870	DFT study of gas-phase adsorption of benzotriazole on Cu(111), Cu(100), Cu(110), and low coordinated defects thereon. 2011 , 13, 20408-17	57
869	Hydrates and ammonium salts of 4-nitrobenzenesulfonic acid: supramolecular organization and its relation to proton conductivity. 2011 , 60, 1185-1195	4
868	Calculations of ionization energies and electron affinities for atoms and molecules: A comparative study with different methods. 2011 , 6, 269-279	17
867	Comparative theoretical and experimental analysis of hydrocarbon Fadical cations. 2011, 47, 1293-1299	8
866	Prediction of Charge Mobility in Amorphous Organic Materials through the Application of Hopping Theory. 2011 , 7, 2556-67	23
865	Efficient Calculation of QM/MM Frequencies with the Mobile Block Hessian. 2011 , 7, 496-514	29
864	How Well Can Modern Density Functionals Predict Internuclear Distances at Transition States?. 2011 , 7, 1667-76	140
863	A Modern First-Principles View on Ligand Field Theory Through the Eyes of Correlated Multireference Wavefunctions. 2011 , 149-220	66
862	Locality and Fluctuations: Trends in Imidazolium-Based Ionic Liquids and Beyond. 2011 , 7, 3040-4	80
861	Dispersion Interactions with Density-Functional Theory: Benchmarking Semiempirical and Interatomic Pairwise Corrected Density Functionals. 2011 , 7, 3944-51	230
860	Density Functional Theory for Reaction Energies: Test of Meta and Hybrid Meta Functionals, Range-Separated Functionals, and Other High-Performance Functionals. 2011 , 7, 669-676	165
859	Nitrile-functionalized pyridinium, pyrrolidinium, and piperidinium ionic liquids. 2011 , 115, 8424-38	52
858	Computational methods to calculate accurate activation and reaction energies of 1,3-dipolar cycloadditions of 24 1,3-dipoles. 2011 , 115, 13906-20	104
857	Density functional theory with London dispersion corrections. 2011 , 1, 211-228	1645
856	Theoretical study of substituent and solvent effects on the thermodynamics for cis/trans isomerization and intramolecular rearrangements of 2,2?-diphenoquinones. 2011 , 22, 615-625	4

855	Conformational analysis of N,N?-dinaphthyl heterocyclic carbenes: imidazol-2-ylidenes and imidazolin-2-ylidenes. 2011 , 22, 1087-1094	6
854	Methanol Adsorption on V2O3(0001). 2011 , 54, 669-684	18
853	Substrate binding and activation in the active site of cytochrome c nitrite reductase: a density functional study. 2011 , 16, 417-30	36
852	Oxygen cleavage with manganese and iron in ribonucleotide reductase from Chlamydia trachomatis. 2011 , 16, 553-65	24
851	Lessons on O2 and NO bonding to heme from ab initio multireference/multiconfiguration and DFT calculations. 2011 , 16, 841-55	48
850	Atomistic simulations of materials for optical chemical sensors: DFT-D calculations of molecular interactions between gas-phase analyte molecules and simple substrate models. 2011 , 17, 1855-62	4
849	A density functional theory study of the hythicLindlar hydrogenation catalyst. 2011 , 128, 663-673	114
848	Bonding in cationic MOH + n (M = K \mathbb{L} a, Hf \mathbb{R} n; n = 0 \mathbb{Z}): DFT performances and periodic trends. 2011 , 129, 389-399	40
847	Computational studies of the interactions of Iland I3 liwith TiO2 clusters: implications for dye-sensitized solar cells. 2011 , 129, 199-208	14
846	Adsorption of catechol on a wet silica surface: density functional theory study. 2011 , 130, 333-339	39
845	High-pressure transitions in bulk mercury: a density functional study. 2011 , 130, 455-462	11
844	Binding energy of gas molecule with two pyrazine molecules as organic linker in metal b rganic framework: its theoretical evaluation and understanding of determining factors. 2011 , 130, 475-482	9
843	Ion beam induced defects in graphene: Raman spectroscopy and DFT calculations. 2011 , 993, 506-509	22
842	Determination of relative configuration of symmetrical bis-Trgers base derivatives. 2011 , 996, 69-74	7
841	noloco: An efficient implementation of van der Waals density functionals based on a Monte-Carlo integration technique. 2011 , 182, 1657-1662	20
840	Applications and validations of the Minnesota density functionals. 2011 , 502, 1-13	568
839	A theoretical study of the structure and conductivity of polycytosineacetylene. 2011 , 506, 243-247	2
838	Solvent induced structural dynamics of ruthenium pentacarbonyl in benzene. 2011 , 508, 43-48	4

837	What happens to hydrophobic interactions during transfer from the solution to the gas phase? The case of electrospray-based soft ionization methods. 2011 , 22, 1167-77	40
836	Heteroleptic Organostannylenes and an Organoplumbylene Bearing Phosphorus-Containing Pincer-Type Ligands Istructural Variations and Insights into the Configurational Stability. 2011 , 637, n/a-n/a	16
835	Graphene on ferromagnetic surfaces and its functionalization with water and ammonia. 2011, 6, 214	22
834	Structure and X-ray spectrum of crystalline poly(3-hexylthiophene) from DFT-van der Waals calculations. 2011 , 248, 1360-1368	58
833	Electron correlation and the stability of substituted alkenes. 2011 , 24, 1222-1228	4
832	Interactions within the alcohol dehydrogenase Zn(II)-metalloenzyme active site: Interplay between subvalence, electron correlation/dispersion, and charge transfer/induction effects. 2011 , 111, 1213-1221	13
831	Atomic radii in molecules for use in a polarizable force field. 2011 , 111, 1763-1772	8
830	Analysis of pair interaction in a bipolar mesogen 4-(4-hydroxylbutyloxy)-4?-cyano-biphenyl: A comparative study based on semiempirical and DFT methods. 2011 , 111, 4113-4123	5
829	Chemoinformatics as a Theoretical Chemistry Discipline. 2011 , 30, 20-32	64
828	An Easy, Stereoselective Synthesis of Hexahydroisoindol-4-ones under Phosphine Catalysis. 2011 , 353, 483-493	17
827	Ethene-Induced Temporary Inhibition of Grubbs Metathesis Catalysts. 2011 , 353, 2701-2707	35
826	Synthesis, Molecular Structure, and Physical Properties of the Complexes [{PhB(pz)2(CH2SMe)}2M] (M = MnII, FeII; pz = pyrazol-1-yl) Containing a Novel [N,N,S]-Heteroscorpionate Ligand. 2011 , 2011, 1709-1718	₃ 8
825	Substrate Hydroxylation by the Oxidolron Intermediate in Aromatic Amino Acid Hydroxylases: A DFT Mechanistic Study. 2011 , 2011, 2720-2732	5
824	A Metallocorrole with Orthogonal Pyrrole Rings. 2011 , 2011, 1865-1870	46
823	Reduction of Nitriles to Amines with H2 Catalyzed by Nonclassical Ruthenium Hydrides Water-Promoted Selectivity for Primary Amines and Mechanistic Investigations. 2011 , 2011, 3381-3386	87
822	Synthesis, Structures, and Aggregation Properties of N-Acylamidines. 2011 , 2011, 861-877	7
821	Assigning predissociation infrared spectra of microsolvated hydronium cations H3O(+)?(H2)n (n=0, 1, 2, 3) by ab initio molecular dynamics. 2011 , 12, 1906-15	20
820	Adsorption of supramolecular building blocks on graphite: a force field and density functional theory study. 2011 , 12, 2242-5	12

819	Reduction potentials and acidity constants of Mn superoxide dismutase calculated by QM/MM free-energy methods. 2011 , 12, 3337-47		34
818	Packed to the rafters: filling up C60 with rare gas atoms. 2011 , 12, 2081-4		13
817	Ultrafast dynamics of UV-excited imidazole. 2011 , 12, 3365-75		32
816	System-dependent dispersion coefficients for the DFT-D3 treatment of adsorption processes on ionic surfaces. 2011 , 12, 3414-20		188
815	The reaction mechanism of Cytochrome P450 NO reductase: a detailed quantum mechanics/molecular mechanics study. 2011 , 12, 3192-203		32
814	Triazole, benzotriazole, and naphthotriazole as copper corrosion inhibitors: I. Molecular electronic and adsorption properties. 2011 , 12, 3547-55		35
813	Empirical hydrogen-bond potential functionsan old hat reconditioned. 2011 , 12, 3131-42		22
812	Substituent effects on non-covalent interactions with aromatic rings: insights from computational chemistry. 2011 , 12, 3116-30		116
811	Importance of structural motifs in liquid hydrogen fluoride. 2011 , 12, 3474-82		26
810	What are the preferred horizontal displacements in parallel aromatic-aromatic interactions? Significant interactions at large displacements. 2011 , 12, 3511-4		62
809	Benchmarking density functional methods against the S66 and S66x8 datasets for non-covalent interactions. 2011 , 12, 3421-33		252
808	Inter- and intramolecular dispersion interactions. <i>Journal of Computational Chemistry</i> , 2011 , 32, 1117-27	3.5	32
807	Sensitivity analysis and uncertainty calculation for dispersion corrected density functional theory. Journal of Computational Chemistry, 2011 , 32, 1424-30	3.5	39
806	A comparison of the behavior of functional/basis set combinations for hydrogen-bonding in the water dimer with emphasis on basis set superposition error. <i>Journal of Computational Chemistry</i> , 2011 , 32, 1519-27	3.5	109
805	Effect of the damping function in dispersion corrected density functional theory. <i>Journal of Computational Chemistry</i> , 2011 , 32, 1456-65	3.5	10429
804	Physical origins of the stability of aromatic amino acid core ring-polycyclic hydrocarbon complexes: a post-Hartree-Fock and density functional study. <i>Journal of Computational Chemistry</i> , 2011 , 32, 1887-9	5 ^{3.5}	8
803	Interaction of quinacridone derivatives. <i>Journal of Computational Chemistry</i> , 2011 , 32, 2055-63	3.5	10
802	Proton-coupled electron transfer of the phenoxyl/phenol couple: effect of Hartree-Fock exchange on transition structures. <i>Journal of Computational Chemistry</i> , 2011 , 32, 3081-91	3.5	11

801	Zinc-homocysteine binding in cobalamin-dependent methionine synthase and its role in the substrate activation: DFT, ONIOM, and QM/MM molecular dynamics studies. <i>Journal of 3.5 Computational Chemistry</i> , 2011 , 32, 3154-67	13	
800	New insights in quantum chemical topology studies using numerical grid-based analyses. <i>Journal of Computational Chemistry</i> , 2011 , 32, 3207-17	40	
799	Interactions between free radicals and a graphene fragment: physical versus chemical bonding, charge transfer, and deformation. <i>Journal of Computational Chemistry</i> , 2011 , 32, 3264-8	27	
798	Ab Initio Energy Landscape of GeF2: A System Featuring Lone Pair Structure Candidates. 2011 , 123, 4723-4	728 ₄	
797	Hoch asymmetrische NHC-katalysierte Hydroacylierung nichtaktivierter Alkene. 2011 , 123, 5087-5091	56	
796	A Biologically Relevant Co1+???H Bond: Possible Implications in the Protein-Induced Redox Tuning of Co2+/Co1+ Reduction. 2011 , 123, 8861-8864	3	
795	Selbstorganisation und spontane 2D-Racematspaltung eines Dicyano[7]helicens auf Cu(111). 2011 , 123, 10158-10162	18	
794	Taking the Aromaticity out of Aromatic Interactions. 2011 , 123, 7993-7995	31	
793	Solvation and Stabilization of Metallic Nanoparticles in Ionic Liquids. 2011 , 123, 8842-8846	19	
792	Ab initio energy landscape of GeF2 : a system featuring lone pair structure candidates. 2011 , 50, 4627-32	16	
791	Highly asymmetric NHC-catalyzed hydroacylation of unactivated alkenes. 2011, 50, 4983-7	160	
790	A biologically relevant Co1+IIIH bond: possible implications in the protein-induced redox tuning of Co2+/Co1+ reduction. 2011 , 50, 8702-5	16	
7 ⁸ 9	Self-assembly and two-dimensional spontaneous resolution of cyano-functionalized [7]helicenes on Cu111. 2011 , 50, 9982-6	82	
788	Taking the aromaticity out of aromatic interactions. 2011 , 50, 7847-9	151	
787	Solvation and stabilization of metallic nanoparticles in ionic liquids. 2011 , 50, 8683-7	118	
786	Docking on the DNA G-quadruplex: a molecular electrostatic potential study. 2011 , 95, 641-50	6	
7 ⁸ 5	Can enantioselectivity be computed in enthalpic barrierless reactions? The case of Cu(I)-catalyzed cyclopropanation of alkenes. 2011 , 17, 529-39	14	
7 ⁸ 4	Induction-driven stabilization of the anion-Interaction in electron-rich aromatics as the key to fluoride inclusion in imidazolium-cage receptors. 2011 , 17, 1163-70	144	

783	Pnicogen bonds: a new molecular linker?. 2011 , 17, 6034-8	350
782	Three-dimensional potential energy surface of selected carbohydrates' CH/dispersion interactions calculated by high-level quantum mechanical methods. 2011 , 17, 5680-90	26
781	Formation of the iron-oxo hydroxylating species in the catalytic cycle of aromatic amino acid hydroxylases. 2011 , 17, 3746-58	12
780	Contiguous metal-mediated base pairs comprising two Ag(I) ions. 2011 , 17, 6533-44	104
779	Going full circle: phase-transition thermodynamics of ionic liquids. 2011 , 17, 6508-17	42
778	Pyrazolate-based cobalt(II)-containing metal-organic frameworks in heterogeneous catalytic oxidation reactions: elucidating the role of entatic states for biomimetic oxidation processes. 2011 , 17, 8671-95	127
777	Mechanistic insights into ring-closing enyne metathesis with the second-generation Grubbs-Hoveyda catalyst: a DFT study. 2011 , 17, 7506-20	55
776	CO2 and formate complexes of phosphine/borane frustrated Lewis pairs. 2011 , 17, 9640-50	135
775	Neutral nickel oligo- and polymerization catalysts: the importance of alkyl phosphine intermediates in chain termination. 2011 , 17, 14628-42	15
774	Enantioselective and diastereoselective Tsuji-Trost allylic alkylation of lactones: an experimental and computational study. 2011 , 17, 11243-9	30
773	CO2 insertion into metal-carbon bonds: a computational study of Rh(I) pincer complexes. 2011 , 17, 10329-38	42
772	Ionic liquids containing the triply negatively charged tricyanomelaminate anion and a B(C6F5)3 adduct anion. 2011 , 17, 13526-37	10
771	Telomere structure and stability: covalency in hydrogen bonds, not resonance assistance, causes cooperativity in guanine quartets. 2011 , 17, 12612-22	114
770	Supramolecular engineering through temperature-induced chemical modification of 2H-tetraphenylporphyrin on Ag(111): flat phenyl conformation and possible dehydrogenation reactions. 2011 , 17, 14354-9	52
769	Room-temperature palladium-catalyzed Negishi-type coupling: a combined experimental and theoretical study. 2011 , 17, 14389-93	20
768	Enantioselective 1 receptor binding and biotransformation of the spirocyclic PET tracer 1'-benzyl-3-(3-fluoropropyl)-3H-spiro[[2]benzofuran-1,4'-piperidine]. 2011 , 23, 148-54	11
767	Experimental and theoretical investigations of circular dichroism of donor-acceptor 1,1'-binaphthyls: influence of substitution on the coupling amplitude and cotton effect of the charge-transfer band. 2011 , 23 Suppl 1, E22-7	6
766	Carbon dioxide capture-related gas adsorption and separation in metal-organic frameworks. 2011 , 255, 1791-1823	1614

765	Vacancy clusters as entry ports for cesium intercalation in graphite. 2011, 49, 3937-3952	25
764	A through-space charge transfer mechanism for explaining the oxidation of 2-chlorophenol on a tetrasulphonated nickel(III) phthalocyanine. 2011 , 963, 161-167	6
763	A new semi-empirical model for the oxidation of polycyclic aromatic hydrocarbon (PAHs) molecules physisorbed on soot. II. Application to the reaction PAH + OH for a series of large PAH molecules. 2011 , 965, 259-267	3
762	Proline- and thioproline-derived enamines: The theoretical study of torsional and ring-puckering conformations. 2011 , 964, 133-140	2
761	Dispersion energy effects on methane interaction within zeolite straight micropores: A computational investigation. 2011 , 967, 191-198	7
760	Theoretical study of the adsorption and dissociation of azobenzene on the rutile TiO2(110) surface. 2011 , 501, 379-384	16
759	Theoretical study of weak chemical interactions in solid formamide. 2011 , 508, 54-58	10
758	W4-11: A high-confidence benchmark dataset for computational thermochemistry derived from first-principles W4 data. 2011 , 510, 165-178	285
757	Theoretical study on the adsorption of pyridine derivatives on graphene. 2011 , 510, 220-223	32
756	Classical and quantum mechanical rainbow-scattering of fast He atoms from a KCl(001) surface. 2011 , 269, 799-803	9
755	Density-functional theoretical study of fluorination effect on organic/metal interfaces. 2011 , 12, 295-299	12
754	Synthesis of a 2-benzocymantrenylpyridine and further mechanistic insights. 2011 , 696, 2101-2107	9
753	Chemically accurate and computationally-efficient time-dependent density functional theory (TDDFT) modeling of the UV/Vis spectra of Pechmann dyes and related compounds. 2011 , 4, 1157-1166	2
75 ²	The PAW/GIPAW approach for computing NMR parameters: a new dimension added to NMR study of solids. 2011 , 40, 1-20	303
751	Methane adsorption on graphene from first principles including dispersion interaction. 2011 , 605, 746-749	113
750	Acetylene adsorption on silicon (100)-(4½) revisited. 2011 , 605, 1341-1346	12
749	Three-component conformational equilibria of some flexible pyrrolidin-2-(thi)ones in solution by NMR data (ℂ, ℍ, and nJHH) and their DFT predictions: a confrontation of different approaches. 2011 , 67, 6901-6916	16
748	Resolution of pentafluorophenyl 2-phenylpropanoate using combinations of quasi-enantiomeric oxazolidin-2-ones. 2011 , 22, 413-438	3

747	Quantum mechanical inspection of the DielsAlder approach to biaryls mechanism. 2011, 52, 1245-1249	7
746	Assessment of Some Density Functional Theory Methods and Force Field Models in Describing Various Interaction Modes of Benzene Dimer. 2011 , 24, 635-639	7
745	On the mechanism of the reaction of white phosphorus with silylenes. 2011 , 40, 7193-200	9
744	Charging energy and barrier height of pentacene on Au(111): a local-orbital hybrid-functional density functional theory approach. 2011 , 135, 084702	13
743	Hydrogen bonded structure and dynamics of liquid-vapor interface of water-ammonia mixture: an ab initio molecular dynamics study. 2011 , 135, 114510	35
742	Chasing charge localization and chemical reactivity following photoionization in liquid water. 2011 , 135, 224510	70
741	Electronic transport through single noble gas atoms. 2011 , 84,	2
740	Organic-inorganic compounds with strong nonlinear optical properties based on 2,4,6-trimethylpyridinium and tetrahedral BF4[hetworks. 2011 , 83,	5
739	Strain engineering water transport in graphene nanochannels. 2011 , 84, 056329	86
738	Binding configuration, electronic structure, and magnetic properties of metal phthalocyanines on a Au(111) surface studied with ab initio calculations. 2011 , 84,	62
737	s-orbital continuum model accounting for the tip shape in simulated scanning tunneling microscope images. 2011 , 84,	8
736	Static charging of graphene and graphite slabs. 2011 , 98, 131908	22
735	Efficient, long-range correlation from occupied wave functions only. 2011 , 84,	7
734	Adsorption of Alq3 on Mg(001) surface: Role of chemical bonding, molecular distortion, and van der Waals interaction. 2011 , 83,	6
733	Graphene and graphene nanoribbons on InAs(110) and Au/InAs(110) surfaces: An ab initio study. 2011 , 84,	6
732	Engineering the magnetic properties of hybrid organic-ferromagnetic interfaces by molecular chemical functionalization. 2011 , 84,	44
731	Role of dispersion forces in the structure of graphene monolayers on Ru surfaces. 2011 , 106, 186102	123
730	Pressure-induced transitions in solid nitrogen: Role of dispersive interactions. 2011 , 84,	26

729	Templating an organic layer with the Si(111)-7 surface reconstruction using steric constraints. 2011 , 84,	9
728	Interaction of W(CO)6 with SiO2 surfaces: A density functional study. 2011 , 84,	13
7 2 7	Simulation of frictional behavior of Sb nanoparticles on HOPG: Frictional duality and biduality. 2011 , 84,	2
726	Electronic topological transition in sliding bilayer graphene. 2011 , 84,	50
725	Theoretical investigation of xenon-hydrogen solids under pressure using ab initio DFT and GW calculations. 2011 , 84,	11
724	Zeolitic-type Brfisted-Lowry sites distribution imaged on clinochlore. 2011 , 96, 1461-1466	15
723	Electrostatic-field-driven alignment of organic oligomers on ZnO surfaces. 2011 , 107, 146401	26
722	Trends in charge transfer and spin alignment of metallocene on graphene. 2011 , 83,	14
721	Rainbow scattering under axial surface channeling from a KCl(001) surface. 2011 , 84,	14
720	Water adsorption on hydrogen-passivated silicon nanowires from density functional theory with dispersion correction. 2011 , 83,	5
719	van der Waals density functional study of energetic, structural, and vibrational properties of small water clusters and ice Ih. 2011 , 84,	42
718	Unraveling the stability of polypeptide helices: critical role of van der Waals interactions. 2011 , 106, 118102	90
717	Commensurate-incommensurate phase transition in bilayer graphene. 2011 , 84,	63
716	Self-assembly of molecular wires on H-terminated Si(100) surfaces driven by London dispersion forces. 2011 , 84,	9
715	van der Waals interactions in the ground state of Mg(BH4)2 from density functional theory. 2011 , 83,	45
714	The effect of doping on the energetics and quantum conductance in graphene nanoribbons with a metallocene adsorbate. 2011 , 135, 124708	12
713	Self-assembled cyclic oligothiophene nanotubes: Electronic properties from a dispersion-corrected hybrid functional. 2011 , 84,	28
712	First-principles study of liquid and amorphous InGeTe2. 2011 , 83,	23

711	Functionalization of hydrogenated (111) silicon surface with hydrophobic polymer chains. 2011 , 84,	6
710	FeP(Im)-AB Bonding Energies Evaluated with A Large Number of Density Functionals (P = porphine, Im = imidazole, AB = CO, NO, and O(2)). 2011 , 109, 2035-2048	11
709	Alkane adsorption in Na-exchanged chabazite: the influence of dispersion forces. 2011 , 134, 064102	49
708	Ab-Initio Fully Periodic Characterization of MOF-74-M (M = Mg, Mn, Ni, Zn): Structures and Enthalpies of Adsorption. 2011 , 1366, 1	
707	A generalized-gradient approximation exchange hole model for dispersion coefficients. 2011 , 134, 044117	211
706	Theoretical study on the gas and solution phase enthalpies, free energies and equilibrium constants for the isomerisation of [1.1]paracyclophane derivatives as potential molecular switches. 2011 , 37, 369-378	
705	Re-examining the properties of the aqueous vapor-liquid interface using dispersion corrected density functional theory. 2011 , 135, 124712	74
704	Accurately Predicting the Density and Hydrostatic Compression of Hexahydro-1,3,5-Trinitro-1,3,5-Triazine from First Principles. 2011 , 28, 096103	2
703	PAH-related Very Small Grains in photodissociation regions: implications from molecular simulations. 2011 , 46, 223-234	
702	Dependence of dispersion coefficients on atomic environment. 2011 , 135, 234109	29
701	Comparing modern density functionals for conjugated polymer band structures: screened hybrid, Minnesota, and Rung 3.5 approximations. 2011 , 134, 184105	45
700	Ion selectivity in channels and transporters. 2011 , 137, 415-26	127
699	Communication: The effect of dispersion corrections on the melting temperature of liquid water. 2011 , 134, 121105	135
698	A density functional theory study of the adsorption of uracil on the Au(100) surface. 2011 , 467, 1959-1969	10
697	Understanding frictional duality and bi-duality: Sb-nanoparticles on HOPG. 2011 , 22, 085704	21
697 696	Understanding frictional duality and bi-duality: Sb-nanoparticles on HOPG. 2011 , 22, 085704 Molecular Clips and Tweezers with Corannulene Pincers. 2011 , 1-40	21

693	A post-Hartree-Fock study of pressure-induced phase transitions in solid nitrogen: the case of the 理and 🛮 low-pressure phases. 2011 , 134, 074502	22
692	First-principles investigation of the adsorption of the 2,5-pyridine di-carboxylic acid onto the Cu(011) surface. 2011 , 134, 104708	6
691	Communication: efficient counterpoise corrections by a perturbative approach. 2011 , 135, 081105	9
690	Calculating dispersion interactions using maximally localized Wannier functions. 2011 , 135, 154105	31
689	Comparison of free energy surfaces calculations from ab initio molecular dynamic simulations at the example of two transition metal catalyzed reactions. 2011 , 12, 1389-409	12
688	The role of relativity and dispersion controlled inter-chain interaction on the band gap of thiophene, selenophene, and tellurophene oligomers. 2012 , 136, 094904	19
687	Diffusion of Si and C atoms on and between graphene layers. 2012 , 45, 455309	16
686	N2-to-NH3 conversion by excess electrons trapped in point vacancies on 5f-element dioxide surfaces. 10,	О
685	Structures and properties of nano-XNH2 (X = C, Si, Ge, and Sn). 2023 , 13, 015113	0
684	Theoretical Investigation on the Elusive Structure-Activity Relationship of the Bioinspired High-Valent Nickel-Halogen Complexes in the Oxidative Fluorination Reactions.	O
683	Computational Study on the Catalytic Performance of Single-Atom Catalysts Anchored on g-CN for Electrochemical Oxidation of Formic Acid. 2023 , 13, 187	О
682	Mechanistic Understanding of the Electrocatalytic Nitrate Reduction Activity of Double-Atom Catalysts.	О
681	Incorporation of a BoronNitrogen Covalent Bond Improves the Charge-Transport and Charge-Transfer Characteristics of Organoboron Small-Molecule Acceptors for Organic Solar Cells. 2023 , 28, 811	О
680	Doping-induced magnetism and magnetoelectric coupling in one-dimensional NbOCl3 and NbOBr3.	О
679	Metastable-phase platinum oxide for clarifying the Pt ${\mathbb D}$ active site for the hydrogen evolution reaction.	О
678	Phase engineering in tantalum sulfide monolayers on Au(111).	2
677	Enhancement in photocatalytic water splitting using van der Waals heterostructure materials based on penta-layers.	О
676	The ab initio potential energy curves of atom pairs and transport properties of high-temperature vapors of Cu and Si and their mixtures with He, Ar, and Xe gases.	O

675	First-Principles Calculation Guided High-Purity Layer Control of 4 in. MoS2 by Plasma RIE.	O
674	Crystallographic and Computational Analysis of the Solid-Form Landscape of Three Structurally Related Imidazolidine-2,4-dione Active Pharmaceutical Ingredients: Nitrofurantoin, Furazidin, and Dantrolene.	O
673	A Double-Functional Additive Containing Nucleophilic Groups for High-Performance Zn-Ion Batteries.	1
672	Effect of intermacrocyclic interactions: Modulation of metal spin-state in oxo/hydroxo/fluoro-bridged diiron(III)/dimanganese(III) porphyrin dimers. 2023 ,	O
671	Bifunctional Photoassisted LiD2 Battery with Ultrahigh Rate-Cycling Performance Based on Siloxene Size Regulation.	О
670	Unveiling Charge Transport Mechanisms in Electronic Devices based on Defect-engineered MoS 2 Covalent Networks. 2211157	O
669	Three-Electron Two-Centered Bond and Single-Electron Transfer Mechanism of Water Splitting via a Copper B ipyridine Complex. 2023 , 127, 160-168	O
668	Corrosion inhibition at emergent grain boundaries studied by DFT for 2-mercaptobenzothiazole on bi-crystalline copper. 2023 , 7,	0
667	High Sensitivity Polarized Light Detector of 2D WS 2 /Mo 2 CF 2 Van Der Waals Heterostructure.	0
666	Computational design of novel MAX phase alloys for potential hydrogen storage media combining first principles and cluster expansion methods.	0
665	S-functionalized 2D V2B as a promising anode material for rechargeable lithium ion batteries.	O
664	Conformational dynamics and putative substrate extrusion pathways of the N-glycosylated outer membrane factor CmeC from Campylobacter jejuni. 2023 , 19, e1010841	0
663	The surface charge induced high activity of oxygen reduction reaction on the PdTe2 bilayer.	0
662	Density Functional Study of transition metal (Fe,Co,Ni) doped C60 fullerenes as 6-thioguanine delivery system.	0
661	Carrier and Phonon transport in 2D InSe and its Janus structures.	0
660	Enhanced reversibility of fluorine substituted bis-BN cyclohexane for hydrogen storage: A first-principles approach. 2023 ,	O
659	Two-Dimensional EBe2C with Hepta-Coordinated Carbons: A Highly Stable Direct-Band-Gap Semiconductor Predicted by First-Principles Calculations.	О
658	Experimental and Computational Investigation of Benperidol and Droperidol Solid Solutions in Different Crystal Structures.	O

657	Improving Lurasidone Hydrochloride Solubility and Stability by Higher-Order Complex Formation with Hydroxypropyl-tyclodextrin. 2023 , 15, 232	Ο
656	Vacancy Engineering for High-Efficiency Nanofluidic Osmotic Energy Generation.	Ο
655	Interaction of organic pollutants with TiO2: a density functional theory study of carboxylic acids on the anatase (101) surface.	0
654	Selective etching mechanism of silicon oxide against silicon by hydrogen fluoride: a density functional theory study.	0
653	Two-dimensional AlN/g-CNs van der Waals type-II heterojunction for water splitting.	0
652	Deterministic organic functionalization of monolayer graphene via high resolution surface engineering.	O
651	Molecular Dynamics-Assisted Interaction of Vanadium ComplexMMPK: From Force Field Development to Biological Application for Alzheimer Treatment.	0
650	Is Structural Precision of Platonic Micelles Controlled Solely by Close-Packed Head Groups or Also by Hydrophobic Tail Packing? A DFT Exploration.	Ο
649	Effective carrier doping and quantum capacitance manipulation of graphene through two-dimensional solid electrolytes of ScI3 and YBr3. 2023 , 156443	0
648	Coverage-driven selectivity switch from ethylene to acetate in high-rate CO2/CO electrolysis.	3
647	Relativistic Quantum Calculations to Understand the Contribution of f-type Atomic Orbitals and Chemical Bonding of Actinides with Organic Ligands.	0
646	Benchmarking the Computed Proton Solvation Energy and Absolute Potential in Non-aqueous Solvents. 2023 , 141785	Ο
645	ExperimentalEheoretical study of laccase as a detoxifier of aflatoxins. 2023, 13,	2
644	Structural, Hirshfeld surface and three-dimensional interaction energy studies of 2-(6-iodo-4-oxo-3,4-dihydroquinazolin-3-yl)ethanesulfonyl fluoride. 2023 , 79,	0
643	Multiple Pathways for Dissociative Adsorption of SiCl4 on the Si(100)-c(42) Surface. 2023 , 15, 213	0
642	Kinetic Modeling of a Poly(N-vinylcaprolactam-co-glycidyl methacrylate) Microgel Synthesis: A Hybrid In Silico and Experimental Approach. 2023 , 62, 893-902	0
641	Generation of magnetic skyrmions in two-dimensional magnets via interfacial proximity. 2023, 107,	0
640	Fabrication of polydopamine nanoparticles-based electrochemical sensor for geometry-sensitive detection of chloramphenicol. 2023 , 929, 117127	O

639	High-pressure-induced Multiple Phase Transitions of Parabanic Acid.	0
638	Insight at atomic scale of corrosion inhibition: DFT study of 8-hydroxyquinoline and derivatives on oxidized aluminum surface.	О
637	Room-temperature synthesis of nanometric and luminescent silver-MOFs. 10,	0
636	Structural Diversity in Divalent Group 14 Triflate Complexes Involving Endocyclic Thia-Macrocyclic Coordination. 2023 , 62, 853-862	o
635	Structural, electronic and optical properties of fluorinated bilayer silicene. 2023, 136, 113418	O
634	Hydrated manganese hydrogen phosphate coated membrane with excellent anticrude oil-fouling property for separating crude oil from diverse wastewater. 2023 , 454, 129215	0
633	Chromate ions chemisorption over the exterior surface of pristine boron nitride (B12N12) nanocage: A computational study. 2023 , 148, 110370	0
632	Effects of external electric field on the structural and electronic properties of SeZrS/SeHfS van der Waals heterostructure: A first-principles study. 2023 , 767, 139675	O
631	Mechanical and electronic properties of MX/YTe (M´=´Ge, Sn; X´=´S, Se, Te) van der Waals heterostructures. 2023 , 36, 102604	O
630	Effect of preadsorbing gas molecules on the adsorption of SO2 molecule on Hf2CO2 MXene by first-principles study. 2023 , 36, 102639	o
629	Biphenylene with doping B/N as promising metal-free single-atom catalysts for electrochemical oxygen reduction reaction. 2023 , 558, 232613	0
628	Monolayer of B3O3 as a promising material in anode of magnesium-ion batteries: A theoretical study. 2023 , 1220, 114008	0
627	A universal multifunctional rare earth oxide coating to stabilize high-voltage lithium layered oxide cathodes. 2023 , 56, 155-164	1
626	Highly sensitive and selective sensing-performance of 2D Co-decorated phthalocyanine toward NH3, SO2, H2S and CO molecules. 2023 , 36, 102641	0
625	Polyaniline anchoring environment facilitates highly efficient CO2 electroreduction of cobalt phthalocyanine over a wide potential window. 2023 , 441, 141800	0
624	Construction of two-dimensional lateral heterostructures by graphenelike ZnO and GaN monolayers for potential optoelectronic applications. 2023 , 36, 102635	O
623	Volatile organic compounds gas molecule adsorption on Fe-MoS2 monolayer: The first-principles study. 2023 , 813, 140298	0
622	Calculation of tunable electronic and optical properties of AlSb/CdSe heterojunction based on first principles. 2023 , 614, 156261	o

621	Microwave-accelerated hydrolysis for hydrogen production over a cobalt-loaded multi-walled carbon nanotube-magnetite composite catalyst. 2023 , 333, 120538	О
620	Data-driven many-body potentials from density functional theory for aqueous phase chemistry. 2023 , 4, 011301	Ο
619	Theoretical study for exploring the adsorption behavior of aniline and phenol on pristine and Cu-doped phosphorene surface. 2023 , 614, 156194	1
618	Experimental and density functional theory study of benzohydroxamic acid as a corrosion inhibitor in chemical mechanical polishing of Co interconnects. 2023 , 660, 130848	Ο
617	Mechanism of Pt3Co nanocatalysts to improve the performance for oxygen reduction reactions: DFT study on oxygen adsorption and durability of different facets. 2023 , 289, 116202	0
616	Surface reaction mechanism of atomic layer deposition of niobium oxide: In situ characterization and first-principle study. 2023 , 615, 156340	Ο
615	Influence of N-doped concentration on the electronic properties and quantum capacitance of Hf2CO2 MXene. 2023 , 210, 111826	0
614	Curvature effect on graphene-based Co/Ni single-atom catalysts. 2023 , 615, 156357	Ο
613	Functionalized Mo2BX2 (X = H, OH, O) MBenes as a promising sensor, capturer and storage material for environmentally toxic gases: A case. 2023 , 615, 156299	0
612	DFT and ab-initio molecular dynamics of pyrochlore surface dissolution in aqueous media Effect of cleavage plane and surface atomic vacancies. 2023 , 615, 156425	Ο
611	Tuning the electronic properties of WS2 monolayer by doping transition metals: DFT Approach. 2023 , 157, 107339	O
610	MXene V2CO2 monolayer:a promising adsorbent to capture toxic NH3 gas. 2023 , 148, 115651	Ο
609	Giant band gap bowing in two dimensional Pb1\(\mathbb{B}\)SnxO alloys and Janus PbSnO monolayers. 2023 , 175, 111203	1
608	COF-C4N Nanosheets with uniformly anchored single metal sites for electrocatalytic OER: From theoretical screening to target synthesis. 2023 , 325, 122366	O
607	Design of novel type-I (type-II) band alignment in GeC-VXY ($V'='Cl$, Br; $Y'='Se$, Te) van der Waals heterostructure for optoelectronic and renewable energy application. 2023 , 615, 156260	1
606	Effect of benzotriazole on the prevention of electroless nickellimmersion gold treated copper corrosion. 2023 , 176, 111226	O
605	Band modulation and optoelectronic properties of 2D Janus Ge2SeTe/Sn2SSe van der Waals heterostructures. 2023 , 257, 119682	0
604	Ab Initio Calculations of Chitosan Effects on the Electronic Properties of Unpassivated Triangular ZnO Nanowires Oriented along [0001] Directions. 2023 , 8, 2337-2343	O

603	Electronic contacts and lubricity characters between monolayer WSe2 and $Zr2C$, $Zr2CY2$ (Y = F or OH).	O
602	Embedding Group VIII Elements into a 2D Rigid pc-C3N2 Monolayer to Achieve Single-Atom Catalysts with Excellent OER Activity: A DFT Theoretical Study. 2023 , 28, 254	O
601	Controlled Synthesis of Submillimeter Non-layered WO 2 Nanoplates via a WSe 2 -Assisted Method. 2207895	О
600	Material Innovation Through Atomistic Modelling for Hybrid Bonding Technology. 2022,	О
599	Atomic-Layer-Deposition Derived Pt subnano Clusters on the (110) Facet of Hexagonal Al2O3 Plates: Efficient for Formic Acid Decomposition and Water Gas Shift. 2023 , 13, 887-901	O
598	4H-SiC Ohmic contacts formation by MoS2 layer intercalation: A first-principles study. 2022 , 132, 245702	O
597	D-SICharge Transfer Mechanism Guiding Design of a ZnIn2S4/SnSe2/In2Se3 Heterostructure Photocatalyst for Efficient Hydrogen Production. 2023 , 13, 1020-1032	Ο
596	Classical Nuclear Motion: Comparison to Approaches with Quantum Mechanical Nuclear Motion. 2023 , 4, 11-21	O
595	First Ultrathin Pure Polyoxometalate 2D Material as a Peroxidase-Mimicking Catalyst for Detecting Oxidative Stress Biomarkers. 2023 , 15, 1486-1494	1
594	Electric-Field-Tunable Spin Polarization and Carrier-Transport Anisotropy in an A-Type Antiferromagnetic van der Waals Bilayer. 2022 , 18,	O
593	Crystallographic Study of Solvates and Solvate Hydrates of an Antibacterial Furazidin.	O
592	New polymorph of graphene monoxide: all-sp3bonded metal and ambient pressure superconductor.	O
591	Density Functional Theory Studies on Magnetic Manipulation in Nil2 Layers.	O
590	Insights of Platinum Drug Interaction with Spinel Magnetic Nanocomposites for Targeted Anti-Cancer Effect. 2023 , 15, 695	O
589	P-type Ohmic contact to MoS2 via binary compound electrodes.	O
588	Atomic mean square displacement study of the bond breaking mechanism of energetic materials before explosive initiation.	О
587	Collective Magnetic Behavior in Vanadium Telluride Induced by Self-Intercalation.	O
586	In silico capture and activation of methane with light atom molecules.	O

585	Mechanistic insights into hydrogen production from formic acid catalyzed by Pd@N-doped graphene: The role of the nitrogen dopant. 2023 ,	1
584	Activation of Aryl Halides at Gold(I) by N-Heterocyclic Carbenes: L-Shaped Heterobidentate ImPy (Imidazo[1,5-a]pyridin-ylidene) N,C Ligands for Oxidant-Free Au(I)/Au(III) Catalysis.	Ο
583	The synergistic effect of Ti and Nb in TiNbC leads to enhanced anode performance for Na-ion batteries - first-principles calculations. 2023 , 98, 025710	Ο
582	Tetragonal SnOFeSe: A possible parent compound of the FeSe-based superconductor. 2023, 107,	Ο
581	Triggering the mechanism of the initial reaction of energetic materials under pressure based on Raman intensity analysis.	0
580	Heat transport properties of novel carbon monolayer (net-Y): a comparative study with graphene. 2023 , 25, 4915-4922	O
579	Photoinduced Carrier Transfer Dynamics in MoSSe/WSSe Vertical and Lateral Heterostructures. 2023 , 127, 2078-2087	0
578	Tuning the Optical Properties of the Metal-organic Framework UiO-66 via Ligand Functionalisation.	Ο
577	SolarII hermal Fuels and the Role of Carbon Nanomaterials: A Perspective with Emphasis on the Azobenzene System. 2023 , 37, 1731-1756	0
576	Activating the hydrogen evolution reaction in low-dimensional carbon by partial hydrogenation: Role of the hybrid sp2-sp3 orbital interface. 2023 ,	Ο
575	Solvent induced conformational polymorphism. 2023 , 25, 971-980	0
574	Theoretical study of single-nonmetal-modified V2CO2 MXene as an efficient electrocatalyst for overall water splitting. 2023 ,	Ο
573	Proton transfer in layered hydrogen-bonded system MOOH (M = Al, Sc): Robust bi-mode ferroelectricity and 1D superionic conductivity. 2023 , 122, 042901	0
572	Janus Ga2SeTe and In2SeTe nanosheets: Excellent photocatalysts for hydrogen production under neutral pH. 2023 ,	O
571	Effect of Dioldibenzoate Isomers as Electron Donors on the Performances of ZieglerNatta Polypropylene Catalysts: Experiments and Calculations. 2023 , 127, 2294-2302	0
570	Ab Initio Computational Screening and Performance Assessment of van der Waals and Semimetallic Contacts to Monolayer WSe\$_{text{2}}\$ P-Type Field-Effect Transistors. 2023 , 1-8	O
569	The Origin of Amphipathic Nature of Short and Thin Pristine Carbon Nanotubes Eully Recyclable 1D Water-in-Oil Emulsion Stabilizers. 2202407	1
568	Molecular Recognition of Imidazole-Based Drug Molecules by Cobalt(III)- and Zinc(II)-Coproporphyrins in Aqueous Media. 2023 , 28, 964	O

567	The Moir[pattern rule of the twisted bilayer graphene and its electronic property under a strain. 2023 , 138,	0
566	Insights into Photoinduced Carrier Dynamics and Overall Water Splitting of Z-Scheme van der Waals Heterostructures with Intrinsic Electric Polarization. 2023 , 14, 798-808	О
565	Electron Transport through Nanoconfined Ferrocene Solution: Density Functional Theory-Nonequilibrium Green Function Approach. 2023 , 127, 2666-2674	О
564	Birth of the Hydrated Electron via Charge-Transfer-to-Solvent Excitation of Aqueous Iodide. 2023 , 14, 870-878	О
563	XPu(CO)n (X = B, Al, Ga; n = 2 to 4): Back-Bonding in Heterodinuclear Plutonium Boron Group Compounds with an End-On Carbonyl Ligand. 2023 , 127, 1233-1243	0
562	Tuning the Local Coordination of CoP1\(\text{LS} \) between NiAs- and MnP-Type Structures to Catalyze Lithium\(\text{Bulfur Batteries} \).	О
561	Molecular Dynamics and Experimental Study of the Effect of CeF3 and NdF3 Additives on the Physical Properties of FLiNaK. 2023 , 127, 1197-1208	О
560	Engineering Chemo-Mechanical Properties of Zn Surfaces via Alucone Coating. 2023 , 127, 2481-2492	О
559	Can the E1 state in nitrogenase tell if there is an activation process prior to catalysis?. 2023, 25, 3702-3706	О
558	Activation of Aryl Halides at Gold(I) by N-Heterocyclic Carbenes: L-Shaped Heterobidentate ImPy (Imidazo[1,5-a]pyridin-ylidene) N,C Ligands for Oxidant-Free Au(I)/Au(III) Catalysis.	О
557	Dramatic acceleration by visible light and mechanism of AuPd@ZIF-8-catalyzed ammonia borane methanolysis for efficient hydrogen production.	2
556	Demystifying the Chemical Ordering of Multimetallic Nanoparticles. 2023 , 56, 248-257	О
555	Tuning of Second-Harmonic Generation in Zn-Based Metal Drganic Frameworks by Controlling the Structural Interpenetrations: A First-Principles Investigation. 2023 , 127, 2058-2068	0
554	Simulation of O2/N2 behaviors on multi-component polymeric membranes in oxy-fuel combustion system. 2023 , 118288	О
553	Doping and pretreatment optimized the adsorption of *OCHO on bismuth for the electrocatalytic reduction of CO2 to formate.	0
552	Fascinating Electrocatalysts with Dispersed Di-Metals in MN 3 -M?N 4 Moiety as Two Active Sites Separately for N 2 and CO 2 Reduction Reactions and Jointly for C?N Coupling and Urea Production. 2201331	О
551	Investigation of the anchoring and electrocatalytic properties of pristine and doped borophosphene for NaB batteries.	O
550	Efficient adsorption of trinitrotoluene by isoxazoline-based porous polymers prepared from room-temperature stable bis(nitrile oxide).	О

549	Molecular Dynamics with Chemical Accuracy-Alkane Adsorption in Acidic Zeolites. 2023, 13, 2011-2024	О
548	Theoretical design of porous dodecagonal germanium carbide (d-GeC) monolayer. 2023 , 13, 3290-3294	O
547	Catalytic Behavior of Hydrogen Bonded Water in Oligomerization of Silicates. 2023 , 62, 1423-1436	0
546	Understanding the Monomer Deuteration Effect on the Transition Temperature of poly(N-isopropylacrylamide) Microgels in H2O.	O
545	Experimentally Validated Ab Initio Crystal Structure Prediction of Novel Metal®rganic Framework Materials.	О
544	Topology regulation of nanomedicine for autophagy-augmented ferroptosis and cancer immunotherapy. 2023 , 68, 77-94	O
543	First Principles Study of 2D Ring-Te and its Electrical Contact with Topological Dirac Semimetal.	O
542	Yttrium decorated fullerene C30 as potential hydrogen storage material: Perspectives from DFT simulations.	O
541	Substituent Effects of the Nitrogen Heterocycle on Indole and Quinoline HDN Performance: A Combination of Experiments and Theoretical Study. 2023 , 24, 3044	O
540	Accuracy of Intermolecular interaction Energies, Particularly Those of Hetero Atom Containing Molecules Obtained by van der Waals DFT Calculations. 2023 , 8,	O
539	Biaxial strain tunable quantum capacitance and photocatalytic properties of Hf2CO2 monolayer. 2023 , 616, 156579	O
538	Selective semi-hydrogenation of alkynes on palladium-selenium nanocrystals. 2023 , 418, 247-255	O
537	Effects of transition metal intercalation on the electronic and magnetic properties of CrI3/WSe2 heterostructure. 2023 , 158, 107361	O
536	Assembly and electrocatalytic CO2 reduction of two-dimensional bimetallic porphyrin-based conjugated cobalt metal-organic framework. 2023 , 443, 141896	O
535	Influence of C-vacancy-line defect on electronic and optical properties and quantum capacitance of Ti2CO2 MXene: A first-principles study. 2023 , 176, 111254	O
534	Controllable contact types of Janus MoSH and WSi2N4 van der Waals heterostructures via biaxial strain and external electric field. 2023 , 149, 115668	O
533	Nature of the dative Nitrogen-Coinage metal bond in molecular Motors. Evaluation of NHC-M pyrazine bond (M´=´Cu, Ag, Au) from relativistic DFT. 2023 , 549, 121401	O
532	Regulation of the electronic structure and ferromagnetism by implanting topological defects in a bismuth monolayer. 2023 , 161, 112174	O

531	Infinitene as two fused helicoidal trails of fused rings: evaluation of the magnetic behavior of [12]infinitene and anionic species displaying global aromaticity and antiaromaticity. 2023 , 25, 8190-8197	0
530	The regulating effect of boron doping and its concentration on the photocatalytic overall water splitting of a polarized g-C3N5 material. 2023 , 25, 8592-8599	O
529	Accelerated screening and assembly of promising MOFs with open Cu sites for isobutene/isobutane separation using a data-driven approach. 2023 , 25, 8608-8623	0
528	Branching ratios in the dissociative photoionization of iodomethane by photoelectron photoion coincidence. 2023 , 25, 7383-7393	O
527	S- and Cl-functionalized Nb2C MXenes as novel anode materials for sodium-ion batteries: a first-principles study. 2023 , 47, 6412-6419	0
526	Solar cells based on 2D Janus group-III chalcogenide van der Waals heterostructures. 2023 , 15, 7126-7138	O
525	Experimental and theoretical study of catalytic dye degradation and bactericidal potential of multiple phase Bi and MoS2 doped SnO2 quantum dots. 2023 , 13, 10861-10872	0
524	Activating dual atomic electrocatalysts for the nitric oxide reduction reaction through the P/S element.	O
523	First-principles study on electronic states of In2Se3/Au heterostructure controlled by strain engineering. 2023 , 13, 11385-11392	О
522	The PdBi2 monolayer for efficient electrocatalytic NO reduction to NH3: a computational study.	O
521	First-principles study of sodium adsorption on defective graphene under propylene carbonate electrolyte conditions. 2023 , 13, 5627-5633	0
520	Synthesis and properties of p-benzithiahexaphyrin(1.1.1.1.1)s. 2023 , 47, 4720-4729	O
519	Monocarboxylate-Protected Two-Electron Superatomic Silver Nanoclusters with High Photothermal Conversion Performance.	0
518	BN Diamane-like Quasicrystal Based on 30° Twisted H-BN Bilayers and Its Approximants: Features of the Atomic Structure and Electronic Properties. 2023 , 13, 421	O
517	Structural water in amorphous carbonate minerals: ab initio molecular dynamics simulations of X-ray pair distribution experiments. 2023 , 25, 6768-6779	O
516	Ni-Intercalation-Induced Topological Nodal Line States and Superconductivity in NiTe. 2023 , 127, 4303-4309	O
515	Oxide-Metal Interaction Probed by Scanning Tunneling Microscope Manipulation of Cr2O7 Clusters on Au(111). 2023 , 14, 2163-2170	O
514	Inter-quintuple layer coupling and topological phase transitions in the chalcogenide topological insulators. 2023 , 5, 015001	O

513	Adsorption of Carbamazepine in All-Silica Zeolites Studied with Density Functional Theory Calculations**.	Ο
512	Band structure, superconductivity, and polytypism in AuSn4. 2023, 7,	Ο
511	Enabling the transition to ductile MAX phases and the exfoliation to MXenes via tuning the A element. 2023 , 106, 3765-3776	0
510	Carbon nanotubes and nanobelts as potential materials for biosensor. 2023, 13,	O
509	Tailoring WB morphology enables d-band centers to be highly active for high-performance lithium-sulfur battery. 2023 , 108189	О
508	Sandwich Structured Metal oxide/Reduced Graphene Oxide/Metal Oxide-Based Polymer Electrolyte Enables Continuous Inorganic@rganic Interphase for Fast Lithium-Ion Transportation. 2207536	O
507	Work Function-Tailored Nitrogenase-like Fe Double-Atom Catalysts on Transition Metal Dichalcogenides for Nitrogen Fixation. 2023 , 11, 4990-4997	О
506	Direct observation of oxygen vacancy formation and migration over ceria surface by in situ environmental transmission electron microscopy. 2023 ,	O
505	Computational Design of a Two-Dimensional Copper Carbide Monolayer as a Highly Efficient Catalyst for Carbon Monoxide Electroreduction to Ethanol. 2023 , 15, 13033-13041	0
504	A Solar Responsive Battery Based on Charge Separation and Redox Coupled Covalent Organic Framework. 2213667	O
503	Atomically thin metallic Si and Ge allotropes with high Fermi velocities. 2023, 107,	0
502	Microwave measurements, calculations, and analysis for the gas phase ammonia-formic acid dimer. 2023 , 393, 111772	O
501	Inter- vs. Intra-Molecular Hydrogen Bond in Complexes of Nitrophthalic Acids with Pyridine. 2023 , 24, 5248	0
500	Magnetoresistance anomaly in Fe5GeTe2 homo-junctions induced by its intrinsic transition.	O
499	Adsorption and sensing properties of SF6 decomposed gases on Mg-MOF-74. 2023, 363, 115120	0
498	Li, Na and K storage capacity of a novel 2D graphitic carbon-nitride membrane, C9N4: A computational approach. 2023 , 817, 140414	O
497	Interfacial Chemistry in the Electrocatalytic Hydrogenation of CO2 over C-Supported Cu-Based Systems. 5876-5895	О
496	Control of magnetic states and spin interactions in bilayer CrCl3 with strain and electric fields: an ab initio study. 2023 , 13,	Ο

495	Gate switchable spin-orbit splitting in a MoTe2/WTe2 heterostructure from first-principles calculations. 2023 , 107,	O
494	Binuclear spin-crossover [Fe(bt)(NCS)2]2(bpm) complex: A study using first principles calculations. 2023 , 158, 144307	O
493	High-pressure and temperature neural network reactive force field for energetic materials. 2023 , 158, 144117	0
492	Constructing extrinsic oxygen vacancy on the surface of photocatalyst as CO2 and electrons reservoirs to improve photocatalytic CO2 reduction activity. 2023 ,	O
491	First-principles study on the CH 4 adsorption performance of Mn-modified N-doped graphdiyne.	0
490	Thematic Exordium for Special Issue D ensity Functional Theory Application on Chemical Calculation □2023 , 16, 2904	O
489	Atomic structure and bonding in fluorinated graphite intercalated with a strong fluoroxidant. 2023 , 135, 109851	0
488	Contribution of proteins to ceramic membrane fouling at the early stage of membrane filtration. 2023 , 312, 123450	О
487	In-situ construction of hierarchical 2D MoS2/1D Te hybrid for supercapacitor applications. 2023 , 60, 106703	0
486	The Mechanism of Growing MoS 2 via Sulfuration of Molybdenum Hexacarbonyl: First principles study. 2023 , 8,	О
485	Single-atom Pt supported on non-metal doped WS2 for photocatalytic CO2 reduction: a first-principles study. 2023 , 157252	0
484	Promoter not inhibitor: The antidotal effects of arsenic on lead-poisoning V2O5WO3/TiO2 catalyst for selective catalytic reduction of NO with NH3. 2023 , 397, 136621	O
483	Controllable adsorption/desorption of sarin on metallic oxides doped CNTs: First principle calculations. 2023 , 135, 109884	0
482	A density functional study on the sensing behavior of copper doped BC3 nanosheet toward COS gas. 2023 , 110689	O
481	Optimizing CO2RR selectivity on single atom catalysts using graphical construction and identification of energy descriptor. 2023 , 208, 330-337	O
480	Carbon-confined Cu-Pd alloy nanoparticles as high-performance catalysts for acetylene selective hydrogenation. 2023 , 464, 142609	O
479	SizeBelected Cu4 cluster anchored on C2N monolayer for efficient nitrite electroreduction to ammonia: a computational study. 2023 , 620, 156825	0
478	Ga-doped AlN monolayer nano-sheets as promising materials for environmental sensing applications. 2023 , 1223, 114086	O

477	Transition metal doped pyrrole-NC for high-performance CO2 reduction reaction to C1 products. 2023 , 618, 156678	О
476	Oxygen Reduction and Hydrogen Evolution Reactions on Zigzag ReS2 Nanoribbons. 2023, 618, 156677	O
475	Raman spectra and vibrational properties of FOX-7 under pressure and temperature: First-principles calculations. 2023 , 293, 122489	О
474	Site-specific isotope fractionation during Zn adsorption onto birnessite: Insights from X-ray absorption spectroscopy, density functional theory and surface complexation modeling. 2023 , 348, 68-84	Ο
473	First-principles study on the electronic and magnetic properties of BN/CrOBr heterostructures. 2023 , 471, 128789	0
472	Atomic-scale friction of black phosphorus/degraded Cu substrate: A route to robust superlubricity obtained by the critical load. 2023 , 619, 156749	O
471	Water-induced synthesis of Pd nanotetrahedrons on g-C3N4 for highly efficient hydrogenation of nitroaromatic. 2023 , 665, 131201	0
470	Tuning the surface electronic structure of WS2 with Zn- and Cu-phthalocyanine for improved hydrogen evolution reaction: Experimental and DFT investigation. 2023 , 39, 100499	О
469	Li-ion complex enhances interfacial lowest unoccupied molecular orbital for stable solid electrolyte interface of natural graphite anode. 2023 , 449, 142262	О
468	Vacancy on the surface of monolayer MoS2 to improve the sensitivity for DNA/RNA sequencing: A DFT study. 2023 , 1223, 114102	Ο
467	Surface alloy with sulfur leading piezoelectricity from non-piezoelectricity of pentagonal-PdPSe. 2023 , 947, 169640	1
466	Molecular dynamics simulations of CaCl2NaCl molten salt based on the machine learning potentials. 2023 , 254, 112275	Ο
465	Electronic contacts and lubricity characteristics between monolayer WSe2 and Zr2C, Zr2CY2 (Y´=´F or OH). 2023 , 35, 105724	О
464	Through the Self-Optimization process to achieve high OER activity of SAC catalysts within the framework of TMO3@G and TMO4@G: A High-Throughput theoretical study. 2023 , 640, 405-414	О
463	Effect of molybdenum disulfide doping with substitutional nitrogen and sulfur vacancies on lithium intercalation. 2023 , 947, 169689	О
462	Theoretical design toward highly efficient single-atom catalysts for nitrogen reduction by regulating the <code>Bcceptance-donationImechanism</code> . 2023 , 623, 156827	O
461	Calculation of tunable electronic and optical properties of AlP/InSe heterostructure based on first principles. 2023 , 160, 107443	O
460	Computational insight into bilayer NC7 anode material for Li/Na/Mg-ion batteries. 2023, 225, 112194	Ο

459	Construction of diluted magnetic semiconductor to endow nonmagnetic semiconductor with spin-regulated photocatalytic performance. 2023 , 110, 108381	0
458	Design of molecular M N C dual-atom catalysts for nitrogen reduction starting from surface state analysis. 2023 , 640, 983-989	Ο
457	Oxygen-containing functional groups enhance uranium adsorption by aged polystyrene microplastics: Experimental and theoretical perspectives. 2023 , 465, 142730	0
456	Potential use of silicon carbide monolayer as an anode in rechargeable Mg-ion batteries. 2023 , 177, 111270	О
455	Seed-mediated synthesis of a modified micro-mesoporous MIL-101(Cr) for improved benzene and toluene adsorption at room conditions. 2023 , 11, 109558	0
454	The interplay between spin states, geometries and biological activity of Fe(III) and Mn(II) complexes with thiosemicarbazone. 2023 , 237, 116389	O
453	First-principles studies the optical properties of defective-GQDs and -fullerene. 2023, 35, e00793	0
452	The CrBr3 monolayer: Two dimension sodium ion battery anode material to characterize state-of-charge by magnetism. 2023 , 623, 157074	Ο
451	Computational screening of B borophene based single-atom catalysts for N2 reduction. 2023 , 418, 114079	О
450	Performance evaluation and assessment of the corrosion inhibition mechanism of carbon steel in HCl medium by a new hydrazone compound: Insights from experimental, DFT and first-principles DFT simulations. 2023 , 16, 104711	Ο
449	Surface Li effects on the electronic properties of GaAs nanowires: A first principles approach. 2023 , 38, 102745	О
448	A BP3-AlP3 heterobilayer for the bifunctional photocatalysis of CO2 reduction. 2023 , 621, 156890	Ο
447	Copper decorated graphyne as a promising nanocarrier for cisplatin anti-cancer drug: A DFT study. 2023 , 622, 156885	Ο
446	Biaxial strain tunable electronic properties, photocatalytic properties and quantum capacitance of Sc2CO2 MXenes. 2023 , 212, 112016	О
445	Metal-free single atom catalysts towards efficient acetonitrile reduction to ethylamine. 2023, 622, 156891	Ο
444	Adaptive half-metallicity via magnetic proximity in an electrically sensitive 1TEWTe2/CrBr3 vdW heterostructure. 2023 , 623, 157019	О
443	Theoretical investigation of the V2BX2 ($X'=S$, Se, and Te) monolayers as anode materials for Na-ion batteries. 2023 , 35, 105923	0
442	In-situ regeneration of carbon monoliths as an environmental-benign adsorbent for environmental remediation via a flow-through model. 2023 , 314, 123542	O

441	Environmental biotransformation mechanisms by flavin-dependent monooxygenase: A computational study. 2023 , 325, 138403	О
440	Short bandgap of porphyrin molecules (Py) filled in a semiconducting single-walled carbon nanotube (Py@NT17) for highly efficient organic photovoltaic cells. 2023 , 293, 116456	Ο
439	Structure evolution and durability of Metal-Nitrogen-Carbon (M´=´Co, Ru, Rh, Pd, Ir) based oxygen evolution reaction electrocatalyst: A theoretical study. 2023 , 640, 170-178	0
438	DFT study of superlight ambient temperature reversible H2 storage media based on Li decorated on new planar BCN. 2023 , 622, 156947	Ο
437	Unexpected Bi-functional Co-g-GaN monolayer for detecting and scavenging toxic gases. 2023 , 35, 105781	0
436	Atomic-scale engineering of cation vacancies in two-dimensional unilamellar metal oxide nanosheets for electricity generation from water evaporation. 2023 , 110, 108348	Ο
435	Multi-functional lead-free Ba2XSbO6 (X´=´Al, Ga) double perovskites with direct bandgaps for photocatalytic and thermoelectric applications: A first principles study. 2023 , 35, 105617	Ο
434	Heterogeneous catalytic reaction of NO2 to HONO on hematite. 2023 , 733, 122291	O
433	Length-dependent high-frequency response of aromatic and aliphatic molecules: predictions from first-principles calculations. 2023 , 178, 111343	Ο
432	Computational investigation on CO2 capturing capacity of N-doped and Na-decorated Graphdiyne. 2023 , 345, 128169	O
431	New Janus structure photocatalyst having widely tunable electronic and optical properties with strain engineering. 2023 , 155, 142-147	O
430	Evaluating the potential of planar h-BSb monolayer as anode materials for sodium-ion batteries from first principles methods. 2023 , 64, 107260	O
429	Unusual mechanical properties of CO2IV: Auxetic potential in a high-pressure polymorph of carbon dioxide. 2023 , 178, 111349	Ο
428	Boron pretreatment promotes phosphorization of FeNi catalysts for oxygen evolution. 2023 , 330, 122598	Ο
427	Structural studies of a novel tautomeric Schiff base derived from 4-(N,NEdiethylamino)salicylaldehyde and 2-amino-4-methyl phenol: An experimental and theoretical study. 2023 , 1285, 135468	Ο
426	Experimental and theoretical insights into colossal supercapacitive performance of graphene quantum dots incorporated Ni3S2/CoS2/MoS2 electrode. 2023 , 65, 107274	O
425	Design and fabrication of nickel lanthanum telluride microfibers for redox additive electrolyte-based flexible solid-state hybrid supercapacitor. 2023 , 65, 107286	O
424	Noble metal single-atoms for lithium-ion batteries: A booster for ultrafast charging/discharging in carbon electrodes. 2023 , 624, 157161	O

423	Surface symmetry effect on the charge transfer at the black, blue, and green phosphorene/graphene interfaces. 2023 , 733, 122286	O
422	Semi-metallic bilayer borophene for lithium-ion batteries anode material: A first-principles study. 2023 , 571, 111911	O
421	Cu4@C2N for effective electrochemical CO2 reduction and intermediates dependent adsorption behaviours: A computational study. 2023 , 626, 157126	O
420	Construction of triazine-heptazine-based carbon nitride heterojunctions boosts the selective photocatalytic CII bond cleavage of lignin models. 2023 , 331, 122688	O
419	Molecular insights into ions permeation and destruction behavior in methane hydrate driven by electrostatic fields. 2023 , 346, 128211	O
418	Effect of the bipodal Ti species on activity and selectivity of propylene epoxidation with H2O2 over TS-1: A theoretical study. 2023 , 543, 113147	O
417	Infrared and Raman vibrational modelling of ₹C2S and C3S compounds. 2023 , 169, 107162	О
416	High hydrogen production in two-dimensional GaTe/ZnI2 type-II heterostructure for water splitting. 2023 , 178, 111317	O
415	Determine the Complete Configuration of Single-Walled Carbon Nanotubes by One Photograph of Transmission Electron Microscopy.	О
414	Emerging Trends of Computational Chemistry and Molecular Modeling in Froth Flotation: A Review.	O
413	Defect mediated visible light induced photocatalytic activity of Co3O4 nanoparticle decorated MoS2 nanoflower: A combined experimental and theoretical study. 2023 , 9, e14536	O
412	Influence of phosphorus-doped bilayer graphene configuration on the oxygen reduction reaction in acidic solution. 2023 , 118012	O
411	The theoretical study of Rh single atom catalysts decorated C3N monolayer with N vacancy for CO oxidations. 2023 , 129,	O
410	First-principles study of penta-graphene/MoS2 vdW heterostructure as anode material for lithium-ion batteries. 2023 , 109928	O
409	Transport properties in liquids from first-principles: The case of liquid water and liquid argon. 2023 , 158, 134503	O
408	OD Bond Formation and Oxygen Release in Photosystem II Are Enhanced by Spin-Exchange and Synergetic Coordination Interactions.	O
407	Theoretical insights into nonmetal-doped graphyne-supported noble metal electrocatalysts for NH3 synthesis via nitrogen reduction. 2023 , 617, 156550	О
406	A theoretical study of the functionalized carbon dots surfaces binding with silver nanostructures. 2023 , 1223, 114087	O

405	Density Functional Theory Studies of the Direct Conversion of Methane to Methanol Using O2 on Graphitic MN4G-BN ($M = Fe$, Co, Cu) and CuN4G-PN Single-Atom Catalysts.	О
404	High-throughput screening of H2 production catalysts from doped In2SSe monolayer: Valence electrons-based descriptor. 2023 , 224, 112179	О
403	Understanding the hydrogen evolution reaction activity of doped single-atom catalysts on two-dimensional GaPS4 by DFT and machine learning. 2023 , 81, 93-100	О
402	Confined MoS2 nanosheets grown on 3D interconnected N, S co-doped carbon nanofibers as a free-standing anode for sodium-ion batteries. 2023 , 323, 124046	О
401	First-principles calculations investigation on different coverage of H2O adsorption on the Mg-montmorillonite (0 1 0) edge surface. 2023 , 626, 157232	О
400	Promotion of MgO sorbents with eutectic carbonate doping for high-temperature and pressure CO2 capture. 2023 , 625, 157207	O
399	Chemical and interfacial design in the visible-light-absorbing ferroelectric thin films. 2023, 43, 3275-3288	O
398	Investigation on the photocatalytic property of direct Z-type van der Waals g-C3N4/AlN heterojunction and its mechanism. 2023 , 571, 111913	О
397	Large wafer-level two-dimensional h-BN with unintentional carbon doping grown by metalorganic chemical vapor deposition. 2023 , 213, 112083	O
396	Pressure-induced tuning of structure and electronic properties in lead-free hybrid halide perovskite HC(NH2)2SnI3 for photovoltaic solar cells. 2023 , 293, 116468	О
395	Reactivity of diamanes against oxidation: A DFT study. 2023 , 571, 111916	О
394	Removal of methylene blue by using sodium alginate-based hydrogel; validation of experimental findings via DFT calculations. 2023 , 122, 108468	O
393	Adsorption behaviors, electronic and gas-sensing properties of C3N4 monolayers and heterojunctions for SF6 decomposition products. 2023 , 626, 157090	О
392	A new carbon allotrope: Biphenylene as promising anode materials for Li-ion and Li O2 batteries. 2023 , 395, 116214	О
391	Co-adsorption of hydrogen and methane can improve the energy storage capacity of Mn-modified graphene. 2023 , 63, 106973	О
390	Water sorption on pyrochlore Niobium hydration and calcium susceptibility to leaching unraveled by DFT simulations. 2023 , 178, 111372	О
389	Exploring Mg decorated antimonene for promising hydrogen storage material: A DFT outlook. 2023 , 161, 107471	О
388	Adsorption of Pb(II) and Cd(II) hydrates via inexpensive limonitic laterite: Adsorption characteristics and mechanisms. 2023 , 310, 123234	О

387	Theoretical calculation of hydrogen evolution reaction in two-dimensional As2X3(X=S, Se, Te) doped with transition metal atoms. 2023 , 616, 156475	Ο
386	First-principles study of noble metal atom doped Fe(100) as electrocatalysts for nitrogen reduction reaction. 2023 , 297, 127396	O
385	Unidirectional domain growth of hexagonal boron nitride thin films. 2023, 30, 101734	0
384	Tuning gas-sensitive properties of the twin graphene decorated with transition metal via small electrical field: A viewpoint of first principle. 2023 , 133, 109707	O
383	A specific defect type of Cu active site to suppress Water-Gas-Shift reaction in syngas conversion to methanol over Cu catalysts. 2023 , 269, 118496	O
382	First-principles calculations to investigate structural and mechanical properties of MoS2/MoSe2 vertical and lateral Superlattice. 2023 , 45, 106234	O
381	Electronic structures and photovoltaic applications of vdW heterostructures based on Janus group-IV monochalcogenides: insights from first-principles calculations. 2023 , 25, 5663-5672	O
380	Tunable local piezopotential properties of zinc oxide nanowires grown by remote epitaxy. 2023 , 157, 107345	O
379	Efficient H2O2 dissociation and formation on zinc chalcogenides: A density functional theory study. 2023 , 616, 156495	О
378	DFT perspective of gas sensing properties of Fe-decorated monolayer antimonene. 2023 , 616, 156520	О
377	Photo-Initiated in situ synthesis of polypyrrole Fe-Coated porous silicon microspheres for High-performance Lithium-ion battery anodes. 2023 , 459, 141543	0
376	Role of axial coordination in the adsorption configuration of $M(II)$ -tetraphenylporphyrins ($M = Co$, Ni , Cu , Zn) on r-TiO2(110). 2023 , 616, 156548	1
375	Van der Waals stacking of multilayer In2Se3 with 2D metals induces transition from Schottky to Ohmic contact. 2023 , 617, 156557	О
374	Wave-layered dendrite-free lithium deposition with unprecedented long-term cyclability. 2023 , 560, 232697	O
373	The adhesive energies between Poly(3-hexylthiophene) and Polyvinylpyrrolidone for organic electronic devices: Hybrid-exchange density-functional-theory studies.	О
372	A detailed experimental performance of 4-quinolone derivatives as corrosion inhibitors for mild steel in acid media combined with first-principles DFT simulations of bond breaking upon adsorption. 2023 , 375, 121299	O
371	Understanding the adsorption behavior of oxygen on the 3CBiC(1 1 0) surface: A first-principles study. 2023 , 106, 3676-3687	0
370	Electronic and optical properties of of GaSe/ZnSe vdW heterojunction as photocatalyst by biaxial strain: A DFT study. 2023 , 814, 140333	O

369	First principles study of electronic properties and optoelectronic performance of type-II SiS/BSe heterostructure. 2023 , 47, 4537-4542	О
368	Screening of single-atom catalysts of transition metal supported on MoSe2 for high-efficiency nitrogen reduction reaction. 2023 , 537, 112967	1
367	Experimental and first-principles study on the interfacial interactions between vertically aligned carbon nanotubes and growth substrates: Prospects for better substrate adhesion. 2023 , 133, 109734	О
366	Strong phonon mode induced by carbon vacancy accelerating hole transfer in SiC/MoS2 heterostructure. 2023 , 617, 156554	О
365	Electrocatalytic nitrogen fixation performance of two-dimensional Metal-Organic Frameworks Cu3(C6O6) and TM/Cu3(C6O6) from first-principle study. 2023 , 568, 111837	О
364	Two-dimensional conjugated metal@rganic frameworks TM3(HAT)2: a new family of promising single-atom electrocatalysts for efficient nitrogen fixation. 2023 , 10, 024002	О
363	Superconducting state of the van der Waals layered PdH2 structure at high pressure. 2023,	О
362	Reaction profiles for quantum chemistry-computed [3 + 2] cycloaddition reactions. 2023 , 10,	О
361	On the Trail of Molecular Hydrophilicity and Hydrophobicity at Aqueous Interfaces. 2023, 14, 1301-1309	O
360	N-doped rutile TiO2 composite g-C3N4 with Z-Scheme boosts photocatalytic hydrogen production under visible light.	О
359	Role of Magnetic Defects in Tuning Ground States of Magnetic Topological Insulators. 2209951	О
358	Coupling a Main-Group Metal with a Transition Metal to Create Biatom Catalysts for Nitric Oxide Reduction. 2023 , 19,	O
357	Ni-Decorated PtS2 Monolayer as a Strain-Modulated and Outstanding Sensor upon Dissolved Gases in Transformer Oil: A First-Principles Study. 2023 , 8, 6090-6098	О
356	On the Cation-Lapabilities of infinitene ($\mbox{\em L}$ Evaluation of bonding and circular dichroism properties for Infinitene-Ag(I)n ($\mbox{\em n}'='1\mbox{\em L}$) complexes from relativistic DFT calculations. 2023 , 234, 116323	О
355	Partial Oxidation of Methane to Methanol on the MDAg/Graphene (M = Ag, Cu) Composite Catalyst: A DFT Study. 2023 , 39, 2422-2434	О
354	Effects of dispersion corrections on the theoretical description of bulk metals. 2023, 107,	О
353	Interaction between [(ြB-p-cym)M(H2O)3]2+ (MII = Ru, Os) or [([B-Cp*)M(H2O)3]2+ (MIII = Rh, Ir) and Phosphonate Derivatives of Iminodiacetic Acid: A Solution Equilibrium and DFT Study. 2023 , 28, 1477	О
352	Linear Conjugated Coordination Polymers for Electrocatalytic Oxygen Evolution Reaction. 2207720	О

351	Tunable sliding ferroelectricity and magnetoelectric coupling in two-dimensional multiferroic MnSe materials. 2023 , 9,	Ο
350	Adsorption and gas-sensing properties of SF6 decomposition components (SO2, SOF2 and SO2F2) on Co or Cr modified GeSe monolayer: a DFT study. 2023 , 28, 101382	Ο
349	Potential application of two-dimensional PC6 monolayer as an anode material in alkali metal-ion (Li, Na, K) batteries. 2023 , 769, 139734	0
348	DFT study of Mg decorated on the planar B2N as a novel hydrogen storage media. 2023 , 46, 106263	O
347	Halogenated and chalcogenated Ti2C MXenes: High capacity electrode materials for lithium-ion batteries. 2023 , 814, 140356	1
346	Temperature-swing molecular exclusion separation of hexane isomers in robust MOFs with double-accessible open metal sites. 2023 , 460, 141743	O
345	Enhanced reversible hydrogen storage performance of Mg-decorated g-C2N: First principles calculations. 2023 , 220, 112046	0
344	Development and Validation of a ReaxFF Reactive Force Field for Modeling SiliconCarbon Composite Anode Materials in Lithium-Ion Batteries. 2023 , 127, 2818-2834	O
343	Theoretical Mechanistic Investigation of the Dynamic Kinetic Resolution of N-Protected Amino Acid Esters using Phase-Transfer Catalysts.	0
342	Quantum capacitance of iron metal doped boron carbide monolayer-based for supercapacitors electrodes: A DFT study. 2023 , 150, 110480	O
341	Molecular dynamics simulation studies of 1,3-dimethyl imidazolium nitrate ionic liquid with water. 2023 , 158, 084505	0
340	Interfacial interaction of monolayer MX2 (M=Mo, W; X=S, Se, Te)/SiO2 interfaces for composite optical fibers. 2023 , 37, 102739	O
339	Reversible Hydrogen Storage Media by g-CN Monolayer Decorated with NLi4: A First-Principles Study. 2023 , 13, 647	0
338	[2,1,3]-Benzothiadiazole-Spaced Co-Porphyrin-Based Covalent Organic Frameworks for O2 Reduction. 2023 , 17, 3492-3505	O
337	Model Chemistry Recommendations for Scaled Harmonic Frequency Calculations: A Benchmark Study. 2023 , 127, 1715-1735	0
336	Machine learning based modeling of disordered elemental semiconductors: understanding the atomic structure of a-Si and a-C. 2023 , 38, 043001	O
335	Direct deoxygenation reaction of oxygenated model compounds by biomass pyrolysis on the Ni5P4(001) surface: a computational study. 2023 , 7, 1415-1432	0
334	Theoretical simulations on metal nanocluster systems. 2023 , 201-231	Ο

333	High-Performance N-Butanol Gas Sensor Based on Iron-Doped Metal Organic Framework-Derived Nickel Oxide and DFT Study.	О
332	A comparative ab initio study of acetylene activation over Au9 cluster and Au9 supported over ZnO monolayer. 2023 , 1222, 114072	O
331	Effect of strain and electric field on electronic structure and optical properties of Ga₂SeTe/ln₂3</sub> heterojunction. 2023 , 72, 076301	О
330	Computational Approaches in Some Important Organometallic Catalysis Reaction. 2023, 375-407	Ο
329	Investigation of intrinsic catalytic mechanism for NO oxidation to NO2 in CeO2 used for NO removal. 2023 , 460, 141801	O
328	SpinBrbit and exchange proximity couplings in graphene/1T-TaS2 heterostructure triggered by a charge density wave. 2023 , 10, 025013	O
327	Structural Significance of Hydrophobic and Hydrogen Bonding Interaction for Nanoscale Hybridization of Antiseptic Miramistin Molecules with Molybdenum Disulfide Monolayers. 2023 , 28, 1702	0
326	Scalable synthesis of nitrogen and nitrogenBilicon co-doped graphene: SiC4 and SiN1C3 as new active centers for boosting ORR performance. 2023 ,	O
325	Ferromagnetism Induced by Magnetic Dilution in Van der Waals Material Metal Thiophosphates. 2023 , 6, 2200105	0
324	Pyridinic-nitrogen on ordered mesoporous carbon: A versatile NAD(P)H mimic for borrowing-hydrogen reactions. 2023 , 419, 80-98	Ο
323	Two-Dimensional Ferroelectricity in a Single-Atom Adsorbed Bil3 Monolayer. 2023, 127, 3898-3903	O
322	Three-Dimensional Carbon Foam Modified with Mg3N2 for Ultralong Cyclability of a Dendrite-Free Li Metal Anode.	O
321	Comparison study of vibration frequencies and electronic properties by quantum mechanical calculation for open geodesic polyarene molecules. 2023 ,	0
320	Impact of Hydrogen Coverage Trend on Methyl Formate Adsorption on MoS2 Surface: A First Principles Study. 2023 , 8, 6523-6529	O
319	A polymeric hydrogel electrocatalyst for direct water oxidation. 2023 , 14,	1
318	Extending density functional theory with near chemical accuracy beyond pure water. 2023, 14,	O
317	Experimental and DFT study of Cu(II) removed by Na-montmorillonite. 2023, 87, 834-851	0
316	Different Doping of VSe2 Monolayers as Adsorbent and Gas Sensing Material for Scavenging and Detecting SF6 Decomposed Species. 2023 , 39, 2618-2630	1

315	Possible Origin of Low-Frequency Magnetic Flux Noise in Superconducting Devices. 2023, 14, 1854-1861	O
314	Layer Dependence of Thermally Induced Quantum Confinement and Higher Order Phonon Scattering for Thermal Transport in CVD-Grown Triangular MoS2. 2023 , 127, 3787-3799	O
313	Electronic structures and ligand effect on redox potential of iron and cobalt complexes: a computational insight.	0
312	Statistical Equivalence of Quantum Chemical Methods for Energy Distribution in Water Clusters.	O
311	The oxygen reduction reaction activity and selectivity of porous-carbon supported transition metals (M-C: M Mn, Fe, Co, Ni, Cu) electrocatalysts. 2023 , 134, 109776	0
310	Metal-Free Carbon Nitride Nanosheet Supported the Pentacoordinated Silicon Intermediates for Photocatalytic Overall Water Splitting. 2023 , 14, 1918-1927	O
309	Single Atom Catalysis for Hydrogen Evolution Reaction using Transition-metal Atoms Doped g-C 3 N 3 : A Density Functional Theory Study. 2023 , 8,	O
308	Machine Learning-Guided Computational Screening of New Candidate Reactions with High Bioorthogonal Click Potential.	O
307	Why Is Quantum Chemistry So Complicated?. 2023, 145, 4343-4354	0
306	Toward Pair Atomic Density Fitting for Correlation Energies with Benchmark Accuracy. 2023 , 19, 1499-1516	O
305	Toward Pair Atomic Density Fitting for Correlation Energies with Benchmark Accuracy. 2023, 19, 1499-1516 P-Stereogenic Ir-MaxPHOX: A Step toward Privileged Catalysts for Asymmetric Hydrogenation of Nonchelating Olefins. 2023, 13, 3020-3035	0
	P-Stereogenic Ir-MaxPHOX: A Step toward Privileged Catalysts for Asymmetric Hydrogenation of	
305	P-Stereogenic Ir-MaxPHOX: A Step toward Privileged Catalysts for Asymmetric Hydrogenation of Nonchelating Olefins. 2023 , 13, 3020-3035 Indirect Z-scheme hydrogen production photocatalyst based on two-dimensional GeC/MoSi2N4 van	1
3°5 3°4	P-Stereogenic Ir-MaxPHOX: A Step toward Privileged Catalysts for Asymmetric Hydrogenation of Nonchelating Olefins. 2023, 13, 3020-3035 Indirect Z-scheme hydrogen production photocatalyst based on two-dimensional GeC/MoSi2N4 van der Waals heterostructures. 2023, Improving lithium polysulfides adsorption by oxygen-vacancy defects: By first-principles	0
3°5 3°4 3°3	P-Stereogenic Ir-MaxPHOX: A Step toward Privileged Catalysts for Asymmetric Hydrogenation of Nonchelating Olefins. 2023, 13, 3020-3035 Indirect Z-scheme hydrogen production photocatalyst based on two-dimensional GeC/MoSi2N4 van der Waals heterostructures. 2023, Improving lithium polysulfides adsorption by oxygen-vacancy defects: By first-principles calculation. 2023, 220, 112038 Direct Experimental Determination of Ag Adatom Locations in TCNQ-Ag 2D Metal©rganic	1 0
3°5 3°4 3°3 3°2	P-Stereogenic Ir-MaxPHOX: A Step toward Privileged Catalysts for Asymmetric Hydrogenation of Nonchelating Olefins. 2023, 13, 3020-3035 Indirect Z-scheme hydrogen production photocatalyst based on two-dimensional GeC/MoSi2N4 van der Waals heterostructures. 2023, Improving lithium polysulfides adsorption by oxygen-vacancy defects: By first-principles calculation. 2023, 220, 112038 Direct Experimental Determination of Ag Adatom Locations in TCNQ-Ag 2D Metal©rganic Framework on Ag(111). 2023, 127, 4266-4272 Simulation of Cocrystal Formation in Planetary Atmospheres: The C6H6:C2H2 Cocrystal Produced	1 0 0
305 304 303 302 301	P-Stereogenic Ir-MaxPHOX: A Step toward Privileged Catalysts for Asymmetric Hydrogenation of Nonchelating Olefins. 2023, 13, 3020-3035 Indirect Z-scheme hydrogen production photocatalyst based on two-dimensional GeC/MoSi2N4 van der Waals heterostructures. 2023, Improving lithium polysulfides adsorption by oxygen-vacancy defects: By first-principles calculation. 2023, 220, 112038 Direct Experimental Determination of Ag Adatom Locations in TCNQ-Ag 2D Metal@rganic Framework on Ag(111). 2023, 127, 4266-4272 Simulation of Cocrystal Formation in Planetary Atmospheres: The C6H6:C2H2 Cocrystal Produced by Gas Deposition. 2023, 127, 2322-2335 The effect of long-range interactions on the infrared and Raman spectra of aragonite (CaCO3,	1 0 0 0 0

297	Designing Excess Electron Compounds by Substituting Alkali Metals to a Small and Versatile Tetracyclic Framework: A Theoretical Perspective. 2023 , 8, 7978-7988	0
296	Theoretical understanding of stability of mechanically interlocked carbon nanotubes and their precursors. 2023 , 25, 7527-7539	O
295	The important role of surface charge on a new mechanism of nitrogen reduction. 2023, 25, 7986-7993	О
294	A first-principles investigation on the adsorption of octanal and nonanal molecules with decorated monolayer WS2 as promising gas sensing platform. 2023 , 13, 025157	Ο
293	Enhancing the Stability of a Pt-Free ORR Catalyst via Reaction Intermediates. 2023, 10, 2202132	0
292	Substrate-Induced Modulation of Quantum Emitter Properties in 2D Hexagonal Boron Nitride: Implications for Defect-Based Single Photon Sources in 2D Layers. 2023 , 6, 3446-3452	O
291	NAP-XPS Probes the Electronic Structure of the MgAlūl Layered Double Hydroxide upon Controlled Hydration. 2023 , 127, 4144-4153	0
290	Transition metal atoms anchored 2D holey graphyne for hydrogen evolution reaction: Acumen from DFT simulation. 2023 ,	O
289	Density functional theory-based quantum-computational analysis on the strain-assisted electronic and photocatalytic properties of BX-MSSe ($X = P$, As and $M = Mo$, W) heterostructures. 2023 , 129,	0
288	Chlorine-promoted copper catalysts for CO2 electroreduction into highly reduced products. 2023 , 4, 101294	Ο
287	Formation of ibrutinib solvates: so similar, yet so different. 2023 , 10, 210-219	О
286	CO Inversion on a NaCl(100) Surface: A Multireference Quantum Embedding Study. 2023 , 127, 1975-1987	О
285	MoS2/NiSe2/rGO Multiple-Interfaced Sandwich-like Nanostructures as Efficient Electrocatalysts for Overall Water Splitting. 2023 , 13, 752	0
284	Unveiling the latent reactivity of imines on pyridine-functionalized covalent organic frameworks for H2O2 photosynthesis.	O
283	Oxygen-Related Defect Engineering of Amorphous Vanadium Pentoxide Cathode for Achieving High-Performance Thin-Film Aqueous Zinc-Ion Batteries. 2023 , 6, 2719-2727	0
282	Molecular dynamics simulations of the Li-ion diffusion in the amorphous solid electrolyte interphase. 2023 , 108242	O
281	Investigation of Contact Electrification between 2D MXenes and MoS 2 through Density Functional Theory and Triboelectric Probes. 2023 , 33,	0
280	Computational design of a new palladium alloy with efficient hydrogen storage capacity and hydrogenation-dehydrogenation kinetics. 2023 ,	O

279	Ullmann-Like Covalent Bond Coupling without Participation of Metal Atoms. 2023, 17, 4387-4395	O
278	Rh-doped ultrathin NiFeLDH nanosheets drive efficient photocatalytic water splitting. 2023,	O
277	Carboxyl substituted Bambus[6]uril as a novel macrocyclic receptor for cyanide anion: A DFT study. 2023 , 1222, 114081	O
276	How cation nature controls the bandgap and bulk Rashba splitting of halide perovskites.	O
275	Optical Effect Modulation in Polarized Raman Spectroscopy of Transparent Layered HoO 3. 2206932	0
274	A High-Throughput Screening toward Efficient Nitrogen Fixation: Transition Metal Single-Atom Catalysts Anchored on an Emerging ©conjugated Graphitic Carbon Nitride (g-C10N3) Substrate with Dirac Dispersion. 2023 , 15, 11812-11826	O
273	Synergistic promotions between CO2 capture and in-situ conversion on Ni-CaO composite catalyst. 2023 , 14,	O
272	Charge Density Evolution Governing Interfacial Friction. 2023 , 145, 5536-5544	O
271	Metal-Decorated InN Monolayer Senses N2 against CO2. 2023 , 15, 12534-12544	1
270	Vertically Aligned Nanoplates of Atomically Precise Co6S8 Cluster for Practical Arsenic Sensing. 2023 , 5, 893-899	O
269	Comprehensive study on electronic structures of SiGe/Ga\$\$_{2}\$\$SeTe vdW heterobilayer. 2023 , 58, 4020-4030	0
268	Two-dimensional Janus MGeSiP4 (M = Ti, Zr, and Hf) with an indirect band gap and high carrier mobilities: first-principles calculations. 2023 , 25, 8779-8788	O
267	Mo Cluster Support on C $2\mathrm{N}$ as a Highly-efficient Catalyst for Electrocatalytic Nitrogen Reduction Reaction.	0
266	Lithium adsorption on the interface of graphene/boron nitride nanoribbons. 2023, 58, 4513-4524	O
265	The phonon thermal Hall angle in black phosphorus. 2023 , 14,	0
264	Theoretical Study on the Role of Solvents in Lithium Polysulfide Anchoring on Vanadium Disulfide Facets for LithiumBulfur Batteries. 2023 , 127, 4416-4424	O
263	Anharmonicity Reveals the Tunability of the Charge Density Wave Orders in Monolayer VSe2. 2023 , 23, 1794-1800	0
262	Lightweight, ultrastrong and high thermal-stable eutectic high-entropy alloys for elevated-temperature applications. 2023 , 248, 118806	O

261	Mechanistic Insight into the Promotion of the Low-Temperature NH3-Selective Catalytic Reduction Activity over MnxCe1⊠Oy Catalysts: A Combined Experimental and Density Functional Theory Study. 2023 , 57, 3875-3882	O
2 60	Fluorine-based Zn salan complexes. 2023 , 52, 4044-4057	O
259	Drastic Gas Sensing Selectivity in 2-Dimensional MoS2 Nanoflakes by Noble Metal Decoration. 2023 , 17, 4404-4413	О
258	Physical Insights on the Phonon Dispersion of TiS 2. 2200821	O
257	Pd encapsulated core-shell ZIF-8/ZIF-67 for efficient oxygen evolution reaction. 2023 , 447, 142100	O
256	Current transmission pathways in potassium intercalated graphene. 2023 , 221, 112099	O
255	Using ternary steric hindrance synergy of a defective MoS2 monolayer to manipulate the electrocatalytic mechanism toward nitric oxide reduction: a first-principles and machine learning study. 2023 , 11, 7159-7169	О
254	Aculeaxanthones A E , new xanthones from the marine-derived fungus Aspergillus aculeatinus WHUF0198. 14,	O
253	Monolayer and bilayer PtCl3: Energetics, magnetism, and band topology. 2023, 107,	O
252	Hydrated electrons as nodes in porous clathrate hydrates. 2023 , 158, 114504	O
251	Electronic Structure Calculations of Static Hyper(Polarizabilities) of Substrate-Supported Group-IV and -V Elemental Monolayers. 2023 , 8, 9614-9620	O
250	New C2h phase of group III monochalcogenide monolayers AlX (X = S, Se, and Te) with anisotropic crystal structure: first-principles study. 2023 , 13, 6838-6846	O
249	Stacking-dependent topological magnons in bilayer CrI3. 2023 , 7,	О
248	Non-covalent Functionalization of Pristine and Defective WSe2 by Electron Donor and Acceptor Molecules. 2023 , 5, 1660-1669	O
247	Anisotropic Excitons Reveal Local Spin Chain Directions in a van der Waals Antiferromagnet. 2206585	O
246	Two-dimensional rectangular bismuth bilayer: A novel dual topological insulator. 2023, 18,	О
245	Antioxidant Properties of Thymoquinone, Thymohydroquinone and Black Cumin (Nigella sativa L.) Seed Oil: Scavenging of Superoxide Radical Studied Using Cyclic Voltammetry, DFT and Single Crystal X-ray Diffraction. 2023 , 12, 607	O
244	Theoretical Evaluation of Highly Efficient Nitrate Reduction to Ammonia on InBi. 2023, 14, 2410-2415	O

243	Effect of intermolecular interaction of the charge-transfer complex between molecular Eweezers and C60/C70 on second-order nonlinear optical properties. 2023 , 25, 8799-8808	O
242	Encapsulation Studies on closo-Dicarbadodecaborane Isomers in Neutral Tetrahedral Palladium(II) Cages. 2023 , 62, 4035-4042	O
241	Mechanism for the synthesis of medium-chain 1-alkenes from fatty acids catalyzed by binuclear iron UndA decarboxylase. 2023 , 420, 123-133	0
240	Precipitation-free aluminum-air batteries with high capacity and durable service life. 2023 , 462, 142182	O
239	New stable ultrawide bandgap As2O3 semiconductor materials. 2023 , 6, 025003	Ο
238	How Protons Move in Enzymes-The Case of Nitrogenase. 2023 , 127, 2156-2159	Ο
237	Different Dynamic Behavior of Methyl Groups in Crystalline Carbimazole as Revealed by a Multitechnique Experimental and Theoretical Approach. 2023 , 127, 5186-5196	Ο
236	Spinel-Anchored Iridium Single Atoms Enable Efficient Acidic Water Oxidation via Intermediate Stabilization Effect. 2023 , 13, 3757-3767	Ο
235	Interfacial electronic properties and tunable band offset in graphyne/MoSe2 heterostructure with high carrier mobility. 2023 , 47, 7084-7092	Ο
234	Spontaneously enhanced visible-light-driven photocatalytic water splitting of type II PG/AlAs5 van der Waal heterostructure: A first-principles study. 2023 , 108270	Ο
233	Orbital magnetoelectric effect in nanoribbons of transition metal dichalcogenides. 2023, 107,	Ο
232	A DFT Based Approach for NO2 Sensing Using Vander Wall Hetero Monolayer. 1-12	O
231	Brlisted Acids Promote Olefin Oxidations by Bioinspired Nonheme Colll(PhIO)(OH) Complexes: A Role for Low-Barrier Hydrogen Bonds. 2023 , 145, 5739-5749	1
230	Polarization and built-in electric field improve the photocatalytic overall water splitting efficiency of C2N/ZnSe heterostructures. 2023 ,	Ο
229	In-situ growth of low-dimensional perovskite-based insular nanocrystals for highly efficient light emitting diodes. 2023 , 12,	Ο
228	Tunable interlayer excitons and switchable interlayer trions via dynamic near-field cavity. 2023, 12,	1
227	MOFs-alginate/polyacrylic acid/poly (ethylene imine) heparin-mimicking beads as a novel hemoadsorbent for bilirubin removal in vitro and vivo models. 2023 , 235, 123868	0
226	Anthracite based activated carbon impregnated with HMTA as an effectiveness adsorbent could significantly uptake gasoline vapors. 2023 , 254, 114698	O

225	Strain-Driven Superlubricity of Graphene/Graphene in Commensurate Contact. 2023, 10,	0
224	Achieving sustainability of greenhouses by integrating stable semi-transparent organic photovoltaics.	O
223	Interaction Modification of Transition Metal Dichalcogenide Layers by Halogenation. 2023, 127, 5134-5144	О
222	Intrinsic magnetism with high critical temperatures and piezoelectricity in 2D transition metal tetraborides.	O
221	Reactant conversionIntercalation strategy toward interlayer-expanded MoS2 microflowers with superior supercapacitor performance. 2023 , 52, 4537-4547	О
220	Catalytic cycle of formate dehydrogenase captured by single-molecule conductance. 2023 , 6, 266-275	O
219	Semimetallic and semiconducting graphene- hBN multilayers with parallel or reverse stacking. 2023 , 107,	О
218	Interfacial contact barrier and charge carrier transport of MoS2/metal(001) heterostructures. 2023 , 25, 9548-9558	O
217	Two-Dimensional Carbon Networks with a Negative Poisson Ratio. 2023 , 13, 442	О
216	Study on the Half-Auxetic Behavior of Layered Nitrogen-Doped Graphdiyne. 2023 , 12, 1-8	O
215	Dynamical Screening of Local Spin Moments at Metal Molecule Interfaces. 2023, 17, 5974-5983	О
214	C3N2: the missing part of highly stable porous graphitic carbon nitride semiconductors.	О
213	First-Principles Modeling of the Adsorption Mechanism of Carboxylic and Phosphonic Acids onto Pristine and Defective Delafossite CuAlO 2 Surfaces.	О
212	Development of Deep Potentials of Molten MgCl2NaCl and MgCl2NCl Salts Driven by Machine Learning.	O
211	High reactivity of mesoporous CeO2 to dissociate chemical warfare agent sarin.	О
210	Efficient Synthesis of 1H-Benzo[4,5]imidazo[1,2-c][1,3]oxazin-1-one Derivatives Using Ag2CO3/TFA-Catalyzed 6-endo-dig Cyclization: Reaction Scope and Mechanistic Study. 2023 , 28, 2403	O
209	Exploring the adsorption performance of doped graphene quantum dots as anticancer drug carriers for cisplatin by DFT, PCM, and COSMO approaches.	О
208	Comparative studies of hexagonal boron phosphide/V2CS2 heterostructure and homogeneous bilayers as metal-ion battery anodes. 2023 , 25, 10011-10021	O

207	DELTA50: A Highly Accurate Database of Experimental 1H and 13C NMR Chemical Shifts Applied to DFT Benchmarking. 2023 , 28, 2449	Ο
206	Computational studies on functionalized Janus MXenes MM?CT2, (M, M? = Zr, Ti, Hf, M \square M?; T = \square , \square , \square H, \square DH): photoelectronic properties and potential photocatalytic activities. 2023 , 13, 7972-7979	О
205	Experimental and Computational Study on the Effects of High Pressure on the Crystal Structure of Boron Nitrilotriacetate. 2023 , 23, 2745-2754	0
204	Tuning the mechanical anisotropy of biphenylene by boron and nitrogen doping. 2023, 222, 112119	О
203	Intercell moir[exciton complexes in electron lattices.	0
202	A Multiple Proton Transfer Mechanism for the Charging Step of the Aminoacylation Reaction at the Active Site of Aspartyl tRNA Synthetase. 2023 , 63, 1819-1832	O
201	Experimental and ab initio Investigation on the Effect of CO and CO 2 during Hydrodeoxygenation of m-Cresol over Co/SBA-15. 2023 , 15,	0
200	Role of Chalcogen Defect Introducing Metal-Induced Gap States and Its Implications for Metal MDs Interface Chemistry. 2023 , 8, 10176-10184	О
199	Is the impact sensitivity of RDX polymorph dependent?. 2023 , 158, 124115	0
198	Theoretical exploration on the activity of copper single-atom catalysts for electrocatalytic reduction of CO2. 2023 , 11, 7735-7745	О
197	Determining the Electronic Structure and Thermoelectric Properties of MoS 2 /MoSe 2 Type-I Heterojunction by DFT and the Landauer Approach. 2023 , 10,	0
196	Boosting Pseudocapacitive Behavior of Supercapattery Electrodes by Incorporating a Schottky Junction for Ultrahigh Energy Density. 2023 , 15,	О
195	Ab initio studies on graphyne (GY) for the detection of rare bases in DNA. 2023, 25, 10472-10480	0
194	Biphenyl Au(III) Complexes with Phosphine Ancillary Ligands: Synthesis, Optical Properties, and Electroluminescence in Light-Emitting Electrochemical Cells. 2023 , 62, 4903-4921	О
193	First-principles study on unidirectional proton transfer on anatase TiO2 (101) surface induced by external electric fields. 2023 , 25, 9454-9460	0
192	Nucleation Stage for the Oriented Growth of Tantalum Sulfide Monolayers on Au(111). 2023, 127, 5622-5630	0
191	Bio-piezoelectric phenylalanine-时ehydrophenylalanine nanotubes as potential modalities for combinatorial electrochemotherapy in glioma cells.	0
190	Direct Atomic-Level Insight into Oxygen Reduction Reaction on Size-Dependent Pt-based Electrocatalysts from Density Functional Theory Calculations. 2023 ,	O

189	Ferroelectric polarization and interface engineering coupling of Z-scheme ZnIn2S4/\(\perp\)n2Se3 heterostructure for efficient photocatalytic water splitting. 2023 , 133, 105702	О
188	Electron P honon Interaction Contribution to the Total Energy of Group IV Semiconductor Polymorphs: Evaluation and Implications. 2023 , 8, 11251-11260	О
187	Computational design of the novel building blocks for the metal-organic frameworks based on the organic ligand protected Cu4 cluster. 2023 ,	О
186	The Temperature Dependence of the Hexagonal Boron Nitride Oxidation Resistance, Insights from First B rinciple Computations. 2023 , 13, 1041	О
185	Novel energetic salts based on nitrogen-rich fused ring cations: Synthesis, characterization and infrared laser ignition property. 2023 ,	О
184	A DFT study on how vanadium affects hydrogen storage kinetics in magnesium nickel hydride. 2023 ,	O
183	Strain-Modulated Photocatalytic Performance of Janus WSSe/g-GaN Heterostructures. 2023, 127, 5544-5551	О
182	Emerging Metabolic Profiles of Sulfonamide Antibiotics by Cytochromes P450: A Computational Experimental Synergy Study on Emerging Pollutants. 2023 , 57, 5368-5379	О
181	Theoretical Study of Pressure-Induced Phase Transitions in Sb2S3, Bi2S3, and Sb2Se3. 2023 , 13, 498	О
180	Computational and Theoretical Aspects of Structure and Bonding in Doubly Bonded Organogermanium Compounds. 2023 , 1-102	О
179	Direct synthesis of propylene glycol methyl ether from propylene using an Al-TS-1 catalyst: TiAl synergy.	О
178	Classification of doubly excited molecular electronic states. 2023 , 14, 4012-4026	О
177	Compatibility and Interaction Mechanism between the C4F7N/CO2/O2 Gas Mixture and FKM and NBR. 2023 , 8, 11414-11424	O
176	Theoretical design of a photodetector based on a two-dimensional SnSe2/GaP type-II heterostructure. 2023 , 25, 2326-2338	O
175	Engineering electrode/electrolyte interface charge transfer of a TiO2N photoanode with enriched surface oxygen vacancies for efficient water splitting.	O
174	Theoretical Kinetic Isotope Effects in Establishing the Precise Biodegradation Mechanisms of Organic Pollutants. 2023 , 57, 4915-4929	O
173	Spin-phonon interaction and short-range order in Mn3Si2Te6. 2023 , 107,	О
172	Van der Waals Stacked 2D-Layered Co2Ge2Te6 with High Curie Temperature and Large Magnetic Crystal Anisotropy. 2023 , 127, 5991-6001	O

171	First-principles study of ferroelectricity, antiferroelectricity, and ferroelasticity in two-dimensional #AlOOH. 2023 , 107,	Ο
170	Antiferromagnetic Ordering in Bowtie and AA-Stacking Bilayer Trapezoidal Graphene Nanoflakes: A Comparison Study. 2300003	O
169	Rectangular-Phase Tellurene on Ni(111) from Monolayer Films to Periodic Striped Patterns. 2023 , 15, 16144-16152	Ο
168	Superconductivity emerging from a pressurized van der Waals kagome material Pd3P2S8. 2023 , 25, 043001	O
167	Self-Assembly Fabrication of Energetic Perchlorates with High Density and Near-Infrared Laser Ignition Capacity. 2023 , 23, 2702-2709	0
166	Unique features of the structural phase transition in acetylene showing simultaneous characteristics of reconstructive, displacive and orderdisorder. 2023 , 25, 9909-9924	O
165	Nitrogen and sulfur co-doped Ti3C2Tx MXenes for high-rate lithium-ion batteries. 2023 , 25, 10635-10646	Ο
164	Revealing the impact of organic spacers and cavity cations on quasi-2D perovskites via computational simulations. 2023 , 13,	Ο
163	A systematic computational investigation of lithiation-induced structural phase transitions of O-functionalized MXenes. 2023 , 25, 9428-9436	0
162	Enhancement of spin-orbit torque in WS2/Co/Pt trilayers via spin-orbit proximity effect. 2023 , 107,	O
161	Insights into the Corrosion Inhibition Performance of Three 2-Isoxazoline-Lactones for Carbon Steel in Acidic Medium: Linking Molecular and Experimental-Level Information with Microscopic-Scale Modeling. 2023 , 11, 141	0
160	Effects of Anions and Protein Structures on Protein-Based Solid Electrolytes. 2201875	О
159	Residual Molecular Groups[Adsorption in Tuning the Transport Properties of Carbon Nanotubes. 2023 , 5, 1853-1858	0
158	Electronic Properties of Vertically Stacked h-BN/B1\AlxN Heterojunction on Si(100). 2023, 15, 16211-16220	O
157	Brfisted Acid Strength Does Not Change for Bulk and External Sites of MFI Except for Al Substitution Where Silanol Groups Form. 2023 , 13, 4470-4487	0
156	Modeling the Electronic and Optical Properties of Lead-Based Perovskite Materials: Insights from Density Functional Theory and Electrostatic Embedding. 2023 , 127, 5968-5981	O
155	Density Functional Theory Study of Oxygen Evolution Reaction Mechanism on Rare Earth Sc-Doped Graphene. 2023 , 9, 175	О
154	Layer-dependent electronic structures and optical properties of two-dimensional PdSSe.	O

153	Reversible Facet Reconstruction of CdSe/CdS Core/Shell Nanocrystals by FacetIligand Pairing. 2023 , 145, 6798-6810	Ο
152	First-principles structure prediction of two-dimensional HCN polymorphs obtained via formal molecular polymerization.	Ο
151	High production of furfural by flash pyrolysis of C6 sugars and lignocellulose by Pd-PdO/ZnSO4 catalyst. 2023 , 14,	Ο
150	How the Conformational Movement of the Substrate Drives the Regioselective CN Bond Formation in P450 TleB: Insights from Molecular Dynamics Simulations and Quantum Mechanical/Molecular Mechanical Calculations. 2023 , 145, 7252-7267	Ο
149	Ni nanoparticle coupled surface oxygen vacancies for efficient synergistic conversion of palmitic acid into alkanes. 2023 , 47, 229-242	О
148	N -Heterocyclic Olefin Type Ionic Liquid with Innate Soft Lewis-Base Character as an Effective Additive for Hybrid Quasi-2D and 3D Perovskite Solar Cells. 2300013	O
147	Intrinsic ferroelectrics and carrier doping-induced metallic multiferroics in an atomic wire. 2023,	О
146	A first-principles study of self-healing binders for next-generation Si-based lithium-ion batteries. 2023 , 29, 101474	O
145	Computational Study on NiAl Bimetal-Catalyzed Twofold CH Annulation Reaction: Mechanism, Origin of Selectivity, and Role of SPO Ligand.	О
144	Transition-Metal-Free, Pure p-Block Alloy Electrocatalysts for the Highly Efficient Nitrate Reduction to Ammonia. 2023 , 35, 2884-2891	O
143	A Buckycatcher in Solution Computational Perspective. 2023, 28, 2841	О
142	Gamma-Ray Irradiation Induced Ultrahigh Room-Temperature Ferromagnetism in MoS2 Sputtered Few-Layered Thin Films. 2023 , 17, 6555-6564	O
141	High electrochemical stability and low-agglomeration of defective Co3O4 nanoparticles supported on N-doped graphitic carbon nano-spheres for oxygen evolution reaction. 2023 ,	Ο
140	Energies Exploration for the Troponine Molecule Supported on Carbon Nanomaterials: DFT Study. 2023 , 8, 12334-12338	Ο
139	Quantum Chemical Study the Removal of Acetone by Using the Pristine and Si-doped C2N Monolayer.	Ο
138	Role of Non-Covalent Interactions in Carbonic Anhydrase Illopiramate Complex Based on QM/MM Approach. 2023 , 16, 479	Ο
137	Superconductivity and charge density wave in transition metal chalcogenides: A first principle study. 2023 , 151, 115714	0
136	Direct Laser Writing of Multimetal Bifunctional Catalysts for Overall Water Splitting. 2023, 6, 3756-3768	0

135	Enhancing efficiency of the ternary tri-chalcogenide MnPSe3 towards hydrogen evolution reaction by activating its basal plane. 2023 ,	O
134	From ultra-low friction to superlubricity state of black phosphorus: Enabled by the critical oxidation and load.	O
133	Role of molecular modelling in the development of metal-organic framework for gas adsorption applications. 2023 , 135,	O
132	Regulated adsorption sites using atomically single cluster over biochar for efficient elemental mercury uptake. 2023 , 5,	O
131	Defect-Engineered 3D Nanostructured MoS2 for Detection of Ammonia Gas at Room Temperature. 2023 , 6, 5284-5297	0
130	Enhanced Photocatalytic Activity of Two-Dimensional Polar Monolayer SiTe for Water-Splitting via Strain Engineering. 2023 , 28, 2971	O
129	Approach of Electronic Structure Calculations to Crystal. 2023 , 209-255	0
128	Polarization Modulation on Charge Transfer and Band Structures of GaN/MoS2 Polar Heterojunctions. 2023 , 13, 563	O
127	Nitrogen adsorption via charge transfer on vacancies created during surfactant assisted exfoliation of TiB2.	0
126	Nonvolatile Electrical Control and Reversible Gas Capture by Ferroelectric Polarization Switching in 2D FeI2/In2S3 van der Waals Heterostructures.	Ο
125	Exploring Spin-Phonon Coupling in Magnetic 2D Metal-Organic Frameworks. 2023 , 13, 1172	0
124	CO and CO2 adsorption mechanism in Fe(pz)[Pt(CN)4] probed by neutron scattering and density-functional theory calculations.	Ο
123	Proton absorption and penetration behaviors in Pt-supported graphene.	0
122	Heterocyclic Diaryliodonium-Based Inhibitors of Carbapenem-Resistant Acinetobacter baumannii. 2023 , 11,	O
121	Large permittivity, low loss and defect structure in (Nb, Zn) co-doped SnO2 ceramics studied through a combined experimental and DFT calculational method. 2023 ,	0
120	Supported Pt Nanoclusters on Single-Layer MoS2 for the Detection of Cortisol: From Atomistic Scale to Device Modeling.	O
119	Selective Uptake of Ethane/Ethylene Mixtures by UTSA-280 is Driven by Reversibly Coordinated Water Defects. 2023 , 35, 2956-2966	0
118	A first principles study of structural and optoelectronic properties and photocatalytic performance of $GeCMX2$ (M = Mo and W; X = S and Se) van der Waals heterostructures.	O

117	Immobilized triatomic CuB2 clusters on 2D carbon nitride: highly selective conversion of CO to ethanol at low potentials.	O
116	Highly Connected Three-Dimensional Covalent Organic Framework with Flu Topology for High-Performance Li-S Batteries. 2023 , 145, 8141-8149	0
115	Structural classification of boron nitride twisted bilayers and ab initio investigation of their stacking-dependent electronic structure. 2023 , 14,	Ο
114	Understanding the Electronic Structure Basis for N2 Binding to FeMoco: A Systematic Quantum Mechanics/Molecular Mechanics Investigation. 2023 , 62, 5357-5375	O
113	Microscopic Linker Distribution in Mixed-Linker Zeolitic Imidazolate Frameworks via Computational Raman Spectroscopy: Implications for Gas Separation. 2023 , 6, 5645-5652	O
112	Construction of Two-Faced (Hetero)hydrocarbyl Diiron Complexes Mediated by the Interplay of Ligands. 2023 , 42, 615-626	O
111	Nonsymmorphic symmetry protected spin-orbit semi-Dirac fermions in two dimensions. 2023 , 107,	О
110	Complexes of a model trimeric acylphloroglucinol with a Cu2+ ion: a DFT study. 2023 ,	O
109	High-throughput screening of highly efficient Cu-based dual-atom catalysts to promote nitrate electroreduction for ammonia synthesis: A computational study. 2023 , 541, 113095	O
108	Metavalent Bonding in Layered Phase-Change Memory Materials.	О
107	Nanocomposites of Quasicrystal Nanosheets and MoS2 Nanoflakes for NO2 Gas Sensors. 2023 , 6, 5952-5962	O
106	Tailored BiVO 4 Photoanode Hydrophobic Microenvironment Enables Water Oxidative H 2 O 2 Accumulation.	О
105	Bibliography. 2023 , 431-464	O
104	Subtle hydrogen bond preference and dual Franck Condon activity Lithe interesting pairing of 2-naphthol with anisole. 2023 , 25, 10427-10439	O
103	Synergistic marriage of CO2 reduction and sulfide oxidation towards a sustainable co-electrolysis process. 2023 , 332, 122718	O
102	Effect of vacancies and edges in promoting water chemisorption on titanium-based MXenes. 2023 , 10,	O
101	Nonvolatile electrical control of spin polarization in the 2D bipolar magnetic semiconductor VSeF. 2023 , 9,	О
100	Isolated Cu-Sn diatomic sites for enhanced electroreduction of CO2 to CO.	O

99	Nanostructured Ni-MoCx: An efficient non-noble metal catalyst for the chemoselective hydrogenation of nitroaromatics.	0
98	Adsorption of water and formic acid molecules on the (104) surface of calcite: a theoretical study by DFT-D3.	O
97	CO 2 Capture and Separation by Mono-Vacancy Doped Graphene in Electric Field: A DFT study. 2023 , 8,	О
96	Fast-Disintegrating Nanofibrous Web of Pullulan/Griseofulvinflyclodextrin Inclusion Complexes.	O
95	Friction properties of black phosphorus: a first-principles study. 2023 , 34, 275703	0
94	Adsorption Behaviors of Small Molecules on Two-Dimensional Penta-NiN2 Layers: Implications for NO and NO2 Gas Sensors. 2023 , 6, 6151-6160	O
93	A Quantum Monte Carlo Study of the Structural, Energetic, and Magnetic Properties of Two-Dimensional H and T Phase VSe2. 2023 , 14, 3553-3560	О
92	Vibrational spectra and lattice dynamics of the 動hase of white phosphorus. 2023 , 178, 111356	O
91	Hydrogen from catalytic non-thermal plasma-assisted steam methane reforming reaction. 2023,	О
90	Biphenylene Nanotube: A Promising Anode Material for Sodium-Ion Batteries.	O
89	Degradation of Perfluorooctanoic Acid on Aluminum Oxide Surfaces: New Mechanisms from Ab Initio Molecular Dynamics Simulations.	О
88	Rational Design of Highly Efficient PdIn I h2O3 Interfaces by a Capture-Alloying Strategy for Benzyl Alcohol Partial Oxidation. 2023 , 15, 19653-19664	0
87	Density functional theory (DFT) simulation and approach to property-driven investigations in ceramic and composites materials. 2023 , 461-490	О
86	Across-Layer Sliding Ferroelectricity in 2D Heterolayers.	0
85	Quantum Chemical Study of the Mechanism of (E,Z)-1,3-Diphenyl-2-Aza-1,3-Diene Stereoselective Formation from N-Benzyl-1-Phenylethane-1-Imine and Acetylene in the KOt-Bu/DMSO Superbasic Environment. 2023 , 64, 386-397	О
84	Oxidation State Dependent Conjugation Controls Electrocatalytic Activity in a Two-Dimensional Di-Copper Metal Drganic Framework. 2023 , 127, 7299-7307	O
83	Formation of active sites on transition metals through reaction-driven migration of surface atoms. 2023 , 380, 70-76	О
82	Two-dimensional half-metallicity in transition metal atoms decorated Cr2Ge2Te6. 11,	0

81	Terahertz (6-18 THz) spectroscopic characterization of benzoic acid class liquid crystals using Fourier Transform Infrared technique. 1-7	О
80	Order-disorder phase transition driven by interlayer sliding in lead iodides. 2023 , 14,	O
79	Insights into the Electrochemical Production of Hydrogen Peroxide over Single-Atom CoNC Catalysts with the Introduction of Carbon Vacancy Defect near the CoN4 Site. 2023 , 14, 3658-3668	O
78	Accurate Interaction Energies of CO2 with the 20 Naturally Occurring Amino Acids.	O
77	Universal microscopic patterned doping method for perovskite enables ultrafast, self-powered ultrasmall perovskite photodiode.	O
76	High-capacity hydrogen storage in Li-decorated defective penta-BN2: A DFT-D2 study. 2023 ,	O
75	Co/CoSe Junctions Enable Efficient and Durable Electrocatalytic Conversion of Polysulfides for High-Performance Liß Batteries.	0
74	Intrinsic Control of Interlayer Exciton Generation in Van der Waals Materials via Janus Layers.	O
73	Nanoclay-Modulated Interfacial Chemical Bond and Internal Electric Field at the Co $3 O 4$ /TiO $2 p$ -n Junction for Efficient Charge Separation.	O
72	Calculated Outstanding Energy-Storage Media by Aluminum-Decorated Carbon Nitride (g-C3N4): Elucidating the Synergistic Effects of Electronic Structure Tuning and Localized Electron Redistribution. 2023 , 13, 655	O
71	Effect of alkyloxy substituents on mesomorphic and photophysical properties of star-shaped tristriazolotriazines. 1-14	O
70	Electronic properties and optical absorption study of Arsene with PtSe2 type-II heterostructure: based on the first-principles calculation.	O
69	Understanding the wetting of transition metal dichalcogenides from an ab initio perspective. 2023 , 5,	0
68	Dehydration of a crystal hydrate at subglacial temperatures. 2023 , 616, 288-292	O
67	Understanding Li interaction in TiO2/graphene composites for high-performance Li-ion battery anodes: A first principles study. 2023 , 660, 414878	О
66	Encapsulation of Astatide by a water cage.	O
65	Morphology-dependent adsorption energetics of Ru nanoparticles on hcp-boron nitride (001) surface la first-principles study.	О
64	Remarkable modulation of the spin transport properties of transition metal dibenzotetraaza[14]annulenes by adsorption of oxygen. 2023 , 474, 128827	О

63	Supramolecular Gel-to-Gel Transition Induced by Nanoscale Structural Perturbation via the Rotary Motion of Feringa's Motor.	O
62	Peroxo-Diiron(III/III) as the Reactive Intermediate for N-Hydroxylation Reactions in the Multidomain Metalloenzyme SznF: Evidence from Molecular Dynamics and Quantum Mechanical/Molecular Mechanical Calculations. 5808-5818	O
61	Probing the Interaction of NO with C60: Comparison between Endohedral and Exohedral Complexes.	O
60	Synthesis, Crystal structure, Hirshfeld surface interactions, anti-corrosion analysis, DFT calculations, Docking studies and evaluation of the antioxidant activity of a new zwitterion Schiff base. 2023 , 1286, 135569	O
59	Theoretical Study on Origin of CVD Growth Direction Difference in Graphene/hBN Heterostructures. 2023 ,	O
58	13C CPMAS NMR as an Alternative Method to Verify the Quality of Dietary Supplements Containing Curcumin. 2023 , 28, 3442	O
57	On the coexistence of ferroelectric and antiferroelectric polymorphs in NaNbO3 fibers at room temperature.	0
56	Electrical tuning of robust layered antiferromagnetism in MXene monolayer. 2023 , 122, 162403	O
55	Synergy of Small Antiviral Molecules on a Black-Phosphorus Nanocarrier: Machine Learning and Quantum Chemical Simulation Insights. 2023 , 28, 3521	O
54	Engineering magic number Au19 and Au20 cage structures using electron withdrawing atoms.	O
53	Changes in breakdown and charge migration of cellulose/oil composite after CO2 adsorption. 2023 , 133, 155103	О
52	Revealing the high activity of WO3BBA-15 with isolated tungsten oxide species in cis-cyclooctene epoxidation.	O
51	Comparison of the Performance of Density Functional Methods for the Description of Spin States and Binding Energies of Porphyrins. 2023 , 28, 3487	0
50	Corrosion inhibition with a perezone-impregnated Mg/Al hydrotalcite coating in AS21 alloy 2023 , 142428	O
49	Simulation of NO x and CO x Gas Sensor based on Pristine Armchair Stanene Nanoribbon.	O
48	First-principles study of structural, electronic and vibrational properties of bulk and monolayer TiS2. 2023 , 111382	O
47	A systematic first-principles exploration of the impact of metal doping on the electronic properties of MOF MIP-177(Ti). 2023 , 112607	O
46	Unraveling Bonding Mechanisms and Electronic Structure of Pyridine Oximes on Fe(110) Surface: Deeper Insights from DFT, Molecular Dynamics and SCC-DFT Tight Binding Simulations. 2023 , 28, 3545	O

45	Magnetic Ordering in TlGa1-xFexSe2 Dilute Magnetic Semiconductors with Various Fe Dilution Ratios.	O
44	Ruthenium (II) Complexes of CNC Pincers and Bipyridine in the Photocatalytic CO2 Reduction Reaction to CO Using Visible Light: Catalysis, Kinetics, and Computational Insights. 5986-5999	O
43	Interaction of Water and Oxygen Molecules with Phosphorene: An Ab Initio Study. 2023, 28, 3570	O
42	Insights into the Corrosion Inhibition Performance of Isonicotinohydrazide Derivatives for N80 Steel in 15% HCl Medium: An Experimental and Molecular Level Characterization. 2023 , 13, 797	O
41	Atomic level mechanisms of graphene healing by methane-based plasma radicals. 2023, 100506	0
40	Electronic properties and photocatalytic water splitting with high solar-to-hydrogen efficiency in a hBNC/Janus WSSe heterojunction: First-principles calculations. 2023 , 107,	O
39	Swelling effect of 2D BC7 anode material in Li-, Na- and Mg-ion energy storage systems. 2023 , 414902	O
38	A DFT study of methanol synthesis from CO2 hydrogenation on Cu/ZnO catalyst. 2023 , 346, 128381	O
37	Unlocking the Facet-Dependent Ligand Exchange on Rutile TiO2 of a Rhenium Bipyridyl Catalyst for CO2 Reduction.	O
36	L-Histidine-based computation devices. 2023 , 97,	O
36 35	L-Histidine-based computation devices. 2023, 97, Magneto-optical Kerr Effect in Ferroelectric Antiferromagnetic Two-Dimensional Heterostructures.	0
35	Magneto-optical Kerr Effect in Ferroelectric Antiferromagnetic Two-Dimensional Heterostructures. Edge atomic Fe sites decorated porous graphitic carbon as an efficient bifunctional oxygen catalyst	0
35	Magneto-optical Kerr Effect in Ferroelectric Antiferromagnetic Two-Dimensional Heterostructures. Edge atomic Fe sites decorated porous graphitic carbon as an efficient bifunctional oxygen catalyst for Zinc-air batteries. 2023, Selective and Sensitive Detection of Formaldehyde at Room Temperature by Tin Oxide	0
35 34 33	Magneto-optical Kerr Effect in Ferroelectric Antiferromagnetic Two-Dimensional Heterostructures. Edge atomic Fe sites decorated porous graphitic carbon as an efficient bifunctional oxygen catalyst for Zinc-air batteries. 2023, Selective and Sensitive Detection of Formaldehyde at Room Temperature by Tin Oxide Nanoparticles/Reduced Graphene Oxide Composite. Rapid Detection of Cd2+ Ions in the Aqueous Medium Using a Highly Sensitive and Selective	0 0
35 34 33 32	Magneto-optical Kerr Effect in Ferroelectric Antiferromagnetic Two-Dimensional Heterostructures. Edge atomic Fe sites decorated porous graphitic carbon as an efficient bifunctional oxygen catalyst for Zinc-air batteries. 2023, Selective and Sensitive Detection of Formaldehyde at Room Temperature by Tin Oxide Nanoparticles/Reduced Graphene Oxide Composite. Rapid Detection of Cd2+ Ions in the Aqueous Medium Using a Highly Sensitive and Selective Turn-On Fluorescent Chemosensor. 2023, 28, 3635 Two-Dimensional Films Based on Graphene/Li4Ti5O12 and Carbon Nanotube/Li4Ti5O12 Nanocomposites as a Prospective Material for Lithium-Ion Batteries: Insight from Ab Initio	0 0
35 34 33 32 31	Magneto-optical Kerr Effect in Ferroelectric Antiferromagnetic Two-Dimensional Heterostructures. Edge atomic Fe sites decorated porous graphitic carbon as an efficient bifunctional oxygen catalyst for Zinc-air batteries. 2023, Selective and Sensitive Detection of Formaldehyde at Room Temperature by Tin Oxide Nanoparticles/Reduced Graphene Oxide Composite. Rapid Detection of Cd2+ Ions in the Aqueous Medium Using a Highly Sensitive and Selective Turn-On Fluorescent Chemosensor. 2023, 28, 3635 Two-Dimensional Films Based on Graphene/Li4Ti5O12 and Carbon Nanotube/Li4Ti5O12 Nanocomposites as a Prospective Material for Lithium-Ion Batteries: Insight from Ab Initio Modeling. 2023, 16, 3270 Synthesis and Characterization of Xylazine Hydrochloride Polymorphs, Hydrates, and Cocrystals: A	00000

27	A Combined Experimental and Computational (DFT, RDF, MC and MD) Investigation of Epoxy Resin as a Potential Corrosion Inhibitor for Mild Steel in a 0.5 M H2SO4 Environment. 2023 , 15, 1967	О
26	Characterizing Grain Boundary Effects on Mg2+ Conduction in Metal®rganic Frameworks.	O
25	Enabling enhanced lithium storage capacity of two-dimensional pentagonal BN2 by aluminum doping.	О
24	Tribo-catalysis Triggered the In-situ Formation of Amphiphilic Molecules to Reduce Friction and Wear. 2023 , 108541	O
23	Thickness-dependent piezoelecticity of black arsenic from few-layer to monolayer. 2023, 115175	O
22	Extreme Flexibility and Unusual Piezomechanical Properties of Zinc-Alkyl-Based Metal-Organic Frameworks: A First Principles Study. 2023 , 106054	O
21	Eco-friendly synthesis of graphene oxidepalladium nanohybrids. 2023, 106007	O
20	Site selective behaviour of B, C and N doping in MgO monolayers towards spintronic and optoelectronic applications. 2023 , 162, 107514	O
19	Tuning the Sharing Modes and Composition in a Tetrahedral GeX2 (X = S, Se) System via One-Dimensional Confinement. 2023 , 17, 8734-8742	O
18	Spin-Topological Electronic Valve in Ni/hBNt raphenetBN/Ni Magnetic Junction. 2023 , 9, 113	O
17	Synthesis of nanosized MFI zeolites using Cu-containing complexes. 2023 , 357, 112625	0
16	Single-Wall-Carbon-NanotubelVSe2 Nanohybrid for Ultrafast Visible-To-Near-Infrared Third-Order Nonlinear Optical Limiters. 2023 , 19,	O
15	Theoretical study of a novel porous penta-TaB with two-dimensional furrow surface as an anode for lithium-ion batteries. 2023 , 47, 9852-9860	O
14	Theoretical study on the electronic properties and quantum capacitance of Zr 2 CO 2 MXene with atomic swap.	O
13	2D Cobalt Chalcogenide Heteronanostructures Enable Efficient Alkaline Hydrogen Evolution Reaction.	O
12	Adsorption and Dissociation of R-Methyl p-Tolyl Sulfoxide on Au(111). 2023 , 8, 16471-16478	O
11	Thermostable 1T-MoS 2 Nanosheets Achieved by Spontaneous Intercalation of Cu Single Atoms at Room Temperature and Their Enhanced HER Performance.	O
10	Encapsulation of antioxidant beta-carotene by cyclodextrin complex electrospun nanofibers: Solubilization and stabilization of beta-carotene by cyclodextrins. 2023 , 423, 136284	O

CITATION REPORT

9	Hydrogen storage on tin carbide monolayers with transition metal adatoms. 2023,	О
8	Adsorption mechanism of hydrazine and methane on Li3B12 cluster: DFT investigations.	O
7	Multiple redox mechanisms for water-gas shift reaction on Fe3O4 (1 1 1) surface: A density functional theory and mean-field microkinetic modeling study. 2023 , 630, 157501	О
6	2D/2D SnS2/SnSe2 van der Waals heterostructure for highly sensitive room-temperature NO2 sensor: Key role of interface contact. 2023 , 466, 143369	O
5	Mechanisms of adsorption and diffusion of Na on a VSe2 monolayer with engineering-induced vacancies.	O
4	Dry ball-milling preparation and characterization of graphitephthalocyanine composites. 1-13	О
3	Effect of Intercalated LiF on Interface Contact Characteristics of MoS 2 Field Effect Transistor: A First-Principles Study.	О
2	First-principles study of SiC and GeC monolayers with adsorbed non-metal atoms. 2023 , 13, 14879-14886	О
1	Pd-functionalized 2D TMDC MoTe2 monolayer as an efficient glucose Sensor: A First-principles DFT study. 2023 , 631, 157525	O